THE SYNTHESIS AND REACTIVITY OF SOME HYDROCARBYL COMPLEXES OF IRON AND RUTHENIUM

A thesis submitted to the

UNIVERSITY OF CAPE TOWN

in partial fulfilment of the requirements for the degree of

MASTER OF SCIENCE

by

MANSOOR AHMED GAFOOR

B. Sc (Hons)

Department of Chemistry

University of Cape Town

Rondebosch

South Africa

September 1991

ACKNOWLEDGEMENTS

My sincere thanks and appreciation are extended to:

My supervisor, Professor J. R. Moss, for his interest, encouragement and support during the course of this project.

Mr G. P. Benin-Casa for microanalyses and recording the mass spectra.
Mr N. Hendricks, Mr Z. Brown and Miss M Nair for all the NMR spectra, efficiently run - often at short notice. Miss S. Bourne for recording the DSC thermographs. Mr N. Ahmed for the synthesis of $[CpRu(CO)_2]_2$.

Dr M. L. Niven and Dr A. Hutton for determining the crystal structures.
Dr H. B. Friedrich for proofreading this manuscript.

My colleagues and friends in the Chemistry Department, especially
Mr M. Naidoo, Mr M. R. Domingo, Dr H. B. Friedrich, Mrs J. M. Andersen, Mr R. O. Hill and Mr Y-H Liao for their support and friendship.

The University of Cape Town, FRD and DAAD for financial support.

To my family for their continuous support and encouragement.

ABSTRACT

We have reviewed the synthesis and properties of ethylene-bridged dinuclear transition metal complexes.

The ethylene-bridged ruthenium complex $[CpRu(CO)_2]_2[\mu\text{-}(CH_2CH_2)]$ has been prepared. The characterization data (IR, ^1H and ^{13}C NMR, and Mass spectral) and properties of this complex are discussed. The crystal structure of this complex has also been determined. The reactivity of this complex with donor ligands (CO, PMe_2Ph and PPh_3), protic acids (CF_3COOH and HCl), bromine, MeOH and with oxidants (Ph_3CPF_6 and $AgBF_4$) has been investigated.

The new ruthenium complexes $[\{CpRu(CO)_2\}_2\{\mu\text{-}(C_nH_{2n-1})\}]PF_6$ (n = 3 or 5), as well as their known iron analogues have been prepared. The crystal structures of $[\{CpM(CO)_2\}_2\{\mu\text{-}(C_3H_5)\}]PF_6$ (M = Fe or Ru) have been determined. The fluxional behaviour of the complex $[\{CpRu(CO)_2\}_2\{\mu\text{-}(C_3H_5)\}]PF_6$ has also been determined and discussed in comparison with the analogous iron complexes. A sequence of reactions of $[CpM(CO)_2]_2[\mu\text{-}(CH_2)_5]$ (M = Fe or Ru) with Ph_3CPF_6, CF_3COOH and NaI has been shown to give high yields of 1-pentene; the relevance of this reaction sequence is discussed.

The synthesis and properties of the known ruthenium ethyl complex $[CpRu(CO)_2(CH_2CH_3)]$ are compared with $[CpRu(CO)_2]_2[\mu\text{-}(CH_2CH_2)]$. The synthesis, characterization and properties of the ruthenium haloalkyl complexes $[CpRu(CO)_2\{(CH_2)_nX\}]$ (n = 3, X = Cl, Br or I; n = 4 or 5, X = Br or I) are also described.

ABBREVIATIONS

Å	=	Ångstrom
Cp	=	η^5-C_5H_5
Cp^*	=	η^5-$C_5(CH_3)_5$
COSY	=	correlated spectroscopy
DSC	=	differential scanning calorimetry
Et	=	ethyl group
ether	=	diethyl ether
h	=	hours
HETCOR	=	heteronuclear correlation
IR	=	infrared (vs = very strong, s = strong, w = weak)
L, L_m	=	ligand(s)
M	=	transition metal
M^+	=	molecular ion
Me	=	methyl group
m/e	=	mass to charge ratio (mass spectrometry)
m.p.	=	melting point
NMR	=	nuclear magnetic resonance (m = multiplet, qn = quintet, q = quartet, t = triplet, d = doublet, dd = doublet of doublets, tt = triplet of triplets)
	=	1,10-phenanthroline
OEP	=	octaethylporphyrin
Ph	=	phenyl group
PMe_2Ph	=	dimethylphenylphosphine
PPh_3	=	triphenylphosphine

ppm	=	parts per million
R	=	alkyl group
THF	=	tetrahydrofuran
TMS	=	tetramethylsilane
TMTAA	=	dibenzotetramethylaza-14-annulene dianion

NOTE: COMPOUNDS, FIGURES, TABLES, SCHEMES, EQUATIONS AND REFERENCE NUMBERS ARE VALID WITHIN EACH INDIVIDUAL CHAPTER ONLY

PUBLICATIONS

PAPERS:

1. "The synthesis, characterization and properties of long chain alkyl complexes of the type [CpM(CO)$_2$R] (Cp = η^5-C$_5$H$_5$; M = Fe or Ru; R = n-C$_6$H$_{13}$ to n-C$_{12}$H$_{25}$)", A. Emeran, M. A. Gafoor, J. K. I. Goslett, Y-H Liao, L. Pimble and J. R. Moss, *J. Organomet. Chem.*, **1991**, 405, 237.

2. "A comparative study of the reactivity of some dinuclear alkanediyl complexes of the type [L(CO)$_2$M(CH$_2$)$_n$M(CO)$_2$L] (where M = Fe, L = η^5-C$_5$H$_5$, η^5-C$_5$H$_4$Me or η^5-C$_5$Me$_5$, and n = 4-6; or M = Ru, L = η^5-C$_5$H$_5$, and n = 5)", K. P. Finch, M. A. Gafoor, S. F. Mapolie and J. R. Moss, *Polyhedron*, **1991**, 10, 963.

3. "A new proposal concerning the mechanism of alkene and alkane formation in the Fischer Tropsch reaction", M. A. Gafoor and J. R. Moss, *manuscript in preparation.*

CONFERENCE CONTRIBUTIONS:

1. Poster titled "C_2 ruthenium chemistry", M. A. Gafoor and J. R. Moss, presented at the Annual General Meeting Catalysis and Catalytic Processing in Gordons Bay, RSA (**1990**).

2. Short talk and poster titled "The reactivity of an ethylene-bridged ruthenium complex", M. A. Gafoor and J. R. Moss, presented at 31 st Convention of the South African Chemical Institute, Grahamstown, RSA (**1991**).

TABLE OF CONTENTS

CHAPTER 1

THE SYNTHESIS AND PROPERTIES OF ETHYLENE-BRIDGED DINUCLEAR TRANSITION METAL COMPLEXES

1.1 INTRODUCTION

Dinuclear complexes containing hydrocarbon bridges hold a pivotal position in the development of dinuclear organometallic chemistry. This is, in part, due to their implication in important catalytic reactions, including CO hydrogenation and polymerisation reactions. Several comprehensive reviews on the complexes having methylene[1], polymethylene[2,3] and hydrocarbon bridges[4,5] have recently appeared which describe their synthesis, as well as chemical and structural properties.

Ethylene-bridged complexes of the type, $[L_mM\overline{\{\mu\text{-}(CH_2CH_2)\}M'}L_m]$ or $[L_mM\{\mu\text{-}(CH_2CH_2)\}M'L_m]$, which are specific examples of the above dinuclear complexes, have also attracted the attention of many theoretical and synthetic chemists because of their chemical and novel structural features. These complexes are relevant to catalysis since they can be models for catalytic intermediates. For example, the surface ethylene species (a) (Scheme 1) has been proposed as a key intermediate in the Fischer-Tropsch reaction.

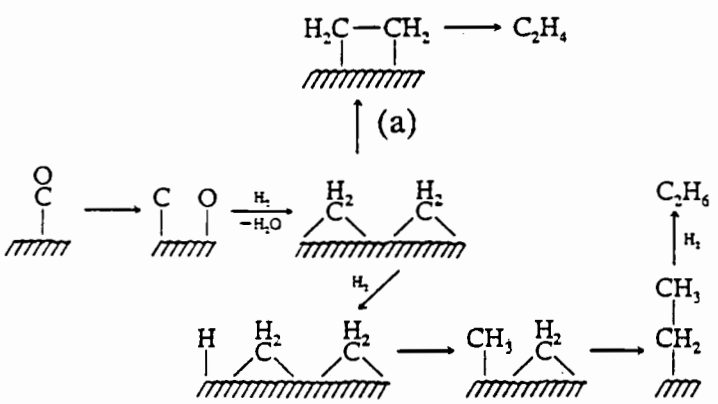

Scheme 1

The carbide mechanism[6] for the Fischer-Tropsch synthesis.

Although much work has been done, particularly in the last five years, on the ethylene-bridged dinuclear transition metal complexes, this work has not been reviewed as a separate subject before. Thus, in this chapter we describe the synthesis and properties of some of the known ethylene-bridged complexes. We have grouped these ethylene-bridged complexes into three major categories: **type A**, complexes without metal-metal bonds (section 1.2), **type B**, complexes with metal-metal bonds (section 1.3) and **type C**, complexes where ethylene is bridged side on between two metals (Section 1.4). These complexes could be homodinuclear (M = M′) (sections 1.2.1 and 1.3) or heterodinuclear (M ≠ M′) (section 1.2.2) (Scheme 2).

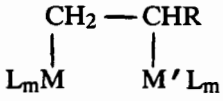

type A

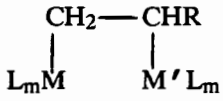

type B

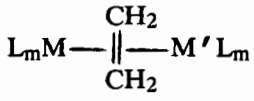

type C

L_mM, L_mM' = Metal with its associated ligand.

Scheme 2

1.2 ETHYLENE-BRIDGED COMPLEXES WITHOUT A METAL-METAL BOND, i.e. type A

Four main synthetic routes have been used for the synthesis of these complexes, i.e. (1) reaction of transition metal anions with cationic alkene complexes, (2) insertion of ethylene into metal-metal bonds, (3) reaction of trialkylaluminium with early-transition metal complexes, and (4) reactions of transition metal anions with 1,2-dihaloalkanes.

1.2.1 HOMODINUCLEAR ETHYLENE-BRIDGED COMPLEXES

Beck and Olgemöller[7] have found that the ethylene-bridged complexes of Mo and W (**1** and **2** respectively) are best synthesized from the reaction of the $K[CpM(CO)_3]$ (M = Mo or W) with the cationic π-coordinated ethylene complexes, $[CpM(CO)_3(C_2H_4)]BF_4$, (Eq. 1).

$$[CpM(CO)_3(C_2H_4)]BF_4 + K[CpM(CO)_3] \rightarrow [Cp(CO)_3M]_2[\mu\text{-}(CH_2CH_2)]$$

1 M = Mo

2 M = W

Eq. 1

Complex **1** is unstable even in the solid state above -20°C while complex **2** is stable at 20°C[8]. The higher thermal stability of the complex **2** is attributed to the greater strength of the W-C bond over the Mo-C bond[9].

The ethylene-bridged complex $[CpW(CO)_2(PPh_3)]_2[\mu\text{-}(CH_2CH_2)]$, **3**, an analogue of complex **2**, in which one of the carbonyl groups is substituted by a triphenylphosphine group has also been reported[10]. Complex **3** can be synthesized from the reaction of $K[CpW(CO)_2(PPh_3)]$ with $[CpW(CO)_2(PPh_3)(C_2H_4)]BF_4$. The infrared and ^1H NMR data for this compound indicate a trans arrangement of CO groups in the tetragonal pyramidal configuration of ligands around the metal atom (Cp at the apical position) (Fig. 1)[11]. This compound is light sensitive and decomposes rapidly with evolution of ethylene in solution at room temperature.

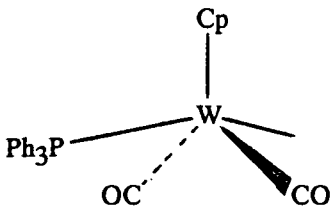

Fig. 1

Beck has also isolated ethylene-bridged complexes of Mn and Re. The reaction of $[(CO)_5Mn(C_2H_4)]BF_4$ with $Na[Re(CO)_5]$ gives a mixture of the complexes, $[Mn(CO)_5]_2[\mu\text{-}(CH_2CH_2)]$ **4**, and $[Re(CO)_5]_2[\mu\text{-}(CH_2CH_2)]$, **5**. The Re complex, $[Re(CO)_5]_2[\mu\text{-}(CH_2CH_2)]$, (Fig. 2) can also be prepared[10] from the reaction of $[(CO)_5Re(C_2H_4)]BF_4$ with $Na[Re(CO)_5]$, as well as replacing the weaker nucleophiles $[CpMo(CO)_3]^-$, $[CpW(CO)_3]^-$ and $[Mn(CO)_5]^-$ from the complexes $[Cp(CO)_3Mo\{\mu\text{-}(CH_2CH_2)\}Re(CO)_5]$, $[Cp(CO)_3W\{\mu\text{-}(CH_2CH_2)\}Re(CO)_5]$ and $[(CO)_5Mn\{\mu\text{-}(CH_2CH_2)\}Re(CO)_5]$ respectively (see later). Complexes **4** and **5** can also be prepared[12] from the reaction of the bistriflates $Y(CH_2)_2Y$ ($Y = CF_3SO_3$) with $K[M(CO)_5]$ (M = Mn or Re).

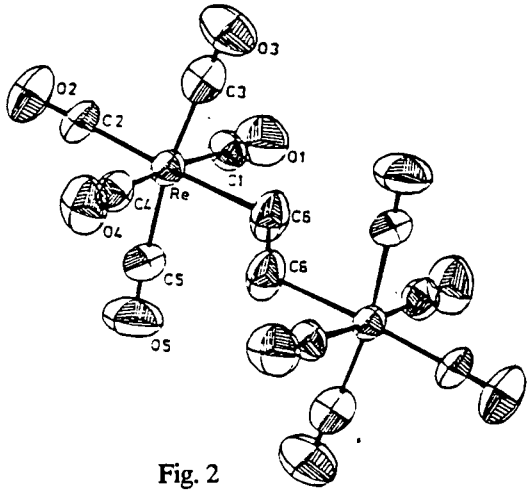

Fig. 2

Another ethylene-bridged rhenium complex $[(CO)_5Re\{(Me)CHCH_2\}Re(CO)_5]$, **6** was also isolated[8] from the reaction of $[(CO)_5Re(MeCH=CH_2)]BF_4$ with $Na[(CO)_5Re]$, (Scheme 3). In complex **6** one of the hydrogen atoms is substituted by a methyl group.

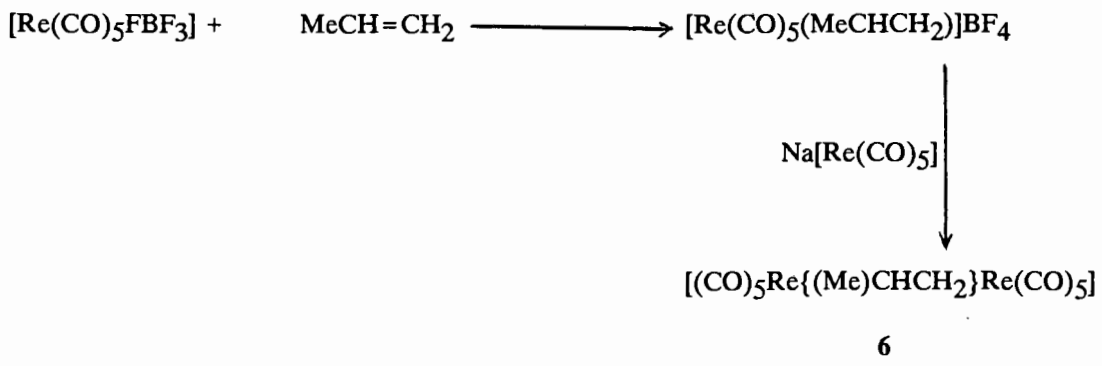

Scheme 3

For the Fe group metals, the ethylene-bridged ruthenium complex of **type A** has briefly been reported by Lin et al.[13]. However, no chemistry of this complex has been described by these authors. We have studied this di-ruthenium ethylene-bridged complex in detail and our results are reported in Chapter 2.

Attempts to prepare the ethylene-bridged complex $[CpFe(CO)_2]_2[\mu\text{-}(CH_2CH_2)]$, either by direct reaction of a 1,2-dihaloethane with $Na[CpFe(CO)_2]$ or by Beck's method[8] have resulted in the formation of ethylene and the dimer[14,15], $[CpFe(CO)_2]_2$. However, Sanders and Giering[16,17] have isolated the ethylene-bridged 3,4-di-iron cyclobutenyl complex, **7**, from the reaction of $Na[CpFe(CO)_2]$ with cis-3,4-dichlorocyclobutene at low temperature (Scheme 4). A trans-monometalated intermediate, **8**, was also isolated. Sanders and Giering proposed that the conversion from **8** to **7** occurs through S_N2 attack of $Na[CpFe(CO)_2]$ at the carbon-carbon double bond on the same side as chlorine. They have also suggested

that iron aids the loss of Cl^- from **8** to form a η-cyclobutadiene intermediate that is subsequently attacked by $[CpFe(CO)_2]^-$ to yield complex **7**.

Reaction of complex **7** with oxidants such as Ag^+ or Ph_3C^+ affords the interesting dinuclear dication complex, **9** (Scheme 4). When complex **7** in toluene is heated under reflux, cyclobutene ring opening occurs to give the 1,4 di-iron butadiene complex **10**.[18]

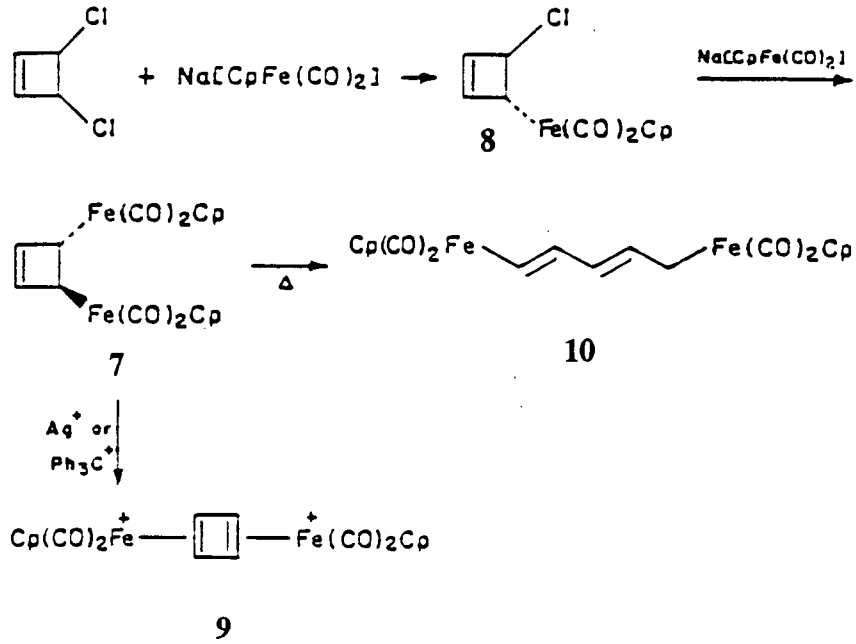

Scheme 4

Another ethylene-bridged complex of iron, **11**, was also synthesized[14] from the reaction of 1,2-dichlorobenzocyclobutene with $Na[CpFe(CO)_2]$ (Fig. 3). This complex is the first ethylene-bridged complex ever to have been prepared. The formulation of this compound as the benzocyclobutene structure **11** and not the *o*-xylene structure **12** follows from its ^1H NMR spectrum and its inability to undergo a Diels-Alder reaction with tetracyanoethylene. It was also observed[14] that the ring

opening of the benzocyclobutene of complex **11** is much slower than that of complex **7** due to the destruction of the benzenoid aromatic system upon ring opening.

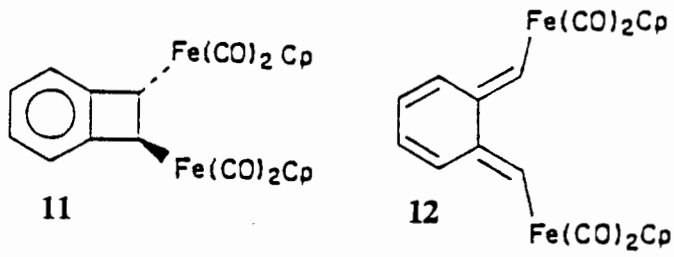

11 12

Fig. 3

Giering et al.[19,20] later studied the mechanism of the formation of complex **11** using trapping experiments and proposed that benzocyclobutadiene was a key intermediate. Benzocyclobutadiene is synthesized by reduction of the starting dichloride by $Na[CpFe(CO)_2]$. Successive additions of two $CpFe(CO)_2$ radicals to benzocyclobutadiene was proposed to lead to complex **11.** Complexes **7** and **11** were found to be stable, probably because elimination would lead to an antiaromatic cyclobutadiene structure.

Related reactions with $CpMo(CO)_3^-$, $CpW(CO)_3^-$, or $Mn(CO)_5^-$ led to the formation of metal-metal bonded dimers[14].

The known ethylene-bridged complexes of rhodium and iridium contain either a macrocycle or porphyrin ligand. Oxidative addition of 1,2-dibromoethane to the macrocyclic rhodium(I) complex, **13**, gave the ethylene-bridged dirhodium complex **14** (Eq. 2).[21] No evidence for a monorhodium alkyl intermediate was seen even when ICH_2CH_2Cl was employed. It was found[21] that the initially formed Rh-CH_2CH_2Cl species is much more reactive than the starting dihalide. Collman[21] has

suggested a cyclic intermediate to explain this neighbouring group effect.

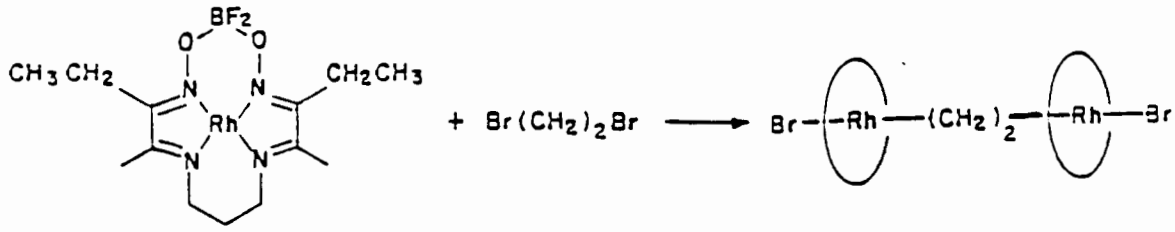

13 14

Eq. 2

An analogous ethylene-bridged complex, **15**, containing a different rhodium macrocycle was reported by Van Voorhees and Wayland[22]. This compound was prepared from the reaction of the rhodium macrocyclic compound $[Rh(TMTAA)]_2$ with ethylene (Eq. 3).

$$[Rh(TMTAA)]_2 + CH_2{=}CH_2 \longrightarrow [(TMTAA)Rh]_2[\mu\text{-}(CH_2CH_2)]$$

15

Eq. 3

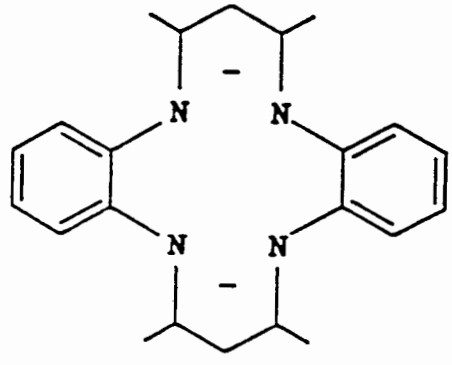

TMTAA

It was found[22] that if the above reaction is carried out in the presence of hydrogen, a mononuclear ethyl species (Eq. 4) is obtained instead of complex **15.**

$$[Rh(TMTAA)]_2 + H_2 + CH_2{=}CH_2 \longrightarrow (TMTAA)RhCH_2CH_3$$

Eq. 4

Wayland[23] et al. have reported the ethylene-bridged complexes of Rh containing an octaethylporphyrin (OEP) ligand. The reaction of $[(OEP)Rh]_2$ with alkenes, $CH_2{=}CHX$ (where X = CH_3 or Ph), gives the desired complexes, **16** (X = CH_3) and **17** (X = Ph), according to equation 5.

$$[(OEP)Rh]_2 + CH_2{=}CHX \longrightarrow [(OEP)Rh]_2[\mu\text{-}(CH_2CHX)]$$

16 X = CH_3

17 X = Ph

Eq. 5

These authors have observed a facile stereospecific 1,2 interchange of the nonequivalent (OEP)Rh group (see equation 6) of complex **16** which is demonstrated by the broadening and subsequent merging of the porphyrin methine ^1H NMR resonances as the temperature is elevated (T = -3 to 47 °C). This exchange, known as a dyotopic process, is defined as an uncatalyzed process in which two σ bonds simultaneously migrate intramolecularly.

$$[(OEP)Rh_1\{\mu\text{-}(CH_2CHX)\}Rh_2(OEP)] \longrightarrow [(OEP)Rh_2\{\mu\text{-}(CH_2CHX)\}Rh_1(OEP)]$$

Eq. 6

Similarly, octaethylporphyrin complexes of iridium $[Ir(OEP)]_2[\mu\text{-}(CH_2CHX)]$ (**18**, X = OH; **19**, X = OEt) have also been reported by Wayland[24] et al.. These complexes are obtained from the reaction of $[Ir(OEP)]_2$ with an alkene, CH_2CHX (X = OH or OEt), as outlined in equation 7.

$$[(OEP)Ir]_2 + CH_2{=}CHX \longrightarrow [(OEP)Ir]_2[\mu\text{-}(CH_2CHX)]$$

18 X = OH

19 X = OEt

Eq. 7

These authors have suggested that the above reactions probably proceed through the intermediacy of the metallo-radical $[(OEP)Ir]^{\bullet}$, formed by homolytic dissociation of the Ir-Ir bond. Furthermore, it has been suggested[24] that the complex **18** could eliminate [(OEP)IrH] due to its instability, whereas complex **19** is relatively more stable as the ethoxy group is substituted for the hydroxy group.

The platinum ethylene-bridged complex, **20**, was reported by Monaghan and Puddephatt[25]. They have found that an oxidative addition of $I(CH_2)_2I$ to dimethyl(1,10-phenanthroline) platinum(II), **21**, gives a mixture of complexes **20** and **22**, as well as ethylene (Scheme 5).

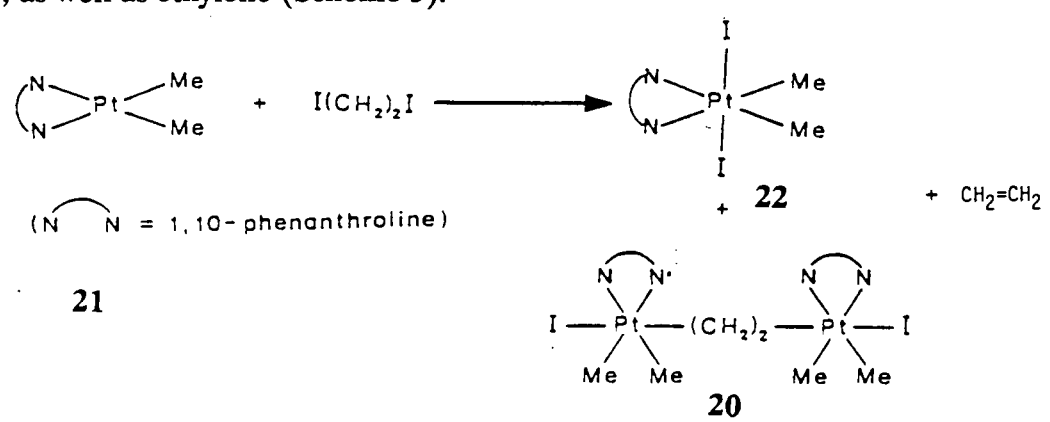

Scheme 5

1.2.2 HETERODINUCLEAR ETHYLENE-BRIDGED COMPLEXES

Heterodinuclear ethylene-bridged complexes of molybdenum, tungsten, manganese, and rhenium were prepared[8] from the nucleophilic addition of the metal anion to ethylene cationic complexes (Eq. 8):

$$[L_mM(C_2H_4)]^+ + [M'L_n]^- \longrightarrow [L_mM(CH_2)_2M'L_n] \qquad \text{Eq. 8}$$

23 L_mM = $CpMo(CO)_3$ and $M'L_n$ = $CpW(CO)_3$

24 L_mM = $CpMo(CO)_3$ and $M'L_n$ = $Re(CO)_5$

25 L_mM = $CpW(CO)_3$ and $M'L_n$ = $Re(CO)_5$

26 L_mM = $Mn(CO)_5$ and $M'L_n$ = $Re(CO)_5$

Complexes **23** and **26** are best synthesized from the reaction of $K[CpMo(CO)_3]$ with $[CpW(CO)_3(C_2H_4)]BF_4$ and from the reaction of the nucleophilic manganese complex, $Na[Mn(CO)_5]$, with the rhenium cationic complex $[Re(CO)_5(C_2H_4)]BF_4$, respectively. The reaction of $[Re(CO)_5]^-$ with the manganese cationic complex, $[(CO)_5Mn(C_2H_4)]^+$, results in the formation of a mixture of the homodinuclear ethylene-bridged complexes (section 1.2.1).

The order of nucleophilicity has been determined[8] to be $[Re(CO)_5]^- >> [CpW(CO)_3]^- > [Mn(CO)_5]^- > [CpMo(CO)_3]^-$. The higher stability of tungsten complexes is also observed for complex **23**. Complex **24** decomposes above -15°C while complex **25** is stable at 20°C. The Re-C bond is known to be particularly

strong; the difference in the stability of these complexes is thus attributed to the differing strengths of Mo-C and W-C bonds[8].

Bullock et al.[26] have reported the preparation of the heterodinuclear ethylene-bridged complex, $[Cp(PMe_3)_2Ru\{\mu\text{-}(CH_2CH_2)\}ZrCp_2Cl]$, **27**, from the reaction of an electron-rich $[Cp(PMe_3)_2Ru]$ fragment and an electron-deficient $[Cp_2ZrHCl]$ moiety. Complexes of this nature (early-late transition metal complexes) exhibit unusual structural and reactivity features. The reaction of $[Cp(PMe_3)_2RuC{\equiv}CH]$[27] with $[Cp_2ZrHCl]$ leads to the formation of the heterodinuclear alkene complex, $[Cp_2(PMe_3)_2RuCH{=}CHZrClCp_2]$, **28**, (Scheme 6)

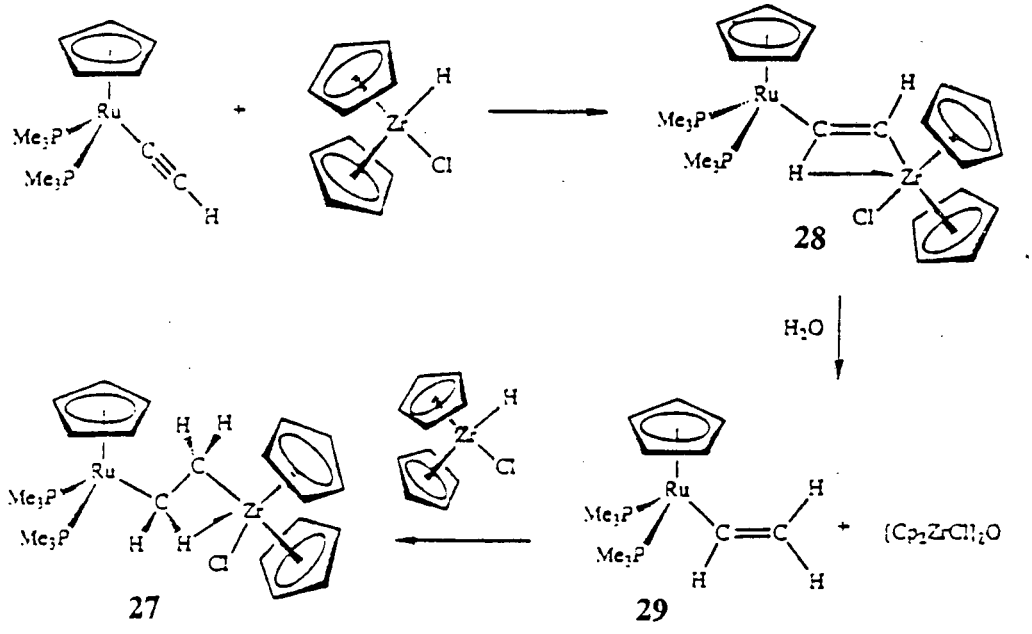

Scheme 6

The heterodinuclear complex **28** is converted to the ruthenium vinyl complex, $[Cp(PMe_3)_2RuCH{=}CH_2]$, **29**, by fission of the Zr-C bond of complex **28**. The reaction of complex **29** with $[Cp_2ZrHCl]$ gives the heterodinuclear ethylene-bridged complex, $[Cp(PMe_3)_2Ru(CH_2)_2ZrClCp_2]$, **27** (Fig. 4). Bullock suggested the

presence of an agostic[27] interaction between the α-hydrogen ($RuCH_2$) and the unsaturated Zr center. The IR spectroscopy, as well as X-ray spectrographic studies of the complex **27**, gave further evidence for this agostic interaction. The X-ray crystallographic study also showed a small Zr-C-C angle of 82.5°. This small M-C-C angle was also found in mononuclear complexes containing agostic ethyl groups[28], i.e. the Ti-C-C angle in $[TiCl_3(dmpe)CH_2CH_3]$[29] is 86.3° and the Co-C-C angle[30] in $[Cp^*P(MeC_6H_4)_3CoCH_2CH_3]^+$ is 63.4°. The C-C bond distance in the $-(CH_2)_2-$ group of 1.485 Å for the complex **27** is significantly shortened compared to a normal C-C single bond length of 1.54 Å, indicating some double bond character.

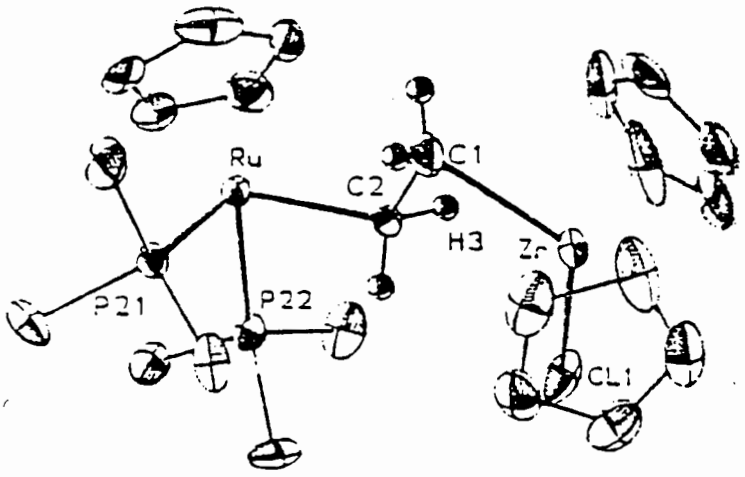

Fig. 4

Beck et al.[31] have recently reported a heterodinuclear ethylene-bridged complex containing Ru and Re, $[Cp(CO)_2Ru\{\mu\text{-}(CH_2CH_2)\}Re(CO)_5]$, **30**. The complex **30** was prepared from the reaction of $Na[CpRu(CO)_2]$ with $[(CO)_5Re(C_2H_4)]^+$. They observed that the ethylene protons, in the ^1H NMR spectrum exhibit an $AA'XX'$ spin system, which was not observed for either $[(CO)_5Re]_2[\mu\text{-}(CH_2CH_2)]$[31] or $[CpRu(CO)_2]_2[\mu\text{-}(CH_2CH_2)]$ (see also Chapter 2)

The ethylene-bridged complex, $[Cp_2ClZr\{\mu\text{-}(CH_2CH_2)\}AlEt_2]$, **31**, was prepared by Kaminsky and Sinn[32,33]. This complex is novel since it contains a main group and a transition metal. The complex **31** was prepared via two different routes during the reaction of $[Cp_2ZrCl_2]$ with $[AlEt_3]_2$ (Scheme 7).

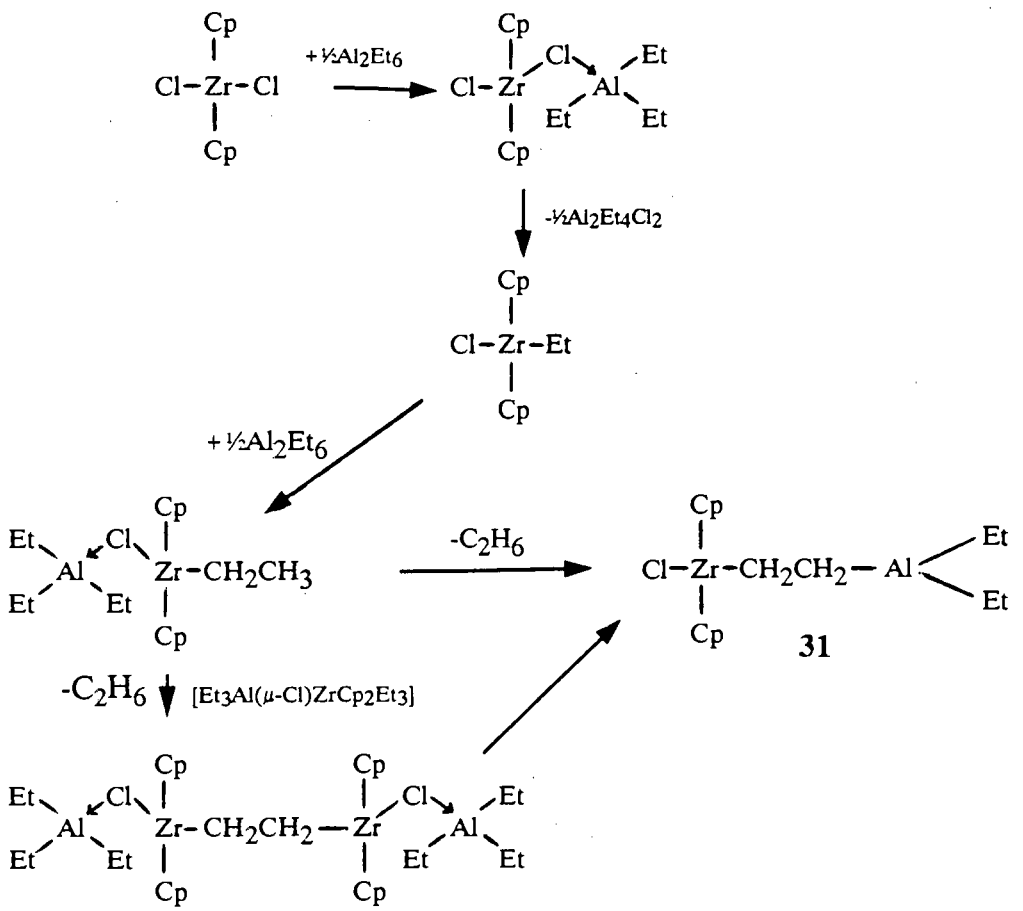

Scheme 7

These authors have also spectroscopically detected a titanium analogue of complex **31**, $[Cp_2ClTi\{\mu\text{-}(CH_2CH_2)\}AlEt_2]$, **32**. They have proposed a mechanism, based on the zirconium system, for the formation of the complex **32** (Scheme 8).

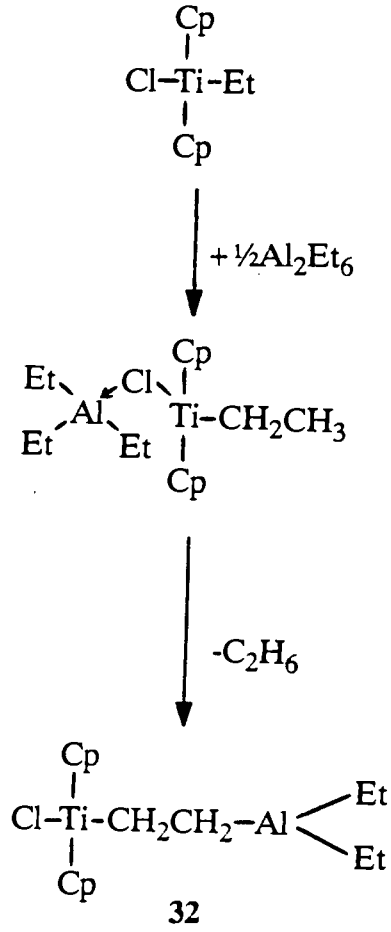

32

Scheme 8

The ethylene-bridged complexes of Nb and Ta metals, $[Cp^*_2M\{(\mu\text{-}(CH_2CH_2)\}AlEt_3]$ have been synthesized by Bercaw[34] and co-workers. The complexes $[Cp^*_2M(H)(C_2H_4)]$ (M = Nb or Ta) reversibly bind trialkylaluminium reagents to give the ethylene-bridged complexes **33**, $[Cp^*_2Nb\{(\mu\text{-}(CH_2CH_2)\}AlEt_3]$ and **34**, $[Cp^*_2Ta\{(\mu\text{-}(CH_2CH_2)\}AlEt_3]$.

A molecular structure (Fig. 5) of the complex **33** was determined at reduced temperature (-53 °C) in order to prove that the aluminium was indeed coordinated to the ethylene ligand and to examine the details of this unusual mode of bonding. The authors observed a C - C bond length of 1.44 Å, which is intermediate between a single and a double C - C bond.

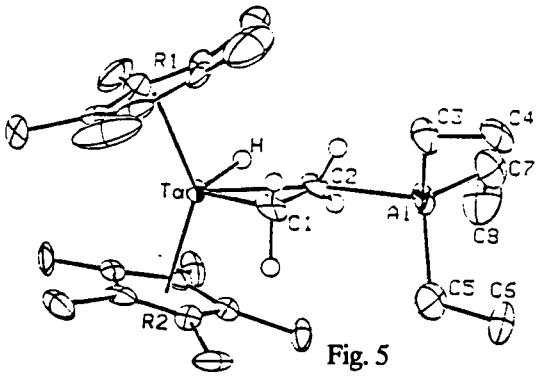

Fig. 5

1.3 ETHYLENE-BRIDGED COMPLEXES WITH A METAL-METAL BOND, i.e. type B

Although examples of the metallacyclobutane ring (b), (Fig. 6), are now fairly common in organometallic complexes[35], the dimetallacyclobutane ring (c), otherwise known as an ethylene-bridged complex with a metal-metal bond, has so far been limited to osmium and cobalt metals.

(b) (c)

Fig. 6

The metallacyclobutane complexes are accepted as being intermediates in the transition metal catalyzed metathesis of olefins; it has also been suggested that they are involved in carbon chain growth in the Fischer-Tropsch synthesis[36].

Norton et al.[37] has shown that the addition of a solution of the dianion $Na_2[Os_2(CO)_8]$, to the difunctional alkylating agents XCH_2CH_2X (X = I or OTs), gives the diosmacyclobutane $[(CO)_4Os]_2[\mu\text{-}(CH_2CH_2)]$, **35** (Eq. 9). The use of $TsOCH_2CH_2OTs$ proved more satisfactory than ICH_2CH_2I. The structure of the diosmacyclobutane, **35**, has been confirmed by X-ray diffraction (Fig. 7). The molecule has approximate C_2 symmetry. A 27° twist about the Os-Os bond keeps the $Os(CO)_4$ units out of the sterically unfavourable eclipsed configuration at the expense of bending the Os_2C_2 ring and slightly compressing[37] (105°) the Os-C-C angles. The ethylene-bridged complex contains a normal (1.53Å) carbon-carbon single bond.

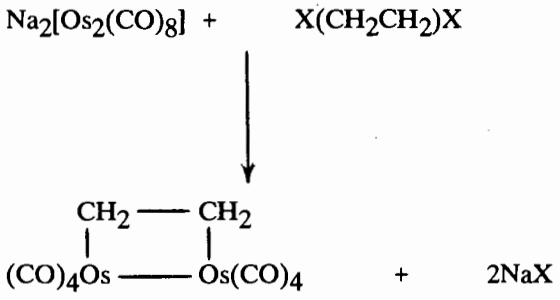

35

Eq. 9

The complex **35** is the first ever example of a 1,2-dimetallacyclobutane.

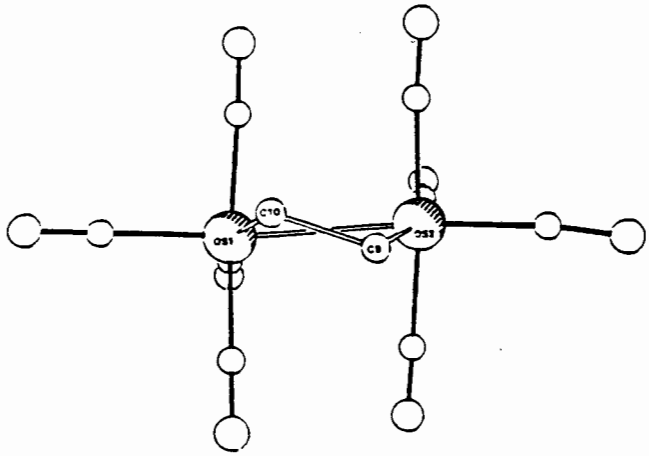

Fig. 7

This diosmacyclobutane, **35**, has been synthesized via a different route by Takats et al.[38], by photolyzing $Os_3(CO)_{12}$ in the presence of ethylene (Eq. 10).

These authors have also isolated the diosmacyclobutane complex, $[(CO)_4Os(\mu\text{-}CH_2CHCO_2Me)Os(CO)_4]$, **36**, from the photolysis reaction of $Os_3(CO)_{12}$ with methyl acrylate (Eq. 10). They have also noted a mononuclear alkene adduct, $[Os(CO)_4(CH_2CHCO_2Me)]$, **37**. The diosmacyclobutane ring is puckered as was observed in the complex **35**.

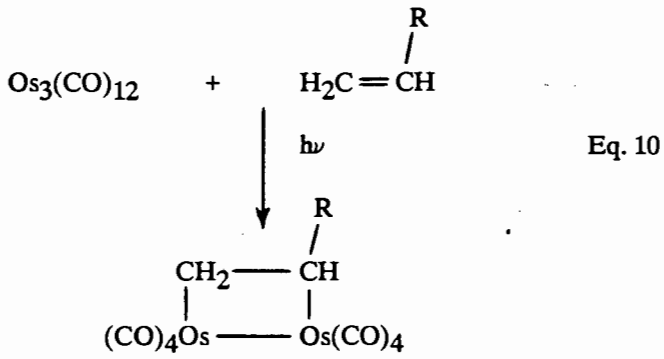

Eq. 10

35 R = H **36** R = CO_2Me **38** R = Me

The X-ray diffraction results confirmed the dinuclear formulation, $[Os_2(CO)_8(CH_2CHCO_2Me)]$ (Fig. 8). The Os-Os bond distance is 2.88Å; and the length of the C-C bond in the bridged ethylene ligand is 1.52 Å, which is consistent with a normal C-C single bond. A 23° twist about the Os-Os bond avoids eclipsing interactions of the carbonyl ligands.

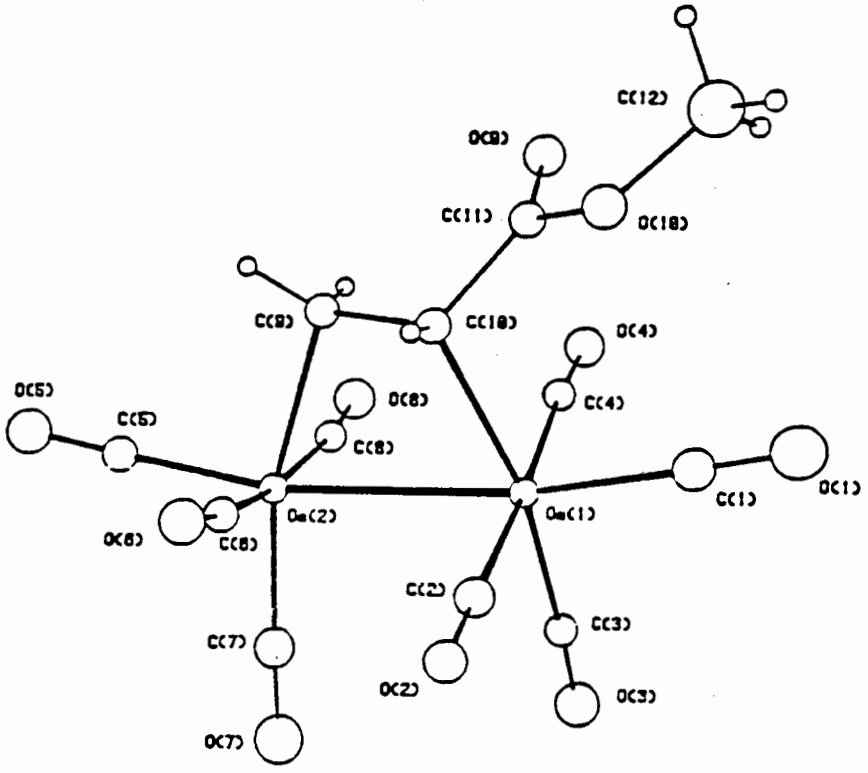

Fig. 8

Similarly, another substituted hydrocarbon diosmacyclobutane complex, **38**, was prepared[38,39] photochemically using propylene (Eq. 10). In both complexes, **36** and **38**, a hydrogen is substituted by a CO_2Me and CH_3 group respectively.

Takats et al.[38] have noted that photolysis of corresponding complexes of other metals (Fe, Ru) in the osmium group did not give the ethylene-bridged or

dimetallacyclobutane complexes. This difference in reactivity of these systems has been attributed to the metal-metal bond strength of the intermediate $M_2(CO)_8$ species. The stronger Os-Os bond allows for trapping of the $Os_2(CO)_8$ intermediate with alkenes, while the weaker bond, for example Ru-Ru readily cleaves to form $Ru(CO)_4$.

Attempted reactions by Theopold and Bergman[40] to synthesize a similar dicobaltacyclobutane from the reaction of ICH_2CH_2I with $Na[Cp_2Co_2(CO)_2]$ were unsuccessful. However, they have synthesized the dicobaltacyclobutane complex, **39**, from the reaction of 1,2-di-iodo-3,4-benzocyclobutene and $Na[Cp_2Co_2(CO)_2]$ (Scheme 9). This product is unstable at room temperature and decomposes to mononuclear benzocyclobutadiene, **40** (Scheme 9). Complex **39** is a rigid compound in which two hydrogen atoms are substituted by the benzocyclobutene. This substituent is also present in complex **11** (see section 1.2.1).

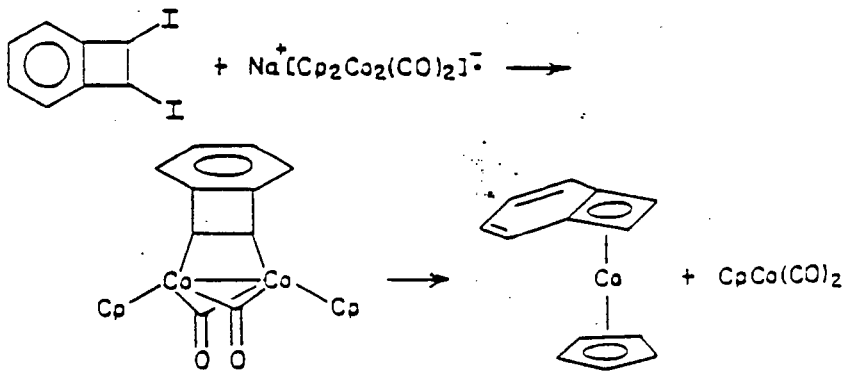

39 **40**

Scheme 9

1.4 ETHYLENE-BRIDGED COMPLEXES WHERE ETHYLENE IS BRIDGED SIDE ON BETWEEN THE TWO METALS, i.e. type C

Some of the ethylene-bridged complexes are categorized into a new type (**type c**) simply because of the way in which the ethylene is bonded to two metals.

Kaminsky and Sinn[32] have isolated three such ethylene-bridged complexes from the reaction of two moles of $[Cp_2ZrCl_2]$ with one mole of $[AlEt_3]_2$. The initial product $[Cp_2ClZrEt]$, **41**, of the above reaction reacts with $[AlEt3]_2$ and $[AlEt_2Cl]_2$ to form two complexes, **42** and **43**, respectively. These complexes are then converted by intermolecular β-hydrogen transfer and elimination of ethane to complexes **44** and **45** respectively. The complex, **46**, was obtained from the complexes **44** and **45** by treating them with THF (Scheme 10).

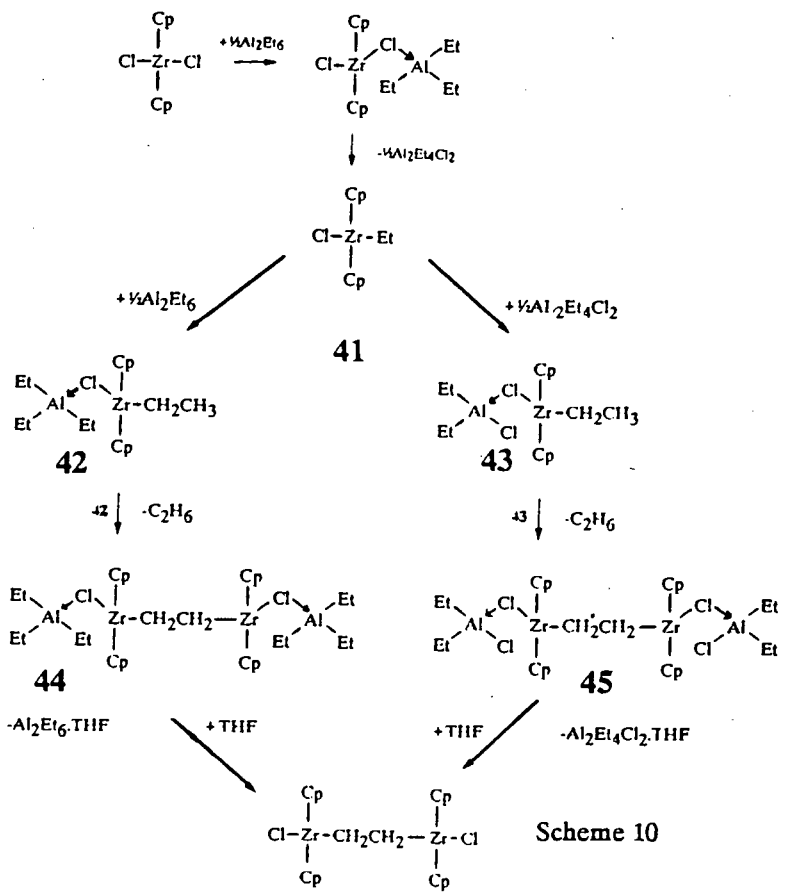

Scheme 10

Complex, **44**, combined with $[AlMe_3]_2$ or $[AlEt_3]_2$, is a very active catalyst for the polymerization of terminal alkenes[41]. Complex **44** has been invoked as a model for the potential CH_2 coupling step ((d) → (e)) of two $Re=CH_2$ species[42] (Fig. 9).

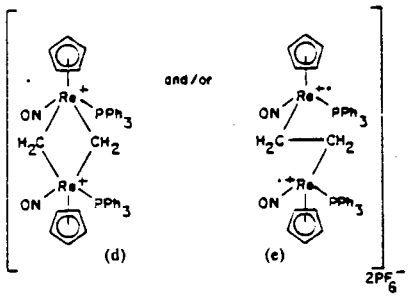

Fig. 9

The X-ray spectrographic investigations[41] of complex **44** show a most interesting structural feature (Fig. 10), i.e. the $Zr\text{-}CH_2\text{-}CH_2$ angle is 75.9°. By contrast an X-ray analysis of the ethylene-bridged rhenium complex, $[(CO)_5Re]_2[\mu\text{-}(CH_2CH_2)]$, reveals no such anomaly. The $Re\text{-}CH_2\text{-}CH_2$ angle[44] is 120°C. The Zr-β-carbon distance in complex **44** is 2.49Å whereas the Zr-α-carbon bond distance is 2.36Å. This suggests that the bonding of the $-(CH_2)_2-$ group is intermediate between a σ and a η^2-(C_2H_4)- type interaction.

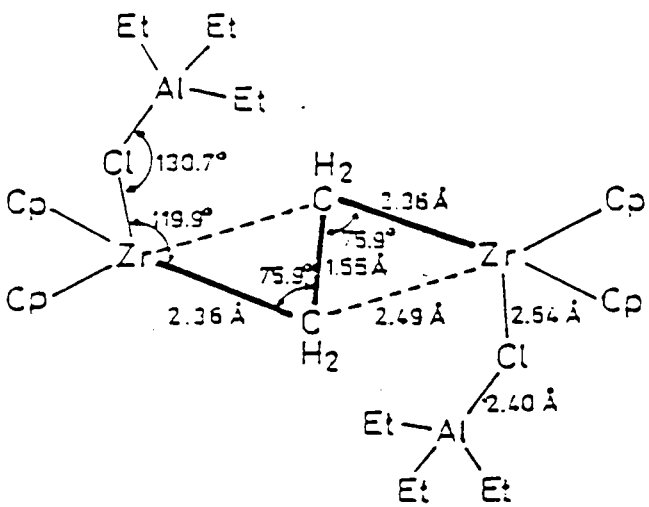

Fig. 10

Elimination of ethylene was observed in the reaction of these ethylene-bridged complexes with HCl. Despite the close proximity of the β-carbons to the Zr atom, a general prerequisite for instability of ethylene-bridged complexes, these complexes show resistance to decomposition via β-elimination. This is partially explained by steric factors; steric crowding in the transition state for β-elimination would disfavour decomposition by this route (Fig. 11).

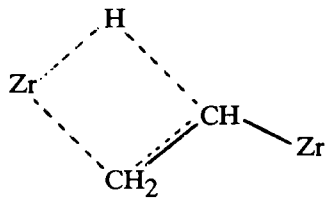

Fig. 11

This steric effect was observed for some zirconium alkyl complexes, for example $[Cp_2ZrBu^n\{CH(SiMe_3)_2\}]$[44]. The dizirconium complexes (**44-46**) are thermally stable up to 96, 110 and 180°C respectively. This in contrast to the ethyl complexes, $[Cp_2ClZrEt]$, which decomposes above 0°C via β-elimination.

Schrock et al.[45] reacted $[ZrCl_3(PEt_3)_2]_2$ and $[ZrCl_3(PBu_3)_2]_2$ with one equivalent or an excess of ethylene to give orange, crystalline complexes **47** and **48**, $[(PR_3)_2ZrCl_3]_2[\mu\text{-}(CH_2CH_2)]$ (**47**, $PR_3 = PEt_3$; **48**, $PR_3 = PBu_3$) (Eq. 11).

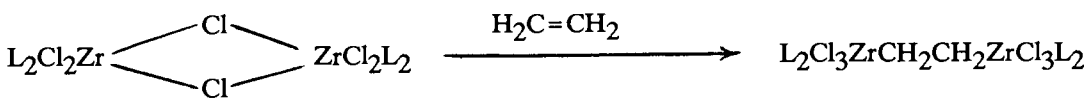

Eq. 11

47 L = PEt_3 **48** L = PBu_3

Schrock and co-workers could not fully characterize complex **47**. However, complex **48** was partially characterized. These authors have suggested that the PBu_3 compound is a dimer with "ethylene" connecting the two octahedral Zr(IV) centers, but could not confirm that the "ethylene" actually was aliphatic. However, Cotton and Kibala[46] later reported the synthesis of complexes **47** and **49** $[MX_3(PEt_3)]_2[\mu\text{-}(CH_2CH_2)]$ (**47**, M = Zr, X = Cl; **49**, M = Zr, X = Br) as well as their hafnium analogues, **50** (X = Cl) and **51** (X = Br) using a different synthetic route (Eq. 12). They have also determined the strutures of these complexes by X-ray crystallography.

$$[M_2X_6(PEt_3)_4] + Cl(CH_2)_2Cl \longrightarrow [MX_3(PEt_3)]_2[\mu\text{-}(CH_2CH_2)]$$

47 M = Zr, X = Cl

49 M = Zr, X = Br

50 M = Hf, X = Cl

51 M = Hf, X = Br

Eq. 12

On the basis of Schrock's method (Eq. 11) and new available spectroscopic evidence ($^{31}P\{H\}$ NMR data), Cotton and Kibala suggested that the complexes $[M_2X_6(PEt_3)_4]$ first react with 1,2-dichloroethane (in the reactions described in equation 12) to form monomeric $MX_3Cl(PEt_3)_2$ and ethylene (Eq. 13):

$$M_2X_6(PEt_3)_4 + Cl(CH_2)_2Cl \longrightarrow 2MX_3Cl(PEt_3)_2 + CH_2{=}CH_2$$

Eq. 13

The released ethylene reacts in turn with another molecule of $M_2X_6(PEt_3)_4$ to give the desired complexes (Eq. 14):

$$M_2X_6(PEt_3)_4 + CH_2{=}CH_2 \longrightarrow [MX_3(PEt_3)]_2[\mu\text{-}(CH_2CH_2)]$$

Eq. 14

A characteristic feature in the crystal stuctures of these complexes is a symmetrical ethylene bridge in which the "olefin" plane is perpendicular to the metal-metal axis, with the midpoint of the ethylene group coinciding with the midpoint of the metal-metal vector. Cotton and co-workers have defined the nearly planar ten-atom arrangement consisting of the two metal atoms, the two bridging carbon atoms of ethylene group, the four phosphorus nuclei, and two of the halide ions as the equatorial plane (see Figures 12 and 13). The structure is then completed with the four axial halide ions, two above and two below the equatorial plane.

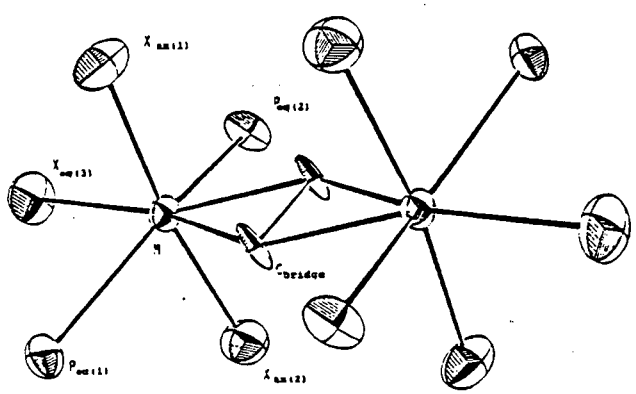

Fig. 12

They also found two main distortions from the octahedral geometry. The first distortion is the bending back of the four equatorial phosphine ligands away from

the central $M_2(\mu\text{-}\eta^4\text{-olefin})$ unit by 27 - 30°. The second distortion is less severe, about 4 - 8°, representing the bending of the axial halide ligands toward the center of the complex.

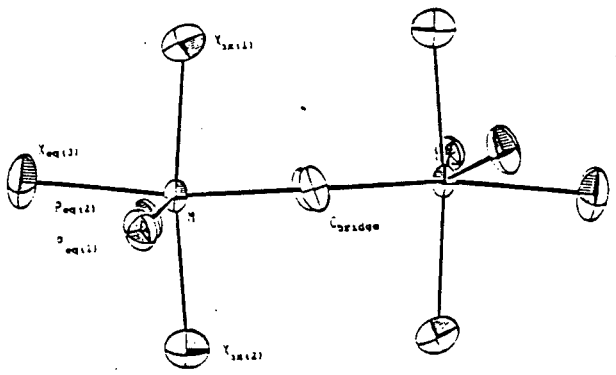

Fig. 13

All metal ligand distances were found to be normal, however, the carbon-carbon bonds were observed to be rather long (> 1.5 Å).

Although many attempts were made by Cotton and Kibala[46] to prepare complexes in which one or more hydrogen atoms of the ethylene group is substituted with an alkyl (CH_3 etc.) group, they were unable to crystallize any solid products from the extremely air-sensitive solutions. However, Schrock et al.[45] have isolated one such ethylene-bridged complex $[(PEt_3)_2Cl_3ZrCH_2CH(Me)ZrCl_3(PEt_3)_2]$, **52**, from the reaction of $[ZrCl_3(PEt_3)_2]_2$ with propylene (Eq. 15). Complex **52** is a dark yellow plate-like crystalline compound which is toluene-soluble. The low - temperature ^{31}P-NMR spectrum (- 40°C) shows two types of phosphine ligands, as expected for a dimer containing the $-CH_2CHMe-$ group. At higher temperatures the two ^{31}P signals coalesce to a single broad peak.

These authors[45] have observed that the CH coupling constants for the bridging CH_2CHMe group which compare well with the coupling constants found for aliphatic compounds. Thus, confirming that propylene "insertion" into the Zr - Zr bond gives a dimer containing two C - Zr bonds.

$$[ZrCl_3(PEt_3)_2]_2 + \quad MeCH{=}CH_2$$

$$\downarrow \text{ toluene}$$

$$[(PEt_3)_2Cl_3ZrCH_2CHMeZrCl_3(PEt_3)_2]$$

52

Eq. 15

The ethylene-bridged complex $[Cp^*_2Yb\{\mu\text{-}(CH_2CH_2\}Pt(PPh_3)_2]$, **53** has been isolated[47] from the reaction of a toluene solution of $[Cp^*_2Yb]$ with $(\eta^2\text{-}CH_2CH_2)Pt(PPh_3)_2$. The solid state structure was determined[47] by X-ray diffraction at -80 °C as shown in figure 14. The C - C bond distance in complex **53** is 1.436 Å, which is larger than a normal C=C distance. The angles at which the planes, defined by H(1)C(1)H(2) and C(1)C(2)Pt, H(3)C(2)H(4) and C(1)C(2)Pt, meet are 89.0° and 85.7°, respectively (see Fig. 14).

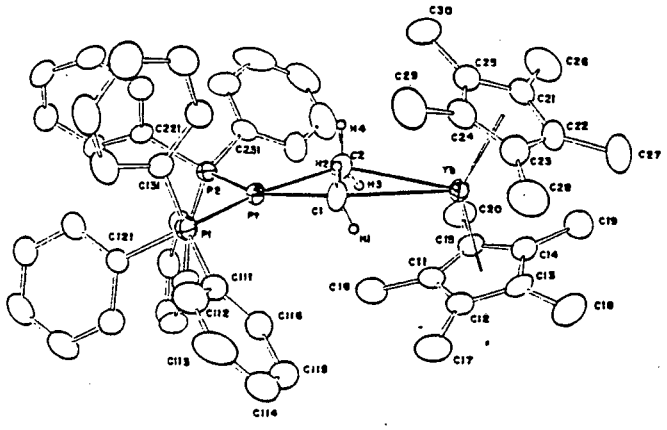

Fig. 14

Attempts were made by Kaminsky and Sinn[48] to isolate the titanium analogue of **44**, $[\{Et_3Al(\mu\text{-}Cl)TiCp_2\}_2\{\mu\text{-}(CH_2CH_2)\}]$, **54**. This complex has been detected spectroscopically during the reaction of $[Cp_2TiClEt]$ with $[AlEt_3]_2$. Based on the findings with the zirconium system, mechanism of the reaction in the analogous titanium system was deduced (Scheme 11).

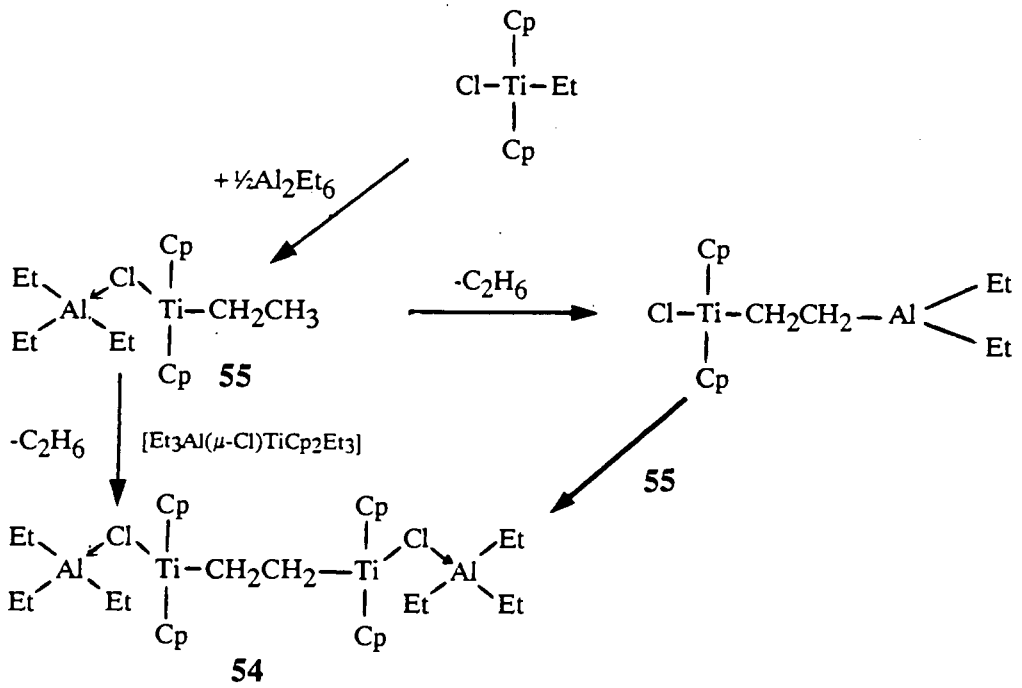

Scheme 11

These authors[48] found that the rate of reaction of the titanium system is ca. 100 times that of zirconium. The complex **54** was also detected in a parallel reaction, in which an intermediate Ti-CH_2-CH_2-Al (see also section 1.2.2) was converted by alkyl exchange with the complex **55**.

1.5 CONCLUSION

A relatively small number of homo- and heteronuclear ethylene-bridged transition metal complexes (**types A - C**) has been synthesized. The mechanistic studies of reactions of these complexes are in their infancy and intense research is still required, since these complexes may provide insight into related heterogeneous catalytic system. Isotopic labeling, crossover experiments and other physical organic techniques are appropriate to fully elucidate the reactivity of these complexes.

TABLE 1 ETHYLENE-BRIDGED COMPLEXES WITH THEIR PRECURSORS

NO.	COMPOUNDS	PRECURSORS	REF
1	$[CpMo(CO)_3]_2[\mu\text{-}(CH_2CH_2)]$	$[Cp(CO)_3Mo(C_2H_4)]^+ + [CpMo(CO)_3]^-$	7
2	$[CpW(CO)_3]_2[\mu\text{-}(CH_2CH_2)]$	$[Cp(CO)_3W(C_2H_4)]^+ + [CpW(CO)_3]^-$	7
3	$[CpW(CO)_2(Ph_3P)]_2[\mu\text{-}(CH_2CH_2)]$	$[Cp(CO)_2W(PPh_3)(C_2H_4)]^+ + [CpW(PPh_3)(CO)_2]^-$	10
4	$[(CO)_5Mn]_2[\mu\text{-}(CH_2CH_2)]$	$[(CO)_5Mn(C_2H_4)]^+ + [Mn(CO)_5]^-$	10
5	$[(CO)_5Re]_2[\mu\text{-}(CH_2CH_2)]$	$[(CO)_5Re(C_2H_4)]^+ + [Re(CO)_5]^-$	10
6	$[(CO)_5Re]_2[\mu\text{-}(CH_2CHMe)]$	$[(CO)_5Re(MeCHCH_2)]^+ + [Re(CO)_5]^-$	7
7	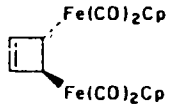	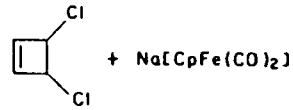	16
11	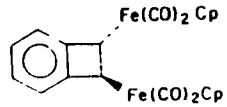		19

NO.	COMPOUNDS	PRECURSORS	REF
14	$[RhLBr]_2[\mu\text{-}(CH_2CH_2)]$	$2RhL + Br(CH_2CH_2)Br$	21
		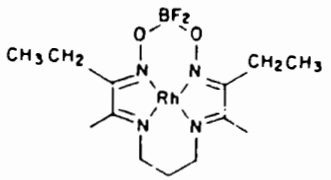 L	
15	$[Rh(TMTAA)]_2[\mu\text{-}(CH_2CH_2)]$	$[Rh(TMTAA)]_2 + CH_2{=}CH_2$	22
		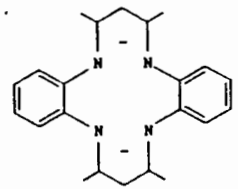 TMTAA	
16	$[(OEP)Rh]_2[\mu\text{-}(CH_2CHMe)]$	$[(OEP)Rh]_2 + CH_2{=}CHMe$	23
17	$[(OEP)Rh]_2[\mu\text{-}(CH_2CHPh)]$	$[(OEP)Rh]_2 + CH_2{=}CHPh$	23
18	$[(OEP)Ir]_2[\mu\text{-}(CH_2CHOH)]$	$[(OEP)Ir]_2 + CH_2{=}CHOH$	24
19	$[(OEP)Ir]_2[\mu\text{-}(CH_2CHOEt)]$	$[(OEP)Ir]_2 + CH_2{=}CHOEt$	24
20	$[PtI(\widehat{N\ N})Me_2]_2[\mu\text{-}(CH_2CH_2)]$	$[Pt(\widehat{N\ N})Me_2] + I(CH_2CH_2)I$	25
23	$[Cp(CO)_3Mo\{\mu\text{-}(CH_2CH_2)\}W(CO)_3Cp]$	$[Cp(CO)_3Mo(C_2H_4)]^+ + [CpW(CO)_3]^-$	8

NO.	COMPOUNDS	PRECURSORS	REF
24	$[Cp(CO)_3Mo\{\mu\text{-}(CH_2CH_2)\}Re(CO)_5]$	$[Cp(CO)_3Mo(C_2H_4)]^+ + [Re(CO)_5]^-$	10
25	$[Cp(CO)_3W\{\mu\text{-}(CH_2CH_2)\}Re(CO)_5]$	$[Cp(CO)_3W(C_2H_4)]^+ + [Re(CO)_5]^-$	7
26	$[(CO)_5Mn\{\mu\text{-}(CH_2CH_2)\}Re(CO)_5]$	$[(CO)_5Mn(C_2H_4)]^+ + [Re(CO)_5]^-$	10
27	$[Cp(PMe_3)_2Ru\{\mu\text{-}(CH_2CH_2)\}ZrCp_2Cl]$	$[CpRu(PMe_3)_2] + [Cp_2ZrHCl]$	26
30	$[CpRu(CO)_2\{\mu\text{-}(CH_2CH_2)_2\}Re(CO)_5]$	$[CpRu(CO)_2]^- + [(CO)_5Re(C_2H_4)]^+$	31
31	$[Cp_2ClZr\{\mu\text{-}(CH_2CH_2)\}AlEt_2]$	Complex **43** - C_2H_6	32
32	$[Cp_2ClTi\{\mu\text{-}(CH_2CH_2)\}AlEt_2]$	Complex **55** - C_2H_6	48
33	$[Cp^*_2Nb\{\mu\text{-}(CH_2CH_2)\}AlEt_3]$	$[Cp^*_2Nb(H)(C_2H_4)] + [AlEt_3]_2$	33
34	$[Cp^*_2Ta\{\mu\text{-}(CH_2CH_2)\}AlEt_3]$	$[Cp^*_2Ta(H)(C_2H_4)] + [AlEt_3]_2$	33
35	$[(CO)_4Os]_2[\mu\text{-}(CH_2CH_2)]$	$Na_2[Os_2(CO)_8] + X(CH_2CH_2)X$	37
		X = I or OTs	
		$[Os_3(CO)_{12}] + CH_2{=}CH_2 + h\nu$	38
36	$[(CO)_4Os]_2[\mu\text{-}(CH_2CHCO_2Me)]$	$[Os_3(CO)_{12}] + CH_2{=}CHCO_2Me + h\nu$	38
38	$[(CO)_4Os]_2[\mu\text{-}(CH_2CHMe)]$	$[Os_3(CO)_{12}] + CH_2{=}CHMe + h\nu$	38
39			40

NO.	COMPOUNDS	PRECURSORS	REF
44	$[ZrCp_2(AlEt_3Cl)]_2[\mu\text{-}(CH_2CH_2)]$	$[Cp_2ZrCl_2]$ + $[AlEt_3]_2$	32
45	$[ZrCp_2(AlEt_2Cl)]_2[\mu\text{-}(CH_2CH_2)]$	$[Cp_2ZrCl_2]$ + $[AlEt_2Cl]_2$	32
46	$[ZrCp_2Cl]_2[\mu\text{-}(CH_2CH_2)]$	Complexes **44** or **45** + THF	32
47	$[Zr(PEt_3)_2Cl_3]_2[\mu\text{-}(CH_2CH_2)]$	$[ZrCl_3(PEt_3)_2]_2$ + C_2H_4	45
48	$[Zr(PBu_3)_2Cl_3]_2[\mu\text{-}(CH_2CH_2)]$	$[ZrCl_3(PBu_3)_2]_2$ + C_2H_4	45
49	$[Zr(PEt_3)_2Br_3]_2[\mu\text{-}(CH_2CH_2)]$	$[ZrBr_3(PEt_3)_2]_2$ + C_2H_4	46
50	$[Hf(PEt_3)_2Cl_3]_2[\mu\text{-}(CH_2CH_2)]$	$[HfCl_3(PEt_3)_2]_2$ + C_2H_4	46
51	$[Hf(PEt_3)_2Br_3]_2[\mu\text{-}(CH_2CH_2)]$	$[HfBr_3(PEt_3)_2]_2$ + C_2H_4	46
52	$[Zr(PEt_3)_2Cl_3]_2[\mu\text{-}(CH_2CHMe)]$	$[ZrCl_3(PEt_3)_2]_2$ + $CH_2{=}CHMe$	45
53	$[Cp^*_2Yb\{\mu\text{-}(CH_2CH_2)_2\}Pt(PPh_3)_2]$	$[Cp^*_2Yb]$ + $[(\eta^2\text{-}CH_2CH_2)Pt(PPh_3)_2]$	47
54	$[TiCp_2(AlEt_3Cl)]_2[\mu\text{-}(CH_2CH_2)]$	[CpTiClEt] + $[AlEt_3]_2$	48

1.6 REFERENCES

1. W. A. Herrmann, *Adv. Organomet. Chem.*,**1982**, 20, 160.
2. C. P. Cassey and J .D .Audett, *Chem. Rev.* **1986**, 86, 339.
3. J. R. Moss and L. G. Scott, *Coord. Chem. Rev.*, **1984**, 60, 171.
4. J. Holton, M. F. Lappert, R. Pearce and P. I. W. Yarrow, *Chem., Rev.*, **1983**, 83, 135.
5. R.J. Puddephatt, *Polyhedron*, **1988**, 7, 767.
6. F. A. Cotton and G. Wilkinson, "Advanced Inorganic Chemistry", 5th Ed., Wiley-Interscience, New York **1988**, p. 1229.
7. W. Beck and B. Olgemöller, *Chem. Ber.* **1981**, 114, 867.
8. W. Beck, *Polyhedron*, **1988**, 7, 2255.
9. F. A. Adedeji, J. A. Connor, H. A. Skinner, L. Galyer and G. Wilkinson, *J. Chem. Soc. Chem. Comm.*, **1967**, 159.
10. W. Beck and B. Olgemöller, *J. Organomet. Chem.*, **1977**. 127, C45.
11. J. W. Faller and A. S. Anderson, *J. Am. Chem. Soc.*, **1969**, 91, 1550; A.R. Manning, *J. Chem. Soc.(A)*, **1967**, 1984.
12. E. Lindner, M. Pabel and K. Eichele, *J. Organomet. Chem.*, **1990**, 386, 187.
13. Y. C. Lin, J. C. Calabrese and S. S. Wreford, *J. Am. Chem. Soc.*, **1983**, 105, 167.
14. R. B. King, A. Efraty and W. C. Zipperer, *J. Organomet. Chem.*, **1972**, 38, 121.
15. L. G. Scott, M. Sc. Thesis, University of Cape Town, **1984**.
16. A. Sanders and W. P. Giering, *J. Am. Chem. Soc.*, **1974**, 96, 5247.
17. A. Sanders and W. P. Giering, *J. Organomet. Chem.*, **1976**, 104, 67.
18. (a) M. R. Churchill, J. Wormald, W. P. Giering and G. F. Emerson, *J. Chem. Soc. Chem. Comm.*, **1968**, 1217; (b) R. E. Davis, *J. Chem. Soc. Chem. Comm.*, **1968**,

1218; (c) M. R. Churchill and J. Wormald, *Inorg. Chem.*, **1969**, 8, 1936.

19. T. Bauch, A. Sanders, C. V. Magatti, P. Waterman, D. Judelson and W. P. Giering, *J. Organomet. Chem.*, **1975**, 99, 269.

20 A. Sanders, T. Bauch, C. V. Magatti and W. P. Giering, *J. Organomet. Chem.*, **1976**, 107, 359.

21. J. P. Collman and M. R. Maclaury, *J. Am. Chem. Soc.*, **1974**, 96, 3019.

22. S. L. Van Voorhees and B. B. Wayland, *Organometallics*, **1987**, 6, 204.

23. B. B. Wayland, Y. Peng and S. Ba, *Organometallics*, **1989**, 8, 1438

24. K. J. Del Rossi and B. B. Wayland, *J. Chem. Soc. Chem. Comm.*, **1986**, 1653.

25. P. K. Monaghan, and R. J. Puddephatt, *Inorg. Chim. Acta*, **1983**, 76, L237.

26. R. M. Bullock, F. R. Lemke and D. J. Szalda, *J. Am. Chem. Soc.*, **1990**, 112, 3244.

27. R. M. Bullock, *J. Chem. Soc. Chem. Comm.*, **1989**, 165-167.

28. M. Brookhart, M. L. H. Green and L. L. Wong, *Prog. Inorg. Chem.*, **1988**, 36, 1.

29. (a) Z. Dawoodi, M. L. H. Green, V. S. B. Mtetwa and K. Prout, *J. Chem. Soc. Chem. Comm.*, 1982, 802; (b) Z. Dawoodi, M. L. H. Green, V. S. B. Mtetwa, K. Prout, A.J.Schultz, J.M.Williams and T.F.Koetzle, *J. Chem. Soc. Dalton Trans.* **1986**, 1629.

30. R. B. Cracknell, A. G. Orpen and J. L. Spencer, *J. Chem. Soc. Chem. Comm.*, **1984**, 326.

31 J. Breimair, B. Niemer, K. Raab and W. Beck, *Chem. Ber.*, **1991**, 124, 1059.

32. W. Kaminsky and H. Sinn, *Justus Liebigs Ann. Chem.*, **1975**, 424.

33. W. Kaminsky and H. Sinn, *Adv. Organometal. Chem.* **1980**, 18, 99.

34. C. McDade, V. C. Gibson, B. D. Santarsiero and J. E. Bercaw, *Organometallics*, **1988**, 7, 1.

35. R. E. Colborn, A. F. Dyke, S. A. R. Knox, K. A. Mead and P.

Woodward, *J. Chem. Soc. Dalton Trans.* **1983**, 2099.

36. R. H. Grubbs, *Prog. Inorg. Chem.* **1978**, 24, 1.
37. K. M. Motyl, J. R. Norton, C. K. Schauer and O. P. Anderson, *J. Am. Chem. Soc.*, **1982**, 104, 7325.
38. M. R. Burke, J. Takats, F. W. Grevels and G. J. A. Reuvers, *J. Am. Chem. Soc.*, **1983**, 105, 4092.
39. A. J. Poë and C. V. Seker, *J. Am. Chem. Soc.*, **1986**, 108, 3673
40. K. H. Theopold and R. G. Bergman, *Organometallics,* **1982**, 1, 1571.
41. W. Kaminsky, J. Kopf, H. Sinn and H-J. Vollmer, *Angew. Chem. Int. Ed. Engl.,* **1976**, 15, 629.
42. J. H. Merrifield, G. Y. Lin, W. A. Kiel, J. A. Gladysz, *J. Am. Chem. Soc.*, **1983**, 105, 5811.
43. N. A. Bailey, P. L. Chell, C. P. Manuel, A. Mukhopadhyay, D.Rogers, H. E. Tabbron and M. J. Winter, *J. Chem. Soc. Dalton. Trans.,* **1983**, 2397.
44. J. L. Atwood, G. K. Parker, J. Holton, W. E. Hunter, M. F. Lappert and R. Pearce, *J. Am. Chem. Soc.*, **1977**, 99, 6645.
45. J. H. Wengrovius, R. R. Schrock and C. S. Day, *Inorg. Chem.,* **1981**, 20, 1844.
46. P. A. Kibala and F. A. Cotton, *Inorg. Chem.*, **1990**, 29, 3192.
47. C. J. Burns and R. A. Anderson, *J. Am. Chem. Soc.*, **1987**, 109, 915.
48. W. Kaminsky and H. Sinn, *Adv. Organometal. Chem.*, **1980**, 18, 61.

CHAPTER 2

THE SYNTHESIS, CHARACTERIZATION AND REACTIVITY OF THE ETHYLENE-BRIDGED COMPLEX, $[CpRu(CO)_2]_2[\mu\text{-}(CH_2CH_2)]$ AND SOME RELATED Fe AND Ru COMPLEXES

2.1 INTRODUCTION

It is clear from the preceding chapter that there has been little research carried out on the reactivity of ethylene-bridged dinuclear transition metal complexes. We have, therefore, investigated the synthesis, structural characterization and reactivity of the ethylene-bridged ruthenium complex, $[CpRu(CO)_2]_2[\mu\text{-}(CH_2CH_2)]$. We have also investigated the reactivity of some related tri- and pentamethylene-bridged complexes of Fe and Ru, viz. $[CpM(CO)_2]_2[\mu\text{-}(CH_2)_n]$ (M = Fe or Ru, n = 3 or 5).

The synthesis of $[CpRu(CO)_2]_2[\mu\text{-}(CH_2CH_2)]$, **1**, was carried out using two different routes. We have characterized this complex by infrared, ^1H and ^{13}C NMR, and proton-coupled ^{13}C NMR spectroscopy, as well as mass spectrometry and elemental analysis. These data have not previously been reported.

The reactions of complex **1** with neutral donor ligands such as CO and tertiary phosphines (PPh_3 and PMe_2Ph), with oxidants (Ph_3CPF_6, and $AgBF_4$), with bromine and with protic acids (HCl and CF_3COOH) have been investigated. The characterization data and the reactivity of complex **1** has been compared with the related dinuclear ruthenium complexes[1-3], $[Cp(CO)_2Ru]_2[\mu\text{-}(CH_2)_n]$ (n = 1 or 3 - 10) as well as with the other ethylene-bridged dinuclear transition metal complexes[4-8]. The thermal decomposition of complex **1** has also been investigated.

The structure of complex **1** has been determined by X-ray crystallography and is reported in section 2.6.

We have also carried out the reactions of tri- and pentamethylene-bridged complexes of iron and ruthenium with Ph_3CPF_6. The structures of the allyl-bridged

complexes, $[\{CpM(CO)_2\}_2\{\mu\text{-}(C_3H_5)\}]^+PF_6^-$ (M = Fe or Ru) have been determined by X-ray crystallography (see section 2.7.2).

2.2 THE SYNTHESIS OF $[CpRu(CO)_2]_2[\mu\text{-}(CH_2CH_2)]$

Two different synthetic routes were used in the synthesis of complex **1**: (a) reaction of $Na[CpRu(CO)_2]$, **2**, with 1,2-dichloroethane in a 2:1 mole ratio in THF at -78°C and (b) reaction of a cationic ethylene complex, **3**, with **2** in a 1:1 mole ratio in THF at 0 °C (scheme 1). The former synthetic route proved to be more efficient as it involves fewer reaction steps. Furthermore, the yield obtained from route (a) is slightly better (43%) than the yield obtained from route (b) (30%).

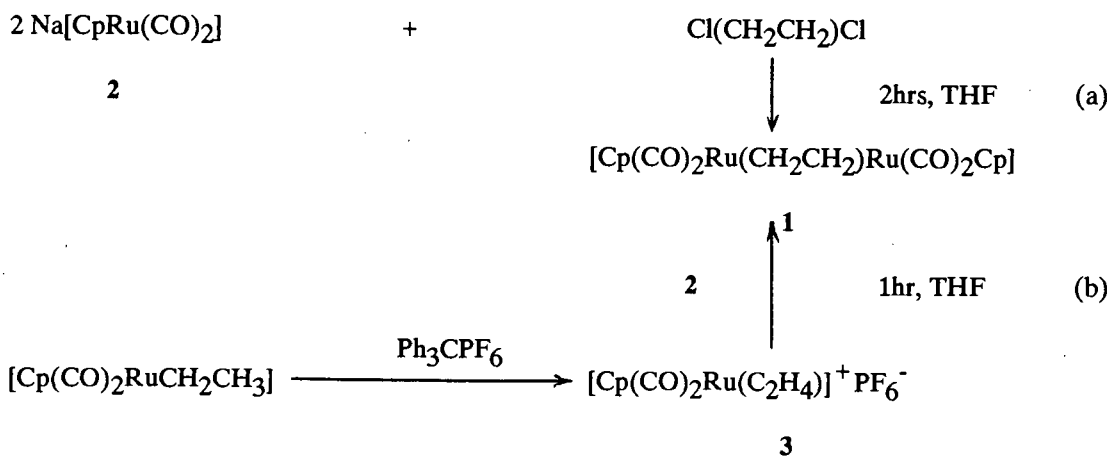

Scheme 1

Difficulty was experienced in purification of complex **1**, because of the similarity in solubility of the dimer, $[CpRu(CO)_2]_2$, and complex **1**. Complex **1** is best isolated by extraction with CH_2Cl_2/hexane (1:1) and recrystallisation from CH_2Cl_2 at -78°C (complex **1** could not be satisfactorily purified by column chromatography, due to its

instability towards the different column materials employed). Complex **1** is a pale yellow crystalline compound (m. p. 130-131 °C). Although complex **1** in its solid state is indefinitely stable under nitrogen, it could only be handled in air for a few hours. Solutions of this compound in hydrocarbon solvents decompose within a few hours in air, but exhibit higher stability in the same solutions under nitrogen (see section 2.5 for the thermal decomposition of complex **1**).

The only other product of the reaction (route (a) and route (b)) was the dimer, $[CpRu(CO)_2]_2$, which was identified by its IR spectrum in the $\nu(CO)$ region. This dimer could have been formed either from the reaction intermediate, $Cp(CO)_2RuCH_2CH_2Cl$ (in route (a)) or from the displacement of ethylene from complex **3** (in route (b)). We believe that the intermediate could undergo β-elimination to form $Cp(CO)_2RuCl$, and that a subsequent replacement of Cl^- by the anion, $[CpRu(CO)_2]^-$, could form the dimer, $[CpRu(CO)_2]_2$.

Complex **1** had previously been synthesized[3] by route (a), but no characterization data or reactivity study has since been reported.

2.3 THE CHARACTERIZATION OF $[CpRu(CO)_2]_2[\mu\text{-}(CH_2CH_2)]$

The ethylene-bridged complex was characterized by infrared, ^1H and ^{13}C NMR spectroscopy, mass spectrometry and elemental analysis.

INFRARED SPECTROSCOPY

The infrared spectrum shows two very strong ν(CO) bands at 2007 and 1953 cm^{-1} (in hexane). These bands are at lower frequencies than those observed for the polymethylene-bridged ruthenium complexes[1,2], $[CpRu(CO)_2]_2[\mu\text{-}(CH_2)_n]$ (n = 3-10), (2019 and 1959 cm^{-1} in hexane). The lowering of the frequencies in complex **1** could be due to greater backbonding in Ru-C≡O, which could be attributed to two factors: (1) increase in electron density due to two Ru centres being close to each other and (2) steric crowding on the complex weakens the Ru-CH_2 bond which consequently enhances the backbonding. Both factors are consistent with the observation that the ν(CO) bands for the polymethylene-bridged complexes, which have two Ru centers far apart and therefore have less steric crowding, appear at higher ν values.

It is interesting to note that the ν(CO) bands of complex **1** are at the same positions as observed in polymethylene-bridged iron complexes[9], $[CpFe(CO)_2]_2[\mu\text{-}(CH_2)_n]$ (n = 3 - 7). It may suggest that the Ru-C (Ru-C≡O) bonds in complex **1** are weaker than the Fe-C (Fe-C≡O) bonds in the aforementioned Fe complexes. This is surprising, but probably true due to steric strain in complex **1**.

^{1}H NMR SPECTROSCOPY

In the ^{1}H NMR spectrum of complex **1** we observe a single resonance at δ = 2.28 ppm for the ethylene protons and another single resonance at δ = 5.22 ppm for the Cp protons (Table 1). The multiplicity of the resonance at 2.28 ppm, remained as singlet even at -60°C. This suggests that rotation about the C-C bond is not restricted down to this temperature.

No significant variations in the Cp proton resonances of complex **1** were observed when compared with methylene and polymethylene-bridged complexes, $[CpRu(CO)_2]_2[\mu\text{-}(CH_2)_n]$ (n = 1 or 3 - 10). However, the resonances of the α-proton ($Ru\text{-}CH_2$) appear at higher field for n>2.

Furthermore, some variations were observed for the α-proton resonances (or ethylene protons) of complex **1** when compared with some analogous ethylene-bridged complexes (Table 2). It is clear from the Table 2 that the ethylene protons of compound **16** resonate upfield at δ = 1.00 ppm (in C_6D_6), while the protons of complex **1** resonate relatively downfield at δ = 2.51 ppm (in C_6D_6). The deshielding of the ethylene protons of complex **1** could be explained in two ways. Firstly, the "$CpRu(CO)_2$" unit could be a stronger electron-withdrawing group than the "$Cp_2Zr(\mu\text{-}Cl)AlEt_3$" unit. Secondly, the "ethylene" could become 'more aliphatic' as the backbonding from the metal increases; this backbonding is rather pronounced in complex **16**.

TABLE 1 **^{1}H NMR data[a] for the complexes $[CpRu(CO)_2]_2[\mu\text{-}(CH_2)_n]$ (n = 1 - 10)**

COMPOUND NO.	n	C_5H_5	$Ru\text{-}CH_2$ (α)	$Ru\text{-}CH_2\text{-}CH_2$ (β)	$\text{-}CH_2\text{-}$
4[b]	1	4.80(10H, s)	2.30(2H, s)		
1	2	5.22(10H, s)	2.28(4H, s)		
5[c]	3	5.30(10H, s)	1.72(6H, br)[d]		
6	4	5.23(10H, s)	1.68(4H, m)	1.55(4H, m)	
7	5	5.22(10H, s)	1.66(4H, m)	1.53(4H, m)	1.28(2H, m)
8	6	5.22(10H, s)	1.67(4H, m)	1.53(4H, m)	1.28(4H, bs)
9	7	5.23(10H, s)	1.67(4H, m)	1.53(4H, m)	1.27(6H, bs)
10	8	5.22(10H, s)	1.67(4H, m)	1.53(4H, m)	1.27(8H, bs)
11	9	5.22(10H, s)	1.67(4H, m)	1.54(4H, m)	1.27(10H, bs)
12	10	5.23(10H, s)	1.67(4H, m)	1.53(4H, m)	1.26(12H, bs)

[a] measured in $CDCl_3$ (or otherwise stated) relative to TMS (δ = 0.00 ppm); [b] spectrum recorded in C_6D_6;

[c] references 1 and 2 for the complexes **5-12**; [d] a broad multiplet was observed for six protons

TABLE 2 **^{1}H NMR data for some of the ethylene-bridged complexes [LmM]$_2$[μ-(CH_2CH_2)]**

COMPD. NO.	LmM	-CH_2CH_2- (ppm)
1	**[CpRu(CO)$_2$]**	**2.51(4H, s)[a]**
13[b]	[Cp(CO)$_2$W(PPh_3)]	2.56(4H, br s)[b]
14[b]	[Re(CO)$_5$]	2.02(4H, s)[b]
15[c]	[Os(CO)$_4$]	1.51(4H, s)[a]
16[d]	[$Cp_2Zr(\mu$-Cl)$AlEt_3$]	1.00(4H, s)[a]
17[d]	[$Cp_2\dot{Z}rCl$]	1.40(4H, m)

[a] measured in C_6D_6; [b] measured in CD_2Cl_2.

[b] reference 5; [c] reference 6; [d] reference 7

^{13}C NMR SPECTROSCOPY

In the ^{13}C NMR spectrum of complex **1** we observe a resonance at δ = 203.25 ppm for the terminal carbonyl ligands, a single sharp resonance at δ = 89.46 ppm for the Cp carbons, and another sharp resonance at δ = 13.13 ppm for the ethylene carbons (Table 3).

From the comparison of the ^{13}C NMR spectroscopic data of complex **1** and the related complexes $[CpRu(CO)_2]_2[\mu\text{-}(CH_2)_n]$ (n = 1 or 3 - 10) (Table 3) we observe that the resonances of Cp carbons and the carbonyl carbon appear in the regions 202-204 ppm and 88-90 ppm respectively, i.e. increase in carbon chain length has no effect on the Cp and CO resonances. However, there appear to be interesting variations in the α-carbon resonances of these complexes, i.e the α-carbon resonance increases from the complex where n = 1 (-37.42 ppm in C_6D_6) to complex where n = 2 (13.13 ppm in $CDCl_3$) then it decreases to complex where n = 3 (0.9 ppm in $CDCl_3$) and decreases further to about -3.3 ppm (in $CDCl_3$) for complexes where n = 4-10 (see Table 3). This suggests that the electronic enviroment of the α-carbon is changing dramatically from n = 1 to 4. This variation is illustrated in the plot of α-carbon resonance versus the carbon number (see Fig. 1).

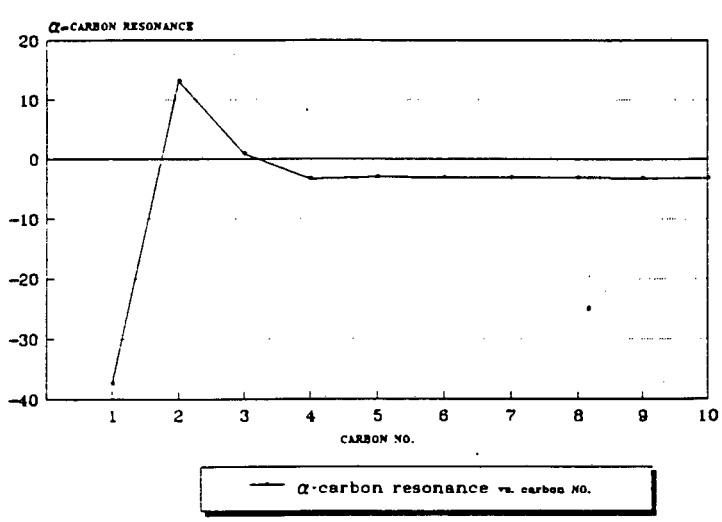

Fig. 1 The plot of α-carbon resonance versus carbon number

TABLE 3 ^{13}C NMR data[a] for the complexes $[CpRu(CO)_2]_2[\mu\text{-}(CH_2)_n]$ (n = 1 - 10)

COMPD NO.	n	CO	C_5H_5	α-CH_2	β-CH_2	γ-CH_2	δ-CH_2	ϵ-CH_2
4[b]	1	203.50	90.41	-37.42				
1	2	203.25	89.46	13.13				
5[c]	3	201.60	87.50	0.90	50.10			
6	4	202.54	88.56	-3.30	45.18			
7	5	202.52	88.54	-2.99	39.65	40.08		
8	6	202.52	88.56	-3.15	34.42	39.86		
9	7	202.52	88.55	-3.12	34.93	39.88	29.05	
10	8	202.50	88.54	-3.16	34.88	39.84	29.44	
11	9	202.50	88.54	-3.18	34.85	39.85	29.38	29.83
12	10	202.50	88.54	-3.18	34.87	39.85	29.37	29.79

[a] measured in $CDCl_3$ relative to TMS (δ = 0.00 ppm)

[b] measured in C_6D_6

[c] references 1 and 2 for complexes **5-12**

A proton-coupled ^{13}C NMR spectrum of complex **1** was also obtained in order to investigate a possible agostic interaction of the type C-H→M. In the spectrum we observe a triplet of triplets at δ = 12.48 ppm ($J(^{13}C,H)$ = 139.4 Hz, $J(^{13}C,CH)$ = 6.1 Hz) for the α-carbon (Table 4). The triplet of triplets arises from the coupling of α-carbon (Ru-CH_2) to its bonded protons, as well as to protons bonded to its adjacent carbon atom (a long range carbon-hydrogen coupling between nuclei separated by two bonds) (Fig. 2). Additional fine structure in the peaks we believe is due to a second order effect (see later).

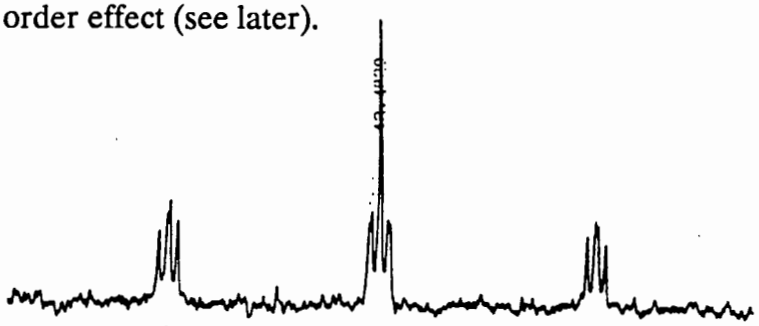

Fig. 2 Resonance for the α-carbon

Another resonance appears as a doublet of quintets at δ = 88.80 ppm ($J(H^{13}C)$ = 177.65 Hz, $J(HC\text{-}C^{13}C)$ = 6.83 Hz) for Cp carbons. This doublet of quintets, we have assigned to the coupling of each Cp carbon to its bonded proton, as well as to the remaining protons on the Cp ligand (Fig. 3).

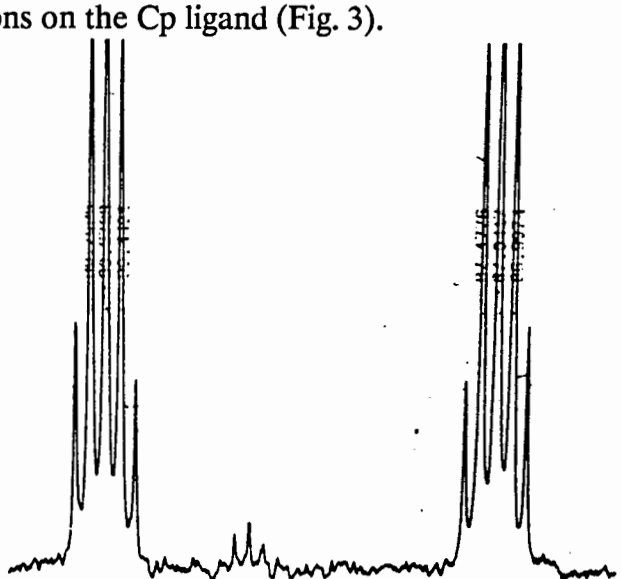

Fig. 3 Resonance for the C_5H_5 carbon.

TABLE 4 **$J(^{13}C\text{-}H)$ data for the complexes $[LmM]_2[\mu\text{-}(CH_2)_n]$ (n = 2, 4 or 5)**

COMPD. NO.	n	LmM	C_5H_5[a]	Ru-C-H[b]	$Ru^{13}CC\text{-}H$[c]	Additional splitting
				(Hz)		
1	**2**	**$[CpRu(CO)_2]$**	**177.7(d)**	**139.4**	**6.1**	**1.7**
			6.8(q)			
14[d]	2	$[Re(CO)_5]$	-	133.3	6.4	-
6[e]	4	$[CpRu(CO)_2]$	177.8(d)	133.8	-	-
			6.8(q)			
7[e]	5	$[CpRu(CO)_2]$	177.9(d)	134.6	-	-
			6.8(q)			

[a] signal occurs as a doublet of quintets; values represent the coupling constants of the doublet (d) and quintet (q) respectively.

[b] signal occurs as a triplet.

[c] signal occurs as a triplet of triplets

[d] reference 5

[e] reference 2

The value of $J(^{13}CH)$ for the C-H bond of the ethylene group of complex **1** lies marginally higher than those characteristic values of normal saturated sp^3 C-H bonds, thus indicating the absence of a possible agostic interaction.

Comparison of this proton-coupled ^{13}C NMR spectral data of complex **1** with the similar data reported[5] for the ethylene-bridged rhenium complex, $[(CO)_5Re]_2[\mu\text{-}(CH_2CH_2)]$ (J(C,H) = 133.3 Hz and J(C,CH) = 6.4 Hz), reveals that the values of J(C,H) for the M-C-H bond obtained for both complexes are in fairly good agreement (Table 4). However, only a triplet of triplets was reported for the rhenium complex, whereas a further splitting (1.7 Hz) of the resonance at 12.48 ppm was observed in the spectrum of complex **1**. We suggest that the further splitting could be due to the phenomenon called, 'indirect electron-coupled nuclear spin-spin splitting'. This occurs because of mutual interaction between different magnetic nuclei (^1H and ^{13}C) within the same molecule[10].

Furthermore, the coupling constant values J(C,H) for the Ru-C-H (triplet of triplets) and Cp carbon (doublet of quintets) of the complexes[2] $[CpRu(CO)_2]_2[\mu\text{-}(CH_2)_n]$ (**12**, n = 4 and **13**, n = 5) and complex **1** are also in good agreement.

MASS SPECTROMETRY

We have obtained a low resolution mass spectrum of complex **1**. This complex exhibit a molecular ion of low intensity at m/e 472 (Fig. 4). The isotopic pattern due to ruthenium (due to six of its most abundant isotopes) was also observed in the spectrum. Probable fragmentation patterns are described in comparison with similar patterns reported for the related ruthenium complexes[2], $[CpRu(CO)_2]_2[\mu\text{-}$

$(CH_2)_n]$ (n = 5 - 10) (see Fig.5 for the possible fragmentation patterns). The intensities and probable assignments of the peaks in the spectrum of complex **1** are presented in Table 5. However, it must be borne in mind that the assignments of these fragmentation patterns are ambiguous, since no high resolution mass spectrometry was employed to distinguish between losses of CO and C_2H_4.

Furthermore, the fragmentation patterns in the spectrum also account for the presence of ruthenium dimer, $[CpRu(CO)_2]_2$, (this dimer could have been formed from the decomposition of complex **1** by elimination of ethylene). Similar fragmentation patterns (due to dimer) were also observed for the mononuclear complexes $[CpRu(CO)_2CH_2CH_3]$ (See section 3.2.1) and $[CpRu(CO)_2CH_2CH_2OCH_3]$ (See section 2.4.2).

Many pathways for the fragmentation of complex **1** are possible. However, we suggest three significant pathways (**A - C**). These are illustrated in figure 5.

The molecular ion, $[Cp_2Ru_2(CO)_4(C_2H_4)]^+$, in the pathway, **A**, could lose ethylene to form $[Cp_2Ru_2(CO)_4]^+$ (m/e 444). A successive loss of CO from this daughter ion could lead to the formation of $[Cp_2Ru_2(CO)_3]^+$ (m/e 416), $[Cp_2Ru_2(CO)_2]^+$ (m/e 388), $[Cp_2Ru_2(CO)]^+$ (m/e 360) and $[Cp_2Ru_2]^+$ (332), all of which peaks are of low intensities. The daughter ion, $[Cp_2Ru_2(CO)_4]^+$ (m/e 444), could also lose $[CpRu]^+$ to form $[CpRu(CO)_4]^+$ (m/e 278), and subsequent loss of carbonyl groups could lead to the formation of $[CpRu(CO)_3]^+$ (m/e 250) (most abundant ion), $[CpRu(CO)_2]^+$ (m/e 223), $[CpRu(CO)]^+$ (m/e 195) and $[CpRu]^+$ (m/e 167) respectively. This route does not account for the presence of the ion of mass, m/e 306.

In another pathway, **B**, loss of CO, instead of ethylene, from the molecular ion could lead to the formation of a daughter ion $[Cp_2Ru_2(CO)_3(C_2H_4)]^+$ (m/e 444). Successive loss of CO from this ion could then lead to the formation of $[Cp_2Ru_2(CO)_2(C_2H_4)]^+$ (m/e 416), $[Cp_2Ru_2(CO)(C_2H_4)]^+$ (m/e 388) and $[Cp_2Ru_2(C_2H_4)]^+$ (m/e 360) respectively. The ethylene is subsequently eliminated to form $[Cp_2Ru_2]^+$ (m/e 332).

The molecular ion, $[Cp_2Ru_2(CO)_4(C_2H_4)]^+$, in pathway, **C**, could lose $[CpRu]^+$ to form $[Ru(CO)_4(C_7H_9)]^+$ (m/e 306), and subsequent losses of CO from this could result in the formation of $[Ru(CO)_3(C_7H_9)]^+$ (m/e 278), $[Ru(CO)_2(C_7H_9)]^+$ (m/e 250) (most abundant ion in the mass spectrum), $[Ru(CO)(C_7H_9)]^+$ (m/e 223) and $[Ru(C_7H_9)]^+$ (m/e 195) respectively.

The combined routes (**A** and **C**) account for all the ions observed. It is interesting to note that while $[CpRu(CO)_3]^+$ (m/e 250) is the most abundant ion in the spectrum of complex **1**, the most abundant ions in the spectra of $[CpRu(CO)_2]_2[\mu\text{-}(CH_2)_n]$ (n = 5 - 10) and ruthenium dimer[11], $[CpRu(CO)_2]_2$, are $[CpRu]^+$ (m/e 167) and $[Cp_2Ru_2]^+$ (m/e 334) respectively.

High resolution mass spectral data would enable definite assignments of the ions to be made and also to distinguish between fragmentation pathways **A** , **B** and **C**.

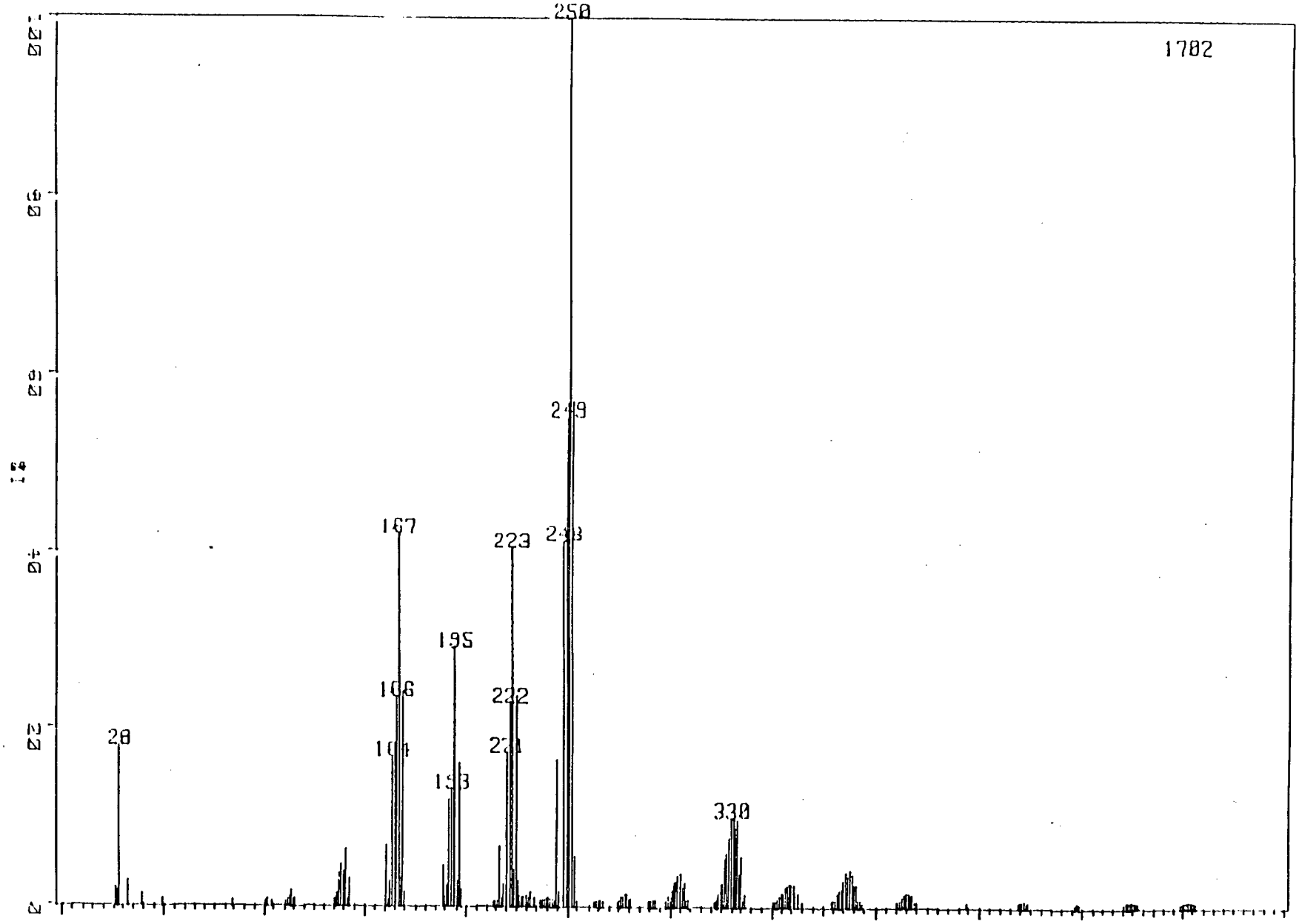

Fig. 4 Mass spectrum of the ethylene-bridged complex, $[CpRu(CO)_2]_2[\mu\text{-}(CH_2CH_2)]$

Table 5 **Mass spectral data for the complex 1, $[CpRu(CO)_2]_2[\mu\text{-}(CH_2CH_2)]$**

ION[a]	(m/e)[b]	RELATIVE PEAK INTENSITY (%)[c]
$[M^d]^+$	472	4
$[M - CO]^+$ or $[M - (C_2H_4)]^+$	444	3
$[M - \{2CO\}]^+$ or $[M - \{CO + C_2H_4\}]^+$	416	6
$[M - \{3CO\}]^+$ or $[M - \{2CO + C_2H_4\}]^+$	388	9
$[M - \{4CO\}]^+$ or $[M - \{3CO + C_2H_4\}]^+$	360	7
$[M - \{4CO + C_2H_4\}$	332	14
$[CpRu(CO)_4(C_7H_9)]^+$	306	7
$[Ru(CO)_3(C_7H_9)]^+$ or $[CpRu(CO)_4]^+$	278	6
$[Ru(CO)_2(C_7H_9)]^+$ or $[CpRu(CO)_3]^+$	250	100
$[Ru(CO)(C_7H_9)]^+$ or $[CpRu(CO)_2]^+$	223	23
$[Ru(C_7H_9)]^+$ or $[CpRu(CO)]^+$	195	16
$[CpRu]^+$	167	24

[a] ion refers to probable assignment, [b] a maximum in envelope of peaks, [c] peak intensities are relative to the base peak m/e 250, and

[d] $M = Cp_2Ru_2(CO)_4C_2H_4$

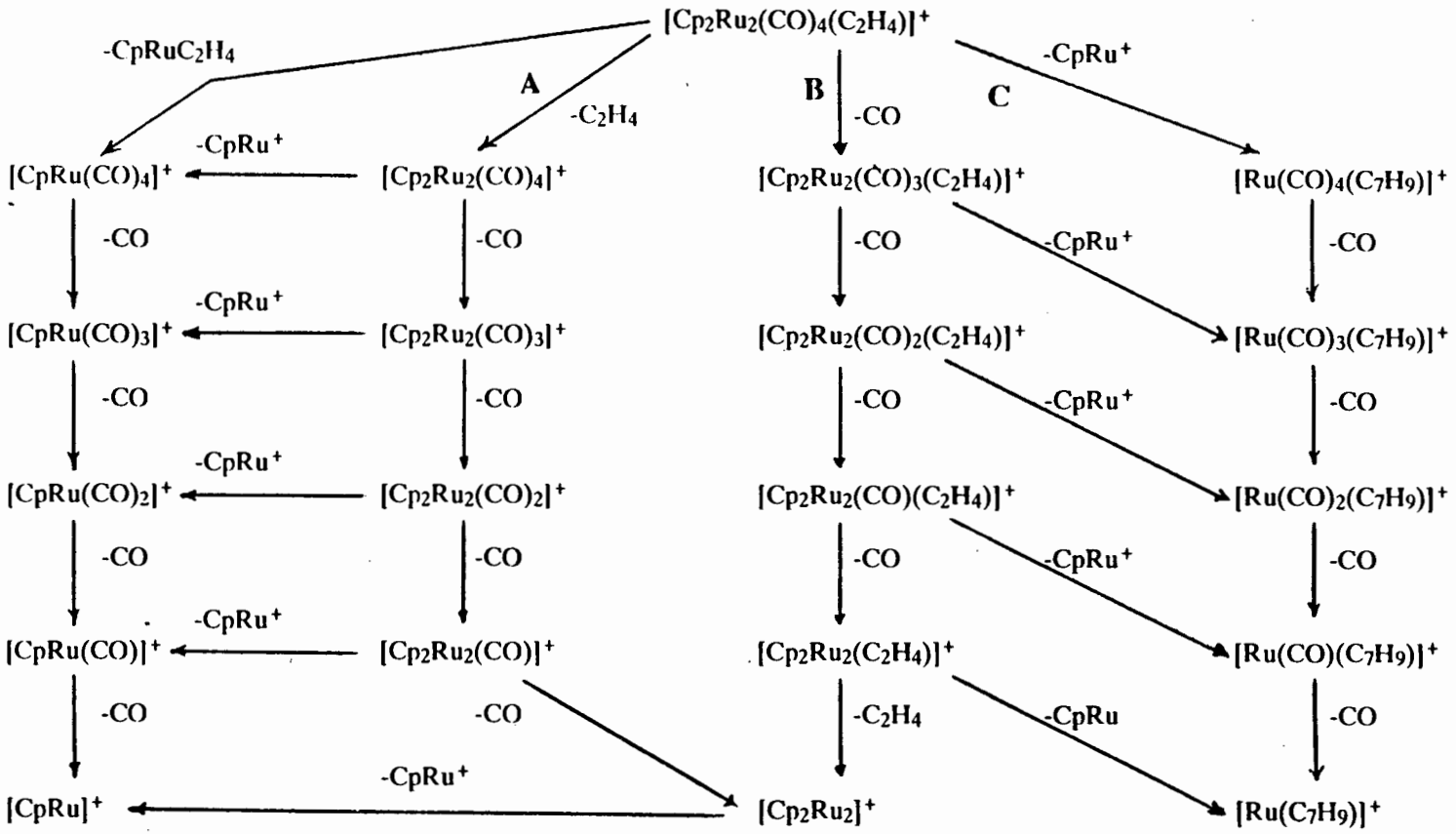

Fig. 5 Fragmentation scheme for the complex **1**, $[CpRu(CO)_2]_2[\mu\text{-}(CH_2CH_2)]$

The molecular ion peak in the mass spectrum of complex **1** further confirms the structure of the ethylene-bridged complex, $[CpRu(CO)_2]_2[\mu\text{-}(CH_2CH_2)]$. In addition, the fragmentation pattern in the spectrum also suggests that the complex **1** could have decomposed by elimination of ethylene to form a dimer, $[CpRu(CO)_2]_2$. Furthermore, many of the peaks observed in the spectrum are common in the spectra reported for the related mono-, $[CpRu(CO)_2(CH_2)_nH]$, (n = 6 - 12), and the dinuclear complexes[11,12], $[CpRu(CO)_2]_2[\mu\text{-}(CH_2)_n]$ (n = 5 - 10).

MELTING POINT

Complex **1** has a sharp melting range of 130 - 131°C. The melting point is surprisingly high, but may be expected, since the trend observed for the related iron[9] and ruthenium[2] complexes $[CpM(CO)_2]_2[\mu\text{-}(CH_2)_n]$ (M = Fe, n = 3 - 10; M = Ru, n = 3 - 10), shows that the melting point of the complexes increase with decrease in chain length (Table 6). A qualitative plot of melting point versus n (the number of carbons in the methylene or polymethylene bridge) for the complexes, $[CpRu(CO)_2]_n[\mu\text{-}(CH_2)_n]$ (n = 2 - 10), was obtained (Fig. 6a). Two other plots were obtained for the melting point against n where n = even or n = odd (Fig. 6b).

TABLE 6 **Melting point of the polymethylene bridged complexes, $[CpRu(CO)_2]_2[\mu\text{-}(CH_2)_n]$ (n = 2 - 10)**

COMPOUND NO.	n	MELTING POINT RANGE (°C)
1	2	130 - 131
5[a]	3	84 - 87
6	4	130 -132
7	5	77 - 84
8	6	106 - 109
9	7	65 - 70
10	8	73 - 77
11	9	37 - 43
12	10	45 - 51

[a] references 1 and 2 for complexes **5-12**

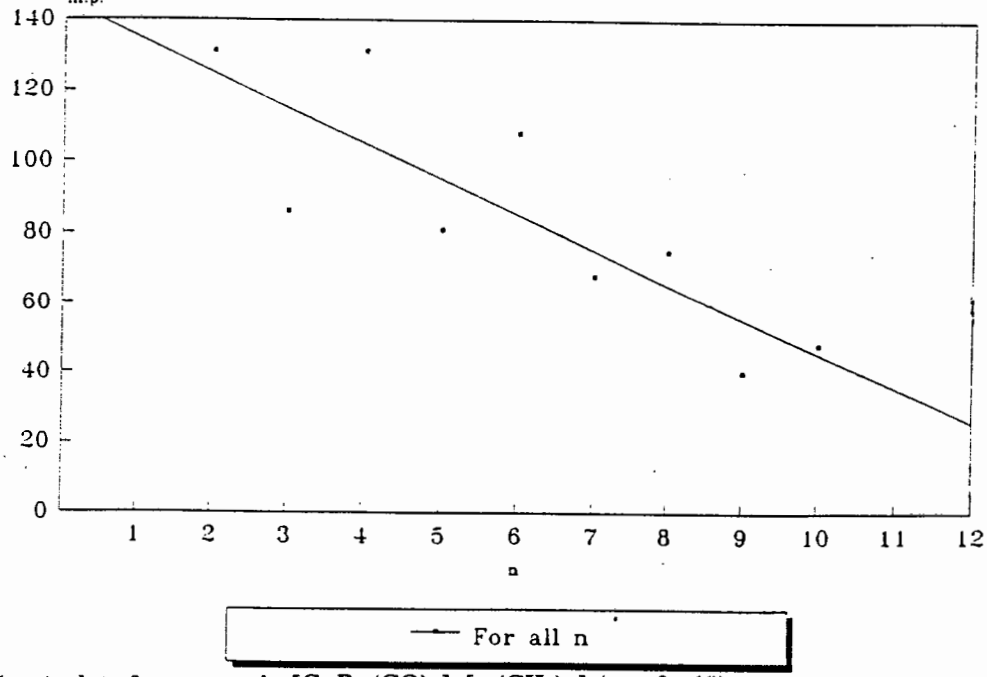

Fig. 6a A plot of m.p. vs. n in $[CpRu(CO)_2]_2[\mu\text{-}(CH_2)_n]$ (n = 2 - 10).

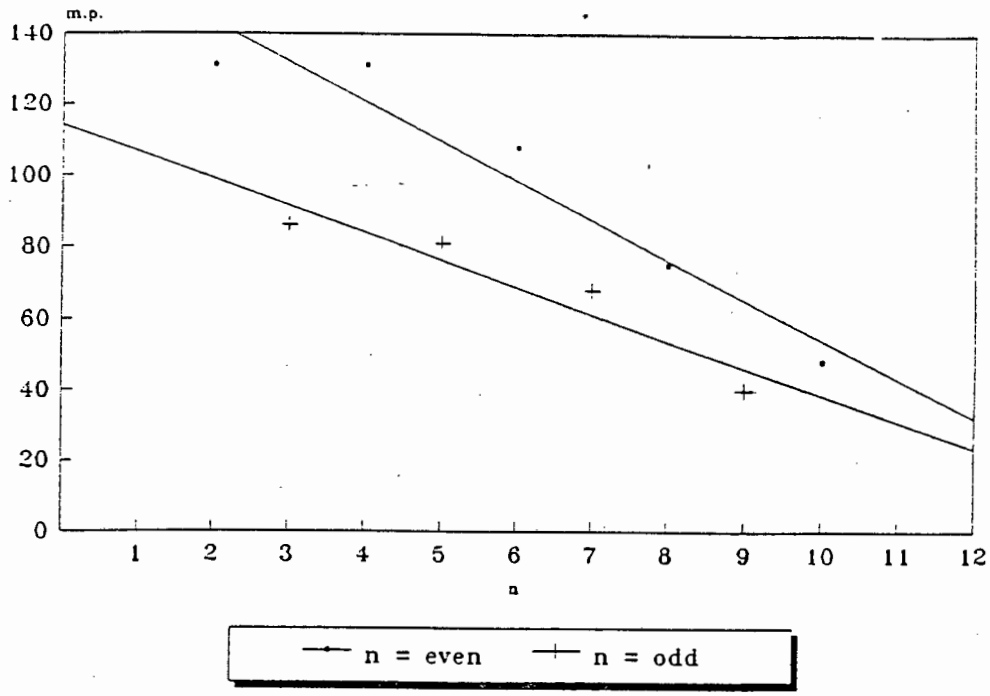

Fig. 6b The plots of m.p. vs. n in $[CpRu(CO)_2]_2[\mu\text{-}(CH_2)_n]$ (where n = odd or n = even).

From the above plot (Fig. 6a) it is clear that the melting points of these complexes decreases as chain length increases. This indicates that the complexes with larger n (longer alkyl chain) have a structure with lower packing density in the crystal than complexes with smaller n, hence we expect the lattice energy for the former to be lower. Complex **1** is, therefore, expected to have a greater lattice energy relative to those related polymethylene-bridged ruthenium complexes and consequently a higher melting point (see Section 2.6 for the crystal structure data).

The plots (Fig. 6b) also shows that the complexes with n = even number have generally higher melting points than those with n = odd numbers, as it was observed for the iron complexes[9b]. The smooth variation in m.p. in the two series, n = even and n = odd, suggest that the compounds in each series are of the same structural type. Furthermore, complexes **1** and **12** melt at the same temperature; an anomaly which can be attributed to a similarity in the packing density in the crystal.

2.4 THE REACTIVITY OF $[CpRu(CO)_2]_2[\mu\text{-}(CH_2CH_2)]$

2.4.1 THE REACTION OF $[CpRu(CO)_2]_2[\mu\text{-}(CH_2CH_2)]$ WITH CO

The carbonyl insertion or alkyl migration reaction, has been known for over 30 years. This reaction was first discovered by Coffield[13] and workers in 1957. Since then this reaction has gained momentum in both chemical and catalysis fields.

This migratory CO insertion reaction is a key step in several catalytic transformations. In hydroformylation reactions, for example, an olefin is converted to an aldehyde, whereas the carbonylation of methanol forms acetic acid, etc[14]. Both these reactions involve a migratory CO insertion step.

Dinuclear μ (α,ω)-alkanediyl complexes[15,16] of the type $[L(CO)_2Fe]_2[\mu\text{-}(CH_2)_n]$ (L = C_5H_5 n = 3, 4 ; L = C_5Me_5 n = 4) have been shown to undergo similar reactions with CO to yield the diacyl insertion products, $[L(CO)_2Fe]_2[\mu\text{-}\{C(O)(CH_2)_nC(O)\}]$. The CO insertion reactions of the analogous ruthenium complexes have not yet been reported, however, carbonylation of a methylene-bridged complex, $[CpRu(CO)_2]_2[\mu\text{-}(CH_2)]$, has been reported by Lin[3] et al. This carbonylation reaction occurs readily at 3 atm and at room temperature to give a monoacyl complex, $[CpRu(CO)_2]_2[\mu\text{-}\{C(O)(CH_2)\}]$.

We have carried out a similar reaction of complex **1** in THF at 30 atm and 50 atm of CO and at room temperature, but no indication of any carbonylation product was observed.

The above reaction as well as the reaction decribed in section 2.4.3, suggest that either the CO insertion in the Ru-C bond of complex **1** is rather difficult, or that the rate of decarbonylation is faster than the rate of carbonylation.

2.4.2 REACTION OF $[CpRu(CO)_2]_2[\mu\text{-}(CH_2CH_2)]$ WITH MeOH

The reaction of complex **1** with CO, as described in section 2.4.1, was repeated using MeOH instead of THF. This reaction led to the formation of an unusual methoxyethyl complex, $[CpRu(CO)_2CH_2CH_2OCH_3]$, **18**, and the dimer, $[CpRu(CO)_2]_2$. Complex **18** and the dimer are formed even in the absence of CO, i.e. when complex **1** in MeOH was heated under reflux for five hours. Complex **18** is an orange oil at room temperature. This complex was characterized by infrared, ^1H NMR, ^{13}C NMR spectroscopy (Table 7) and mass spectrometry (Table 8). The characterization data obtained for an authentic methoxyethyl complex **18**, prepared from the reaction of $Na[CpRu(CO)_2]$ with $ClCH_2CH_2OMe$, is in good agreement with the data obtained in the previous reaction.

Lin[3] and co-workers have also reported a similar reaction for the related complex, $[CpRu(CO)_2]_2[\mu\text{-}(CH_2)]$. They found that the complex reacts with CO in methanol at room temperature, affording methyl acetate and the dimer, $[CpRu(CO)_2]_2$. In the absence of CO, methyl acetate was still formed, but the complex $[CpRu(CO)]_2[\mu\text{-}(CH_2)(\mu\text{-}CO)]$ was produced as a byproduct.

TABLE 7 IR,^{1}H NMR and ^{13}C NMR data for some of the methoxy complexes

COMPOUND	Infrared (cm^{-1})	1H-NMR[a]	^{13}C-NMR[a]
$[CpRu(CO)_2CH_2OCH_3]$[b]	2026s[c]	5.31(C_5H_5, 5H, s)	
	2017vs	4.97($C\underline{H}_2OCH_3$ 2H, s)	
	1965s	3.23(CH_3, 3H, s)	
	1956vs		
$[CpRu(CO)_2CH_2CH_2OCH_3]$	2015s[d]	5.25(C_5H_5, 5H, s)	88.05(C_5H_5)
	1952s	3.44($C\underline{H}_2OCH_3$, 2H, m)	79.84($\underline{C}H_2OCH_3$)
	2021s[c]	3.33(CH_3, 3H, s)	57.47(CH_3)
	2017s	1.74($Ru\text{-}CH_2$, 2H, m)	-6.49($Ru\text{-}CH_2$)
	1962s		
	1958s,sh		
$[IrBr_2(CH_2CH_2OCH_3)(CO)L_2]$[e]	2028[f]	2.96(CH_3, 3H, s)	
(L = $P(CH_3)_2Ph$)		2.26(CH_3-P, 3, t)	
		2.09(CH_3-P, 3, t)	
		2.85($C\underline{H}_2OCH_3$, 2H, m)	
		1.60($Ir\text{-}CH_2$, 2H, m)	

[a] in $CDCl_3$, [b] reference 19 [c] in cyclohexane, [d] in CH_2Cl_2 [e] reference 21, [f] in Nujol

In the infrared spectrum (in cyclohexane) of complex **18** we observe four ν(CO) bands. This fact could be attributed to the existence of two rotamers (Fig. 7). We envisaged that the rotation about Ru-C bond is responsible for the existence of two rotamers.

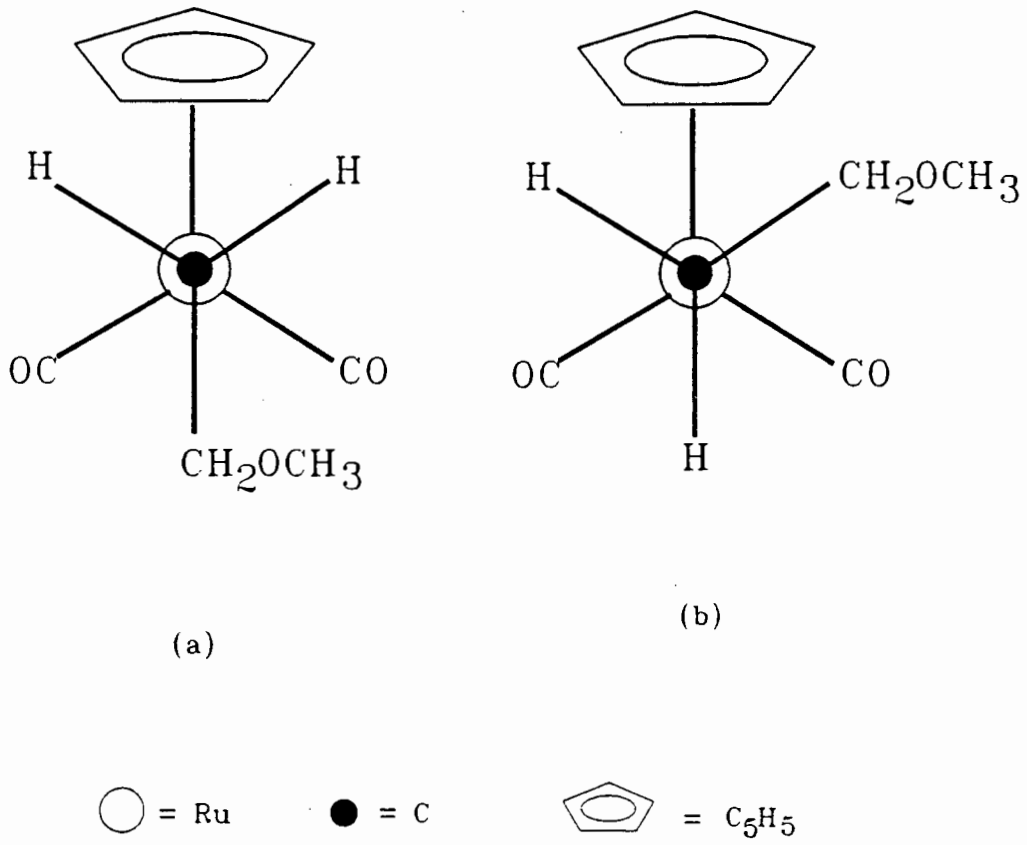

Fig. 7 Possible rotamers of [CpRu(CO)$_2$CH$_2$CH$_2$OCH$_3$]

Rotational isomerism in complexes of the type [CpFe(CO)$_2$(L)R] (L = CO, or a tertiary phosphine, R = ligands) was first reported by Jetz and Graham[17]. It was found that the infrared spectrum for the complex [CpFe(CO)$_2$SiCl$_2$CH$_3$] shows four,

instead of the expected two, ν(CO) bands; a fact which was attributed to the existence of two rotamers (Fig. 8).

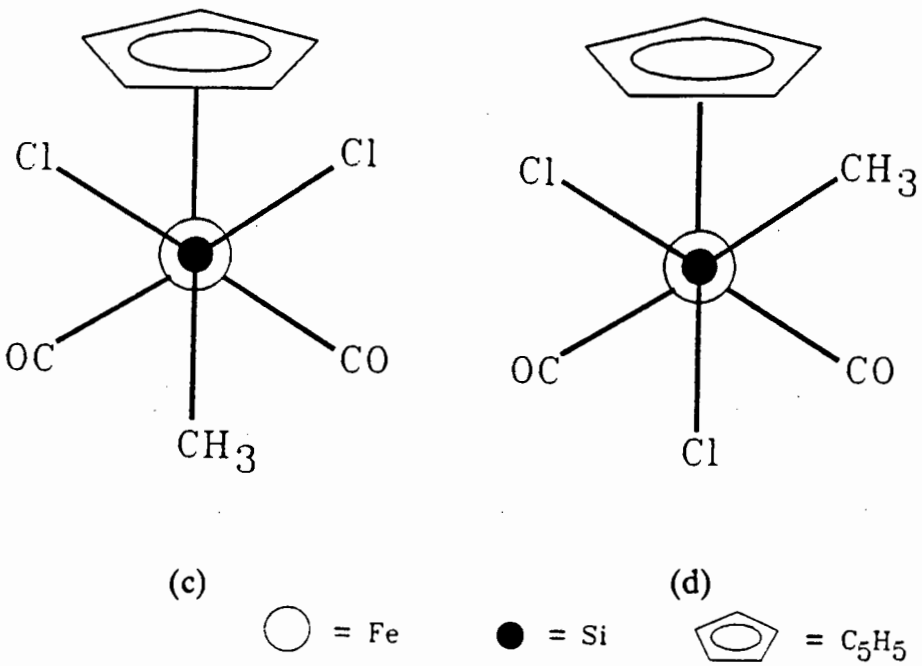

Fig. 8 The rotamers of $[CpFe(CO)_2SiCl_2CH_3]$

These authors expected the rotamer (a) to be the more stable due to steric factors. Although they observed four ν(CO) bands in the infrared spectrum, only one set of ^1H NMR resonances was found. This indicated that the rotation about the Fe - C bond is too rapid to be seen on the NMR time scale.[17] Stanley and Baird[18] have extended this work further by investigating the rotational isomerism of several complexes of the type [CpFe(CO)(L)R] (L = CO or a tertiary phosphine, R = Br, I, CH_3, CH_2Ph, CH_2CH_2Ph, CH_2SiMe_3 or CH_2Naph (Naph = naphthyl)). They have postulated that the presence of four ν(CO) bands in the IR spectra of complexes $[CpFe(CO)_2R]$ (R = CH_2Ph, CH_2SiMe_3, CH_2Naph) was due to the existence of rotational isomers in the complexes. The rotational isomers of the related complex, $[CpRu(CO)_2(CH_2OCH_3)]$ were also reported[19].

In the infrared spectrum (in CH_2Cl_2) of complex **18**, however, we observe two strong ν(CO) bands instead of four (as observed in the IR spectrum recorded in cyclohexane). This may be due to two possible factors. Firstly, broadening of the ν(CO) bands in the more polar solvent may occur and result in overlapping of the bands. Stanley and Baird[18] have also observed the broadening of IR bands of the complexes [CpFe(CO)(L)R] (L = tertiary phosphine, R = CH_2Ph, CH_2SiMe or CH_2Naph). Secondly, the conformations adopted by the complex $[CpRu(CO)_2CH_2CH_2OCH_3]$, could be governed by steric and electrostatic factors, i.e. in a polar solvent (CH_2Cl_2) both steric and dipolar effects may favour one conformation while in a non-polar solvent the other conformation may be favoured. Davies et al.[20] have shown the solvent dependence of conformer populations in the complex $[CpFe(CO)(PPh_3)(CH_2OMe)]$.

In the ^1H NMR spectrum of complex **18** we observe four resonances. Two of them appear as singlets at δ = 5.25 and at δ = 3.3 ppm for the Cp and methyl protons respectively. The other two sets of resonances appear as identical multiplets (Figures 9a and 9b) at δ = 1.77 and at δ = 3.44 ppm for the α (Ru-CH_2) and β-protons (Ru-CH_2-CH_2) respectively (Table 7).

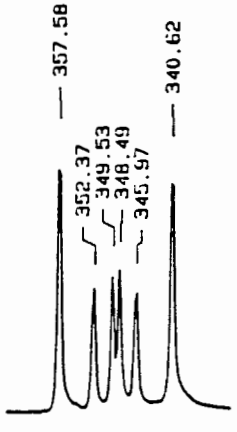

Fig. 9a Resonance for the α-protons (Ru-CH_2).

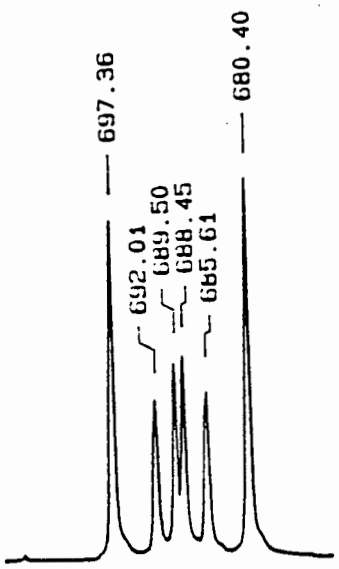

Fig. 9b Resonance for the β-protons (Ru-CH_2-CH_2).

By examining the multiplicity of these peaks (Figures 7a and b) it is clear that the -CH_2CH_2- group exhibits peaks which are an approximation to an AA′XX′ spin system. A similar spin system was observed by Beck[8] and co-workers for a related ruthenium complex, i.e. [$CpRu(CO)_2\{CH_2CH_2\}Re(CO)_5$].

Deeming and Shaw[21] also isolated a similar methoxyethyl complex, [$IrBr_2(CH_2CH_2OCH_3)(CO)(PMe_2Ph)_2$]. Based on our assignments of -CH_2CH_2- protons of complex **18**, we have assigned the resonances due to -CH_2CH_2- protons of the Ir complex which we believe were incorrectly assigned previously (Table 7).

The ^{13}C NMR proton-decoupled spectrum of complex **18** consists of four single resonances which were assigned to the appropriate carbons as shown in Table 8. The α-carbon resonance which appears at high field (-6.49 ppm) is characteristic of a carbon atom bonded to ruthenium[2,12]. Similarly, the assignments of the methyl

Table 8 Mass spectral data for the complex , [CpRu(CO)$_2$(CH$_2$CH$_2$OMe)]

ION[a]	(m/e)	RELATIVE PEAK INTENSITY (%)[b]
$[M^c]^+$	281	9
$[M - \{CO\}]^{+d}$	251	100
$[CpRu(C_2H_4OMe)]^+$	222	17
$[CpRu(C_2H_4)]^+$	194	15
$[CpRu]^+$	167	21
$[C_3H_3Ru]^+$	141	10

[a] ion refers to probable assignment, [b] peak intensities are relative to the base peak m/e 251

[c] M = $CpRu(CO)_2C_2H_4OMe$

[d] a maximum in envelope of peaks,

carbon (OCH_3) and the β-carbon (Ru-C-CH_2) were based on the ^{13}C NMR data of 1,2-dimethoxyethane[22].

We have also obtained a low resolution mass spectrum of complex **18**. In the spectrum we observe a molecular ion peak at m/e 281 corresponding to $[CpRu(CO)_2CH_2CH_2OCH_3]$. The isotope pattern due to ruthenium (arising from six of its most abundant isotopes) were also observed in the spectrum. The intensities and probable assignments of the peaks, which are ambiguous as no high resolution mass spectrometry was employed to distinguish between CO and C_2H_4, are presented in Table 8.

The mass spectral data further confirms the structure of complex **18**. An envelope of peaks at m/e 251 could be attributed to the formation of an ion due to the loss of either the CO or ethylene group (the ethylene could have been lost by β-elimination to form a methoxy complex, $[CpRu(CO)_2OCH_3]$). The remaining fragmentation patterns are characteristic of ruthenium cyclopentadienyl dicarbonyl complexes, which also account for the fragmentation pattern of ruthenium dimer, $[CpRu(CO)_2]_2$.

The suggested mechanism for the above reaction (complex **1** with MeOH) is described in scheme 2. We envisage that an attack by MeOH on the slightly electrophilic α-carbon, $Ru^{\delta-}$-$C^{\delta+}$, of complex **1** leads to the formation the methoxyethyl complex **18** and the hydride, $[CpRu(CO)_2H]$. An oxidation of the hydride could then lead to the formation of the dimer, $[CpRu(CO)_2]_2$ which is an observed product. The hydride could not be detected by infrared spectroscopy probably because the ν(CO) bands of complex **18** and the former appear in the same region {IR (CH_2Cl_2) ν(CO) bands of $[CpRu(CO)_2H]$ 2023,

and 1959 cm^{-1})

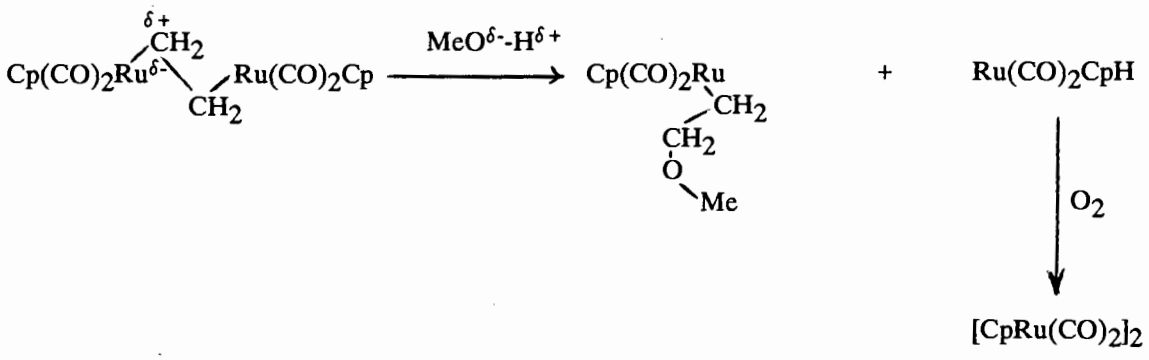

Scheme 2

2.4.3 *REACTIONS OF $[CpRu(CO)_2]_2[\mu\text{-}(CH_2CH_2)]$ WITH THE TERTIARY PHOSPHINES (PPh_3 AND PMe_2Ph)*

The reactivity of the μ (α,ω) - alkanediyl complexes of iron[2,16,23] and ruthenium[16], $[CpM(CO)_2]_2[\mu\text{-}(CH_2)_n]$ (M = Fe, n = 3-7; M = Ru, n = 5) with a range of tertiary phosphines (PPh_3, $PMePh_2$ and PMe_2Ph etc.) have been reported. The thermally induced reactions of $[Cp(CO)_2M]_2[\mu\text{-}(CH_2)_n]$ with tertiary phosphines undergo a CO insertion reaction to yield both monoacyl $[Cp(CO)(PR_3)M(\mu\text{-}\{C(O)(CH_2)_n\})M(CO)_2Cp]$ and diacyl $[Cp(CO)_2M]_2[\mu\text{-}\{C(O)(CH_2)_nC(O)\}]$ (PR_3 = PPh_3, $PMePh_2$ and PMe_2Ph) complexes respectively depending on the molar

ratio of the phosphine employed (Eq.1).

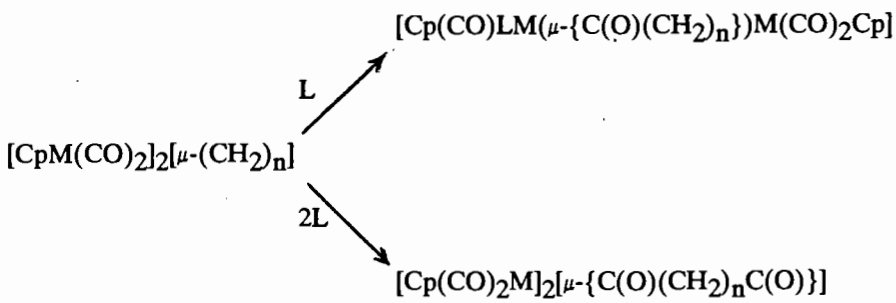

M = Fe n = 3 - 7 L = PPh_3, $PMePh_2$, PMe_2Ph

M = Ru n = 5 L = PPh_3, $PMePh_2$, PMe_2Ph

Eq.1

No reaction was observed when $[CpRu(CO)_2]_2[\mu\text{-}(CH_2CH_2)]$ with PPh_3 in THF or in toluene was heated under reflux. However, a substitution reaction rather than a carbonylation reaction appeared to have occurred when PPh_3 was replaced by PMe_2Ph. In the infrared spectrum we observe a single ν(CO) band at 1951 cm^{-1} (in CH_2Cl_2). In the ^1H NMR spectrum we observe resonances at δ = 7.55 (PPh-H, 10H, m), 4.86 (C_5H_5, 10H, s), 1.97 ($PPhCH_3$, 6H, d), 1.85 ppm (CH_3PPh, 6H, d) and 1.56 ppm (C_2H_4, 4H, s). These data and the fact that no acyl bands were detected in the IR spectrum suggest that the product formed in the above reaction is a disubstituted phosphine complex, $[CpRu(CO)(PMe_2Ph)]_2[\mu\text{-}(CH_2CH_2)]$. However, decarbonylation of the phosphine induced CO insertion product, $[CpRu(CO)(PMe_2Ph)]_2[\mu\text{-}\{C(O)(CH_2CH_2)C(O)\}]$, is possible under the reaction conditions (80 °C) employed.

2.4.4 *REACTIONS OF $[CpRu(CO)_2]_2[\mu\text{-}(CH_2CH_2)]$ WITH OXIDANTS (Ph_3CPF_6 AND $AgBF_4$)*

The trityl salt, Ph_3CPF_6, is well known for its ability to abstract a β-hydride from mononuclear alkyl and dinuclear alkyl-bridged transition metal complexes[16,24-26]. It was, therefore, of interest to investigate whether or not a hydride would be abstracted from complex **1**. The reaction of complex **1** as shown in equation 2, however, afforded two complexes, viz., the mononuclear cationic species, $[CpRu(CO)_2(C_2H_4)]^+PF_6^-$, **19**, and the dimer, $[CpRu(CO)_2]_2$, instead of the expected hydride abstraction product.

$$[CpRu(CO)_2]_2[\mu\text{-}(CH_2CH_2)] + Ph_3CPF_6 \xrightarrow{CH_2Cl_2} [CpRu(CO)_2(C_2H_4)]^+PF_6^- + [CpRu(CO)_2]_2$$

Eq.2

We believe that an oxidative demetallation reaction may have occurred which leads to the formation of the cationic complex, **19**, and the radical, $[CpRu(CO)_2]^\bullet$, which subsequently dimerizes. A similar oxidative demetallation was also observed by Giering et al.[27] for the analogous, but rigid, iron complexes, **20** and **21**.

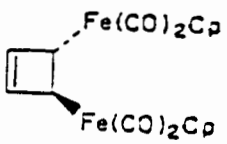

20

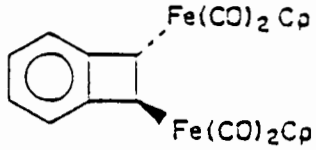

21

A possible mechanism for this reaction is described in scheme 3.

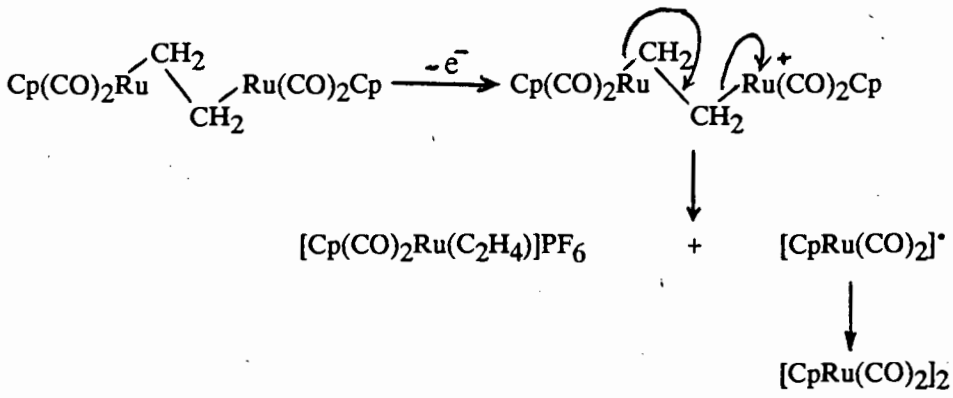

Scheme 3

All our attempts to isolate the trityl dimer, Ph_3CCPh_3, as a possible byproduct (due to coupling of two radicals, $Ph_3C^{\bullet}$) of the above reaction were unsuccessful.

The above reaction was repeated using another oxidant, $AgBF_4$, to verify the oxidative demetallation proposal. From this reaction we have also obtained the expected cationic product $[Cp(CO)_2Ru(C_2H_4)]BF_4$ due to oxidative demetallation of complex **1**.

2.4.5 REACTION OF $[CpRu(CO)_2]_2[\mu\text{-}(CH_2CH_2)]$ WITH PROTIC ACIDS (CF_3COOH AND HCl)

The acid cleavage of a Fe-C bond in $[CpFe(CO)_2R]$ (R = CH_3, CH_2CH_3, n-C_4H_9, etc.) has been investigated by de Luca and Wojciki[28]. These authors have also reported a kinetic study of the cleavage of the Fe-C bond in these complexes by protic acids such as CF_3COOH and $CHCl_2CO_2H$.

We have investigated the possible cleavage of the Ru-C bond in the reaction of the ethylene-bridged complex, $[CpRu(CO)_2]_2[\mu\text{-}(CH_2CH_2)]$, with CF_3COOH (in excess of equimolar). A cationic species was isolated using $NaBPh_4$ and was identified by infrared and ^1H NMR spectroscopy as $[CpRu(CO)_2(C_2H_4)]BPh_4$, **22**. The trifluoroacetato complex, $[Cp(CO)_2RuOC(O)CF_3]$ was isolated as the other product of this reaction. The above reaction was repeated in an NMR tube. In the ^1H NMR spectrum we observe resonances corresponding to $[CpRu(CO)_2(C_2H_4)]^+$, $[Cp(CO)_2RuOC(O)CF_3]$ and $[CpRu(CO)_2]_2$; no ethane was detected. We speculate that in $[CpRu(CO)_2]_2[\mu\text{-}(CH_2CH_2)]$ there is a significant contribution from $[CpRu(CO)_2CH_2CH_2]^+$ and a cleavage of the $Ru^{\delta-}\text{-}C^{\delta+}$ bond by CF_3COOH may lead to the formation of the intermediates $[CpRu(CO)_2(C_2H_4)]^+OC(O)CF_3^-$, **23** and $[CpRu(CO)_2H]$. The latter may react with $^-OC(O)CF_3$ to form $[Cp(CO)_2RuOC(O)CF_3]$, or undergo oxidation to form the dimer $[CpRu(CO)_2]_2$.

A similar reaction of **1** with HCl was also carried out in an NMR tube. In the ^1H NMR spectrum we observe a resonance at δ = 5.43 ppm for the Cp protons corresponding to $[CpRu(CO)_2Cl]$, **24**, another resonance at δ = 5.27 ppm corresponding to Cp protons of $[CpRu(CO)_2]_2$ and two Cp proton resonances at δ = 6.1 ppm and at δ = 4.1 ppm corresponding to the cationic species, $[CpRu(CO)_2(C_2H_4)]^+Cl^-$. We envisaged that complex **24** could have formed from the complex $[CpRu(CO)_2(C_2H_4)]^+Cl^-$ by elimination of ethylene. However, no ethylene was detected. These reactions of complex **1** with acids are thus very different from similar reactions carried out on the mononuclear ethyl complex, $[CpRu(CO)_2CH_2CH_3]$, which we have shown to give ethane (see 3.2.2).

2.4.6 *REACTION OF $[CpRu(CO)_2]_2[\mu\text{-}(CH_2CH_2)]$ WITH BROMINE*

The investigation of the reactions of $[LFe(CO)_2]_2[\mu\text{-}(CH_2)_n]$ (L = C_5H_5, n = 3 or 4; L = C_5Me_5, n = 4; L = C_5H_4Me, n = 4) and $[CpRu(CO)_2]_2[\mu\text{-}(CH_2)_5]$ with halogens (Br_2 or I_2) has been reported[16,20]. It was shown that these polymethylene-bridged complexes react with halogens according to equation 3.

$$[LM(CO)_2]_2[\mu\text{-}(CH_2)_n] \xrightarrow{2X_2} 2LM(CO)_2X + X(CH_2)_nX$$

Eq.3

M = Fe, n = 3 or 4, L = C_5H_5

M = Fe, n = 4, L = C_5Me_5

M = Fe, n = 4, L = C_5H_4Me

M = Ru, n = 5, L = C_5H_5

A similar reaction of complex **1** with bromine led to the formation of the two expected products $[CpRu(CO)_2Br]$ and dibromoethane, $Br(CH_2)_2Br$. This reaction was repeated in an NMR tube. In the ^1H NMR spectrum we observe resonances (other than those corresponding to $[CpRu(CO)_2Br]$ and $Br(CH_2)_2Br$) which originate in an oxidized species, possibly the dinuclear cation, $[Cp_2Ru_2(CO)_4(CH_2)_2]^+$. A related di-iron cationic species $[Cp_2Fe_2(CO)_4(CH_2)_4]^+$, has been observed[20] in a similar reaction. The presence of a triplet at δ = 4.6 ppm, which may be due to CH_2Br (with a coupling constant of J = 5.3 Hz) in the same spectrum suggests the formation of bromoethyl intermediate, $[CpRu(CO)_2CH_2CH_2Br]$ and this resonance appears ca. 1 ppm to lower field than that found for the CH_2X protons in $[CpRu(CO)_2(CH_2)_nX]$ (n = 3-5 , X = Cl, Br or I) (see section 3.3.2). This is because the metal is also affecting the CH_2 resonance.

We believe that the bromoethyl intermediate may be very unstable but we suggest that it could probably be isolated at very low temperatures.

2.5 THERMAL DECOMPOSITION OF $[CpRu(CO)_2]_2[\mu\text{-}(CH_2CH_2)]$

The thermal decomposition of complex **1** was investigated both in solution and in the solid state. A high pressure, thick, glass-walled NMR tube was employed for the thermal decomposition of complex **1** in solution. The NMR tube was filled with a deuterobenzene solution of complex **1**, and was evacuated and sealed off after several freeze/thaw cycles. The sealed tube was heated in a silicone oil bath in the temperature range 80-90°C. The thermal decomposition was monitored by ^1H NMR spectroscopy at intervals. The initially recorded ^1H NMR spectra did not reveal any change in the complex **1**. However, the ^1H NMR spectrum recorded after 122 hours showed some changes. The decrease in the intensities of the resonances of Cp and ethylene protons of complex **1**, as well as the appearance of a new resonance at δ = 5.27 ppm due to free ethylene was observed in the spectrum (other minor peaks in the spectrum were not assigned). An authentic ^1H NMR spectrum of ethylene in deuterobenzene was obtained in order to verify the above result; which proved to be consistent with the previous experiment.

The complete decomposition of **1** occurs after approximately 312 hours. This shows that this complex is more stable than many of its analogues such as $[CpMo(CO)_3]_2[\mu\text{-}(CH_2CH_2)]$ which is unstable even in the solid state above -20°C!

The solid state thermal decomposition of complex **1** was observed by differential scanning calorimetry (DSC) and when recording the melting point (using a Kofler hotstage microscope).

In the DSC analysis, a sample of complex **1** was sealed hermetically under nitrogen. The DSC thermograph (Fig.10) shows an endotherm and an exotherm in the temperature range 125 - 180 °C corresponding to the melting of complex **1** and the formation (or crystallization) of a new complex. The melting range of complex **1** determined by DSC appears somewhat higher than that recorded on the Kofler hotstage microscope (see below) probably because of the heat flow rate in DSC analysis; with this rate being fast (a decrease in the melting point was observed when the heat flow rate was slower).

In order to obtain more information on this solid state thermal decomposition we have investigated this decomposition using a Kofler hotstage melting apparatus with an attached camera. Crystals of complex **1** on the hot stage (see Picture 1 at 20°C) melt at 130 -131 °C to form an "oily" substance. A crystallization then takes place immediately (see Picture 2) to afford crystals with well-defined edges (see Picture 3).

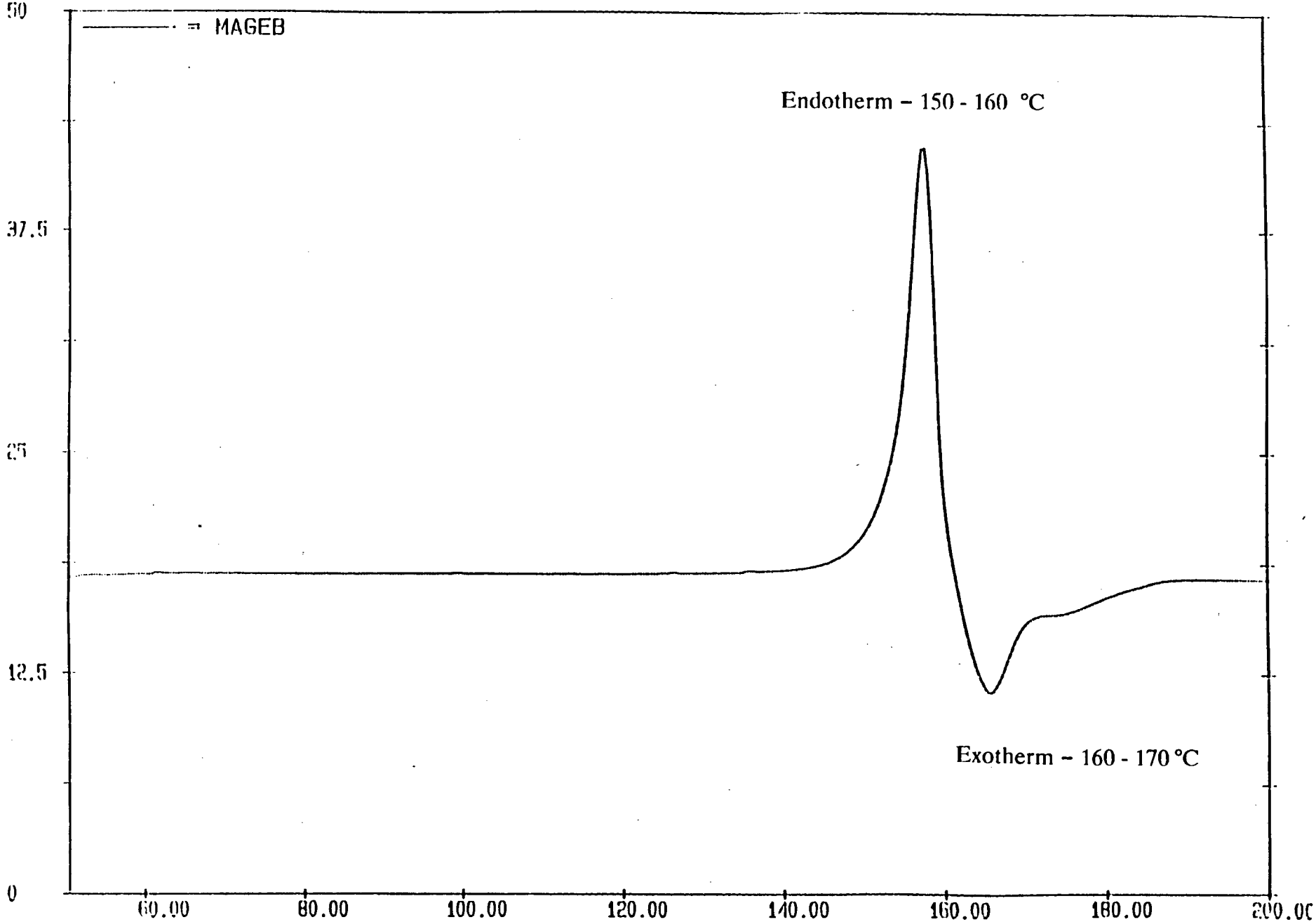

Fig.10 A DSC thermograph for the complex 1

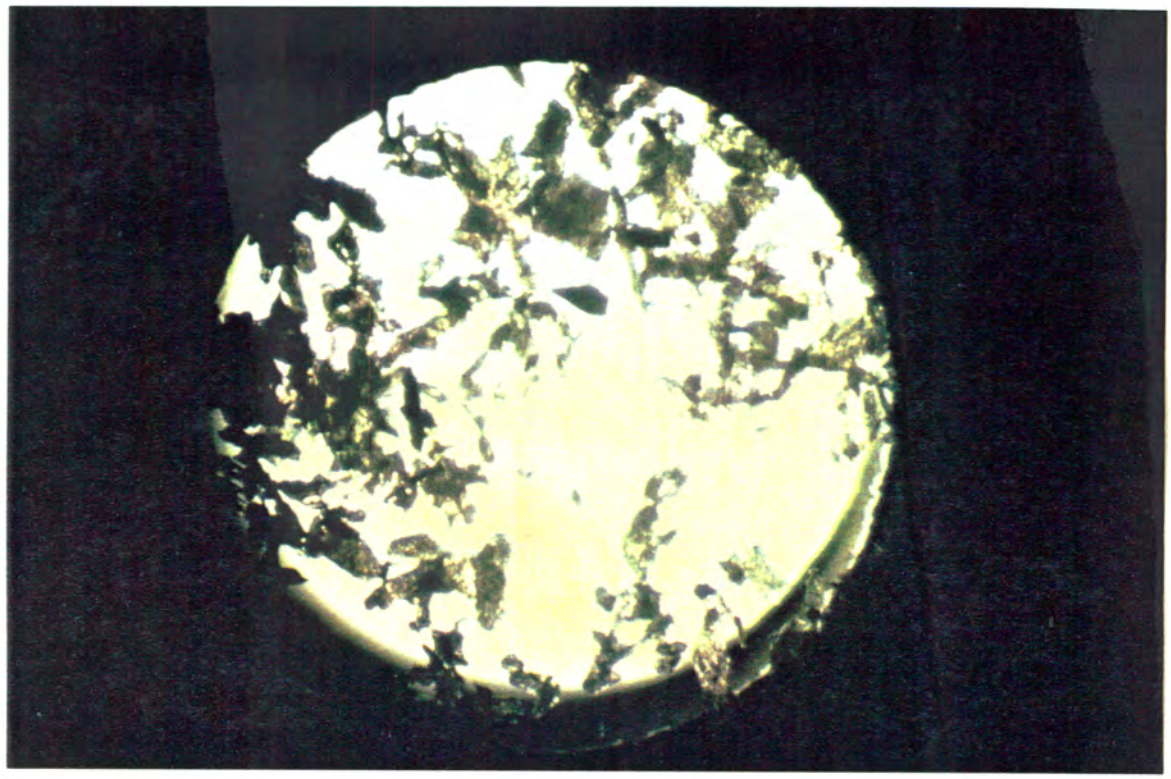

Picture 1 **Crystals of complex 1 at 20 °C.**

Picture 2 **Complex 1 in a molten state.**

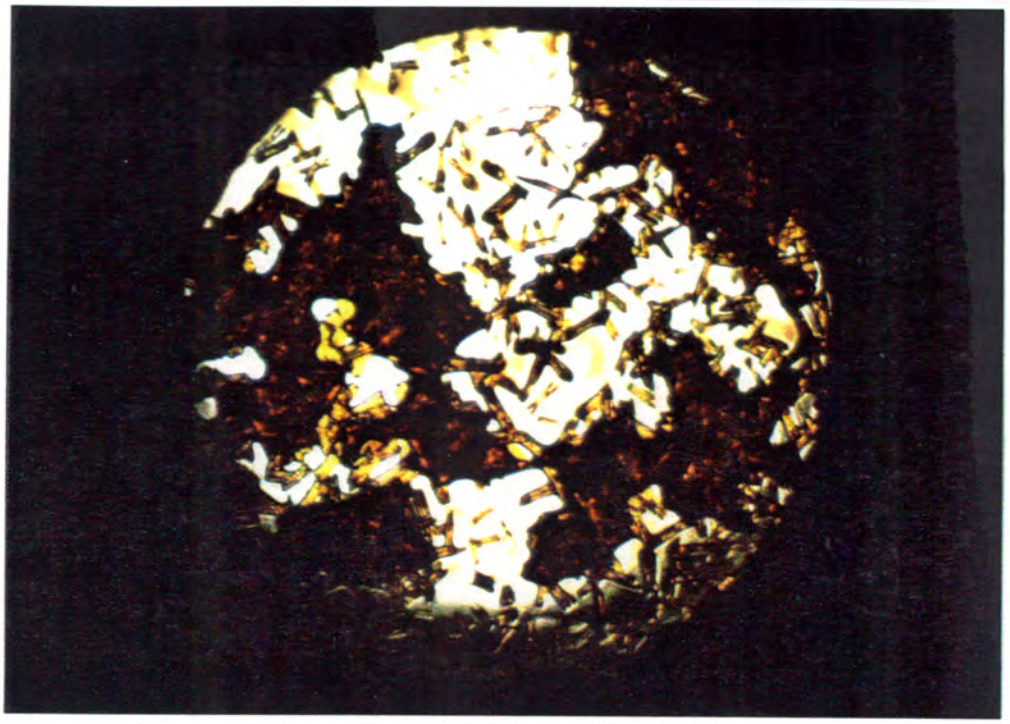

Picture 3 **Crystallisation of Ru dimer, $[CpRu(CO)_2]_2$.**

The infrared spectrum of these crystals shows the four ν(CO) bands corresponding to the ν(CO) bands observed for an authentic sample of the dimer, $[CpRu(CO)_2]_2$. This suggests that the decomposition of the ethylene-bridged complex in the solid state also takes place with a loss of ethylene to form the dimer, $[CpRu(CO)_2]_2$. Furthermore, we believe that the exotherm observed in the DSC thermograph at 160-170 °C could be due to a crystallization of the dimer, $[CpRu(CO)_2]_2$.

The results obtained from both the solution and the solid state thermal decompositions show that thermolysis of the ethylene-bridged complex, $[CpRu(CO)_2]_2[\mu\text{-}(CH_2CH_2)]$, leads to evolution of ethylene and the formation of the dimer, $[CpRu(CO)_2]_2$.

2.6 THE CRYSTAL STRUCTURE OF $[CpRu(CO)_2]_2[\mu\text{-}(CH_2CH_2)]$

Suitable crystals of complex **1** for the X-ray crystal structure determination were obtained by slow crystallization from CH_2Cl_2. Complex **1** crystallizes in space group P1 with Z = 1. Other details concerning the crystal data collection and structure refinement for complex **1** may be found in Table 9. Selected interatomic distances and bond angles are reported in Table 10, fractional atomic coordinates of non-hydrogen atoms are in Table 11. A perspective view of the molecular structure of complex 1 with atomic numbering is shown in Figure 11. A view of the structure along the Ru(1)-Ru axis is shown in Figure 12.

The molecular structure confirms that the $CpRu(CO)_2$ units are bonded to a C_2H_4 fragment. As in the methylene-bridged complex $[CpRu(CO)_2]_2[\mu\text{-}(CH_2)]$, **4**, the two Cp rings in the structure of complex **1** lie on the opposite sides of the Ru(1)-Ru axis in an anti (or trans) orientation (see Fig. 11). This is in contrast with the structure of the pentamethylene-bridged complex $[CpRu(CO)_2]_2[\mu\text{-}(CH_2)_5]$,**7**, where the Cp rings lie on the same side of the metal-metal axis. This could be attributed to the fact that in complex **7** the two metals are further apart than in the complexes **1** and **4**.

The Ru-C bond distance of 2.189 (3) Å is similar to that observed in complexes **4** and **7**. However, the C-C distance in complex **1** is slightly shorter than a normal C-C single bond. The Ru - C(3) - C(3B) angle of 111.3° (1) is slightly larger than expected for the sp^3 hybridization. However, the analogous angle in complex **7** and in complex **4** (Ru - C- Ru) is slightly larger , i.e. 113.5° (6) and 123° respectively. The CO - Ru - CO bond angles are close to 90° in both complexes **1** and **7**. However, the CO - Ru - CH_2 angle in complex **1** is significantly smaller (86.8° (1))

than in complex **7** (88.9° (4)). The Ru(1)-Ru distance of 5.12 Å in complex **1** confirms that the two ruthenium atoms are not bonded to one another. The non-bonded Ru-Ru distance of 3.8 Å was also observed in complex $[CpRu(CO)_2]_2[\mu\text{-}(CH_2)]$[3].

Table 9 Crystal data, experimental details of data collection and structure refinements for $[CpRu(CO)_2]_2[\mu\text{-}(CH_2CH_2)]$

Molecular formula	$C_{16}H_{14}O_4Ru_2$
$M_r/(g\ mol^{-1})$	472.43
space group	P1
a (Å)	6.060 (1)
b (Å)	6.990 (2)
c (Å)	10.097 (1)
α (°)	85.30 (1)
β (°)	76.86 (1)
γ (°)	74.46 (1)
V (Å^3)	401 (2)
D_c for Z = 1 ($g\ cm^{-1}$)	1.96
F(000)	230
μ(MoKα) (cm^{-1})	18.13
Crystal dimension (mm)	0.23 × 0.23 × 0.30
Crystal decay (%)	2.9
Scan mode	ω - 2θ
Scan width (°ω)	(1.00 + 0.35tanθ)
Aperture width (mm)	(1.20 + 1.05tanθ)
θ range (°)	1 - 30
% trans. max./min./ave.	79/100/98
Reflection collected	2460
Reflection observed (with $I_{rel} > 2\sigma I_{rel}$)	2223
No. of parameters	102
R	0.029
R_w	0.034
w	$(\sigma^2F_o + 0.0020F_o^2)^{-1}$
S	1.03

Table 10 **Selected interatomic distances (Å) and angles (°) for complex 1**

Ru(1) - C(3)	2.189 (3)
C(3) - C(3B)	1.499(6)
Ru(1) - C(3)	3.07 (1)
Ru(1) - C(1)	1.860(3)
Ru(1) - C(2)	1.864 (3)
C(1) - O(1)	1.140 (4)
C(2) - O(2)	1.131 (4)
Ru(1) - C(4)	2.265 (3)
Ru(1) - C(5)	2.261 (3)
Ru(1) - C(6)	2.285 (3)
Ru(1) - C(7)	2.269 (3)
Ru(1) - C(8)	2.271 (4)
C(4) - C(5)	1.429 (5)
C(5) - C(6)	1.398 (5)
C(6) - C(7)	1.396 (5)
C(7) - C(8)	1.440 (6)
C(8) - C(4)	1.405 (6)
Ru(1) - C(3) - C(3B)	111.3 (1)
C(1) - Ru(1) - C(3)	86.8 (1)
C(2) - Ru(1) - C(3)	86.4 (1)
C(1) - Ru(1) - C(2)	90.6 (1)

Table 11 **Fractional coordinates of non-hydrogen atoms of complex 1 with e. s. d. s. in parentheses**

Atom	x/a	y/b	z/c
Ru	0.22691 (3)	0.04690 (2)	0.25815 (2)
C(1)	0.4337 (5)	-0.1802 (5)	0.3099 (3)
O(1)	0.5623 (6)	-0.3173 (4)	0.3426 (4)
C(2)	0.1124 (6)	-0.1056 (4)	0.1603 (3)
O(2)	0.0422 (7)	-0.1936 (4)	0.0980 (3)
C(3)	-0.0328 (5)	-0.0134 (5)	0.4347 (3)
C(4)	0.3130 (7)	0.2796 (6)	0.0995 (3)
C(5)	0.0816 (6)	0.3559 (5)	0.1781 (4)
C(6)	0.0988 (6)	0.3751 (5)	0.3120 (3)
C(7)	0.3338 (7)	0.3075 (6)	0.3210 (4)
C(8)	0.4697 (6)	0.2497 (6)	0.1872 (4)

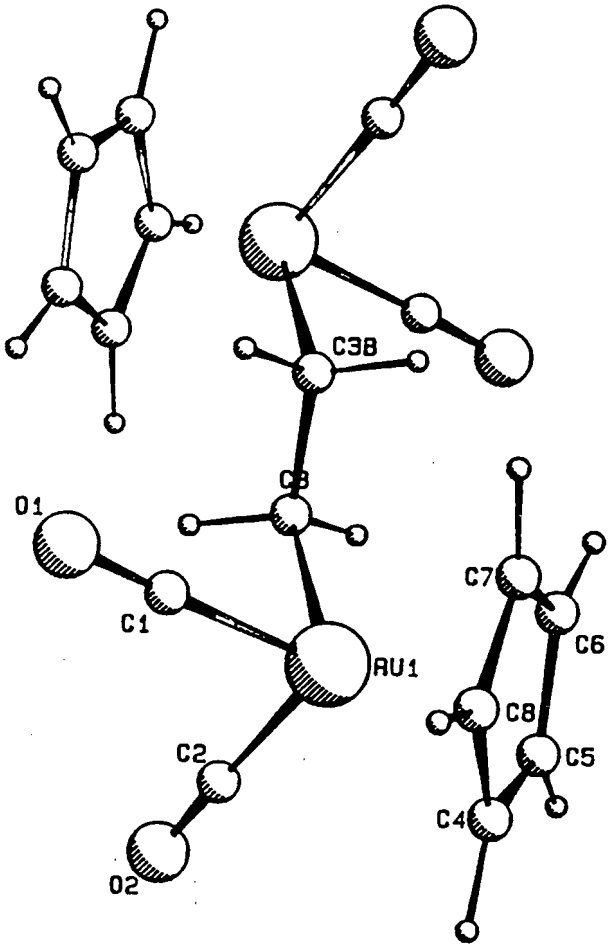

Fig. 11 A perspective view of the molecular structure of complex 1

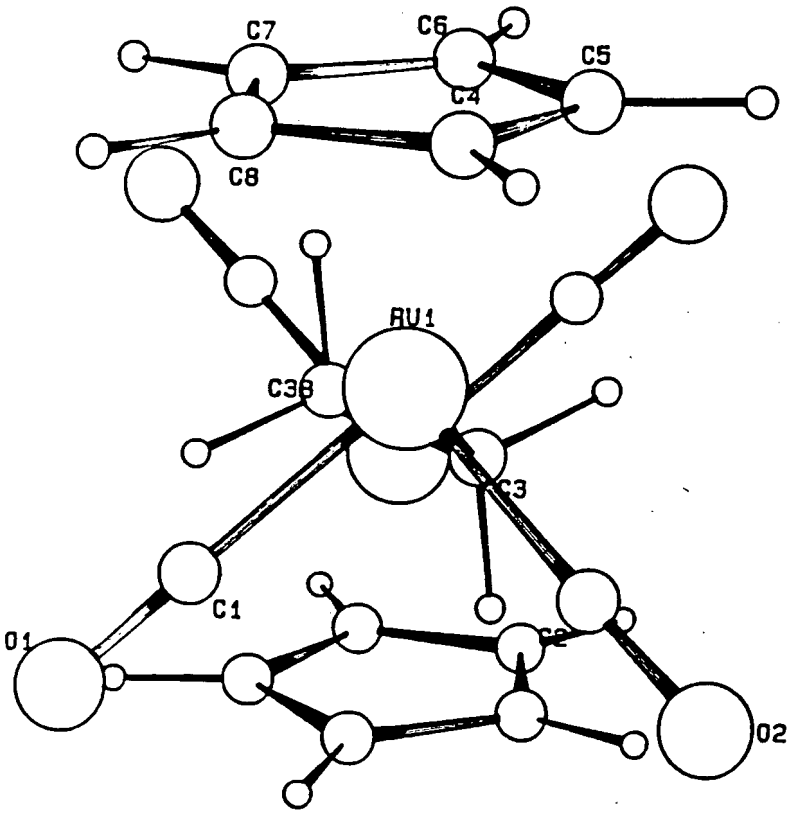

Fig. 12 A view along Ru(1)-Ru axis

2.7 THE SYNTHESIS OF $[\{CpM(CO)_2\}_2\{\mu\text{-}(C_3H_5)\}]^+PF_6^-$ (M = Fe or Ru)

The reactions of the Fe complexes $[CpFe(CO)_2]_2[\mu\text{-}(CH_2)_n]$, (n = 3 - 6) with Ph_3CPF_6 are known to yield the di-iron complexes[26] $[\{CpFe(CO)_2\}_2\{\mu\text{-}(C_nH_{2n-1})\}]^+PF_6^-$ (n = 3 - 6). It was originally thought that analogous ruthenium complexes do not undergo β-hydride abstraction reactions[11]. However, we now find that the complex, $[CpRu(CO)_2]_2[\mu\text{-}(CH_2)_3]$, does react readily with Ph_3CPF_6 to give a bright yellow crystalline complex, $[\{CpRu(CO)_2\}_2\{\mu\text{-}(C_3H_5)\}]^+PF_6^-$, **25** (Eq. 4). Similarly the analogous and known iron complex[24,26], **26**, was also synthesized and new NMR data were obtained (Table 12).

$$[CpM(CO)_2]_2[\mu\text{-}(CH_2)_3] \xrightarrow{Ph_3CPF_6} [\{CpM(CO)_2\}_2\{\mu\text{-}(C_3H_5)\}]^+PF_6^-$$

25 M = Ru

26 M = Fe

Eq. 4

The new complex **25** was characterized by the standard techniques (infrared, ^1H NMR, ^{13}C NMR spectroscopy and elemental analysis). The solution infrared spectrum could not be measured due to the low solubility of the complex. However, the infrared spectrum obtained in hexachlorobutadiene (HCBD) shows two high frequency ν(CO) absorption bands at 2053 and 2015 cm^{-1} and a weak band at 1955 cm^{-1}. In the ^1H NMR spectrum of this complex at room temperature we observe a singlet at δ = 5.80 ppm for the Cp protons and a low field quintet at δ = 6.86 ppm

TABLE 12 IR, ^{1}H NMR and ^{13}C NMR data for the allyl complexes $[\{LmM\}_2\{\mu\text{-}(C_3H_5)\}]^+PF_6^-$ (M = Fe or Ru)

LmM	Infrared[a](cm^{-1})	1H-NMR[b]	^{13}C-NMR[b]
$[CpFe(CO)_2]$	2038s	6.80(CH, 1H, q, J = 10 Hz)	121.76($CH_2\underline{C}H$)
	2012vs	5.50(C_5H_5, 10H, s)	88.07(C_5H_5)
		2.65($C\underline{H}_2CH$ 4H, d, J = 10 Hz)	24.13($\underline{C}H_2CH$)
$[CpRu(CO)_2]$	2053s	6.86($C\underline{H}$, 1H, q, J = 10.0 Hz)	121.87($CH_2\underline{C}H$)
	2015s	5.80($C_5\underline{H}_5$, 10H, s)	90.59(C_5H_5)
	1955w	3.11($C\underline{H}_2CH$, 4H, d, J = 10.0 Hz)	21.05($\underline{C}H_2CH$)

[a] in HCBD

[b] measured in d_6-acetone relative to TMS (δ = 0.00 ppm)

($J(H_{A,B}\ H_X)$ = 10.0 Hz) due to the CH proton. The CH_2 protons appear equivalent at this temperature, hence the resonance appears as a sharp doublet at δ = 3.11 ppm ($J(H_{A,B}\ H_X)$ = 10.0 Hz). The ^{13}C NMR spectrum shows resonances at δ = 121.87 ppm (CH), δ = 90.59 ppm (Cp) and δ = 21.05 ppm (CH_2).

2.7.1 FLUXIONAL BEHAVIOUR OF THE COMPLEX, $[\{CpRu(CO)_2\}_2\{\mu\text{-}(C_3H_5)\}]^+PF_6^-$

Variable temperature ^1H NMR spectra were recorded for the complex, $[\{CpRu(CO)_2\}_2\{\mu\text{-}(C_3H_5)\}]^+PF_6^-$, **25.** In solution, the protons of the allylic group are fluxional and changes in the ^1H NMR spectra occur on varying the temperature. On cooling to -35 °C, the spectrum shows four resonances: (i) the Cp protons remain unchanged as a singlet at δ = 5.78 ppm, (ii) the H_X proton (Fig. 13) is observed as a triplet of triplets at δ = 6.75 ppm ($^3J(H_AH_X)$ = 13.7 Hz and $^3J(H_BH_X)$ = 6.1 Hz), (iii) the H_A protons appear as doublets of doublets at δ = 3.05 ppm ($^3J(H_AH_X)$ = 13.7 Hz and $^2J(H_AH_B)$ = 3.2 Hz), and (iv) the H_B protons also appear as doublets of doublets at δ = 3.10 ppm ($^3J(H_BH_X)$ = 6.1 Hz and $^2J(H_AH_B)$ = 3.2 Hz). These two doublets of doublets are apparently overlapped due to the closeness in the chemical shift values (Fig 14).

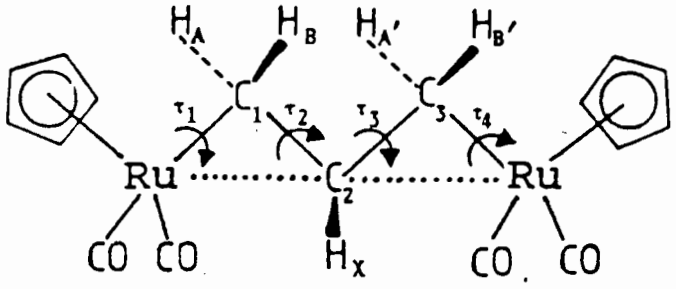

Fig. 13 Diagramatic representation of the structure of complex 25.

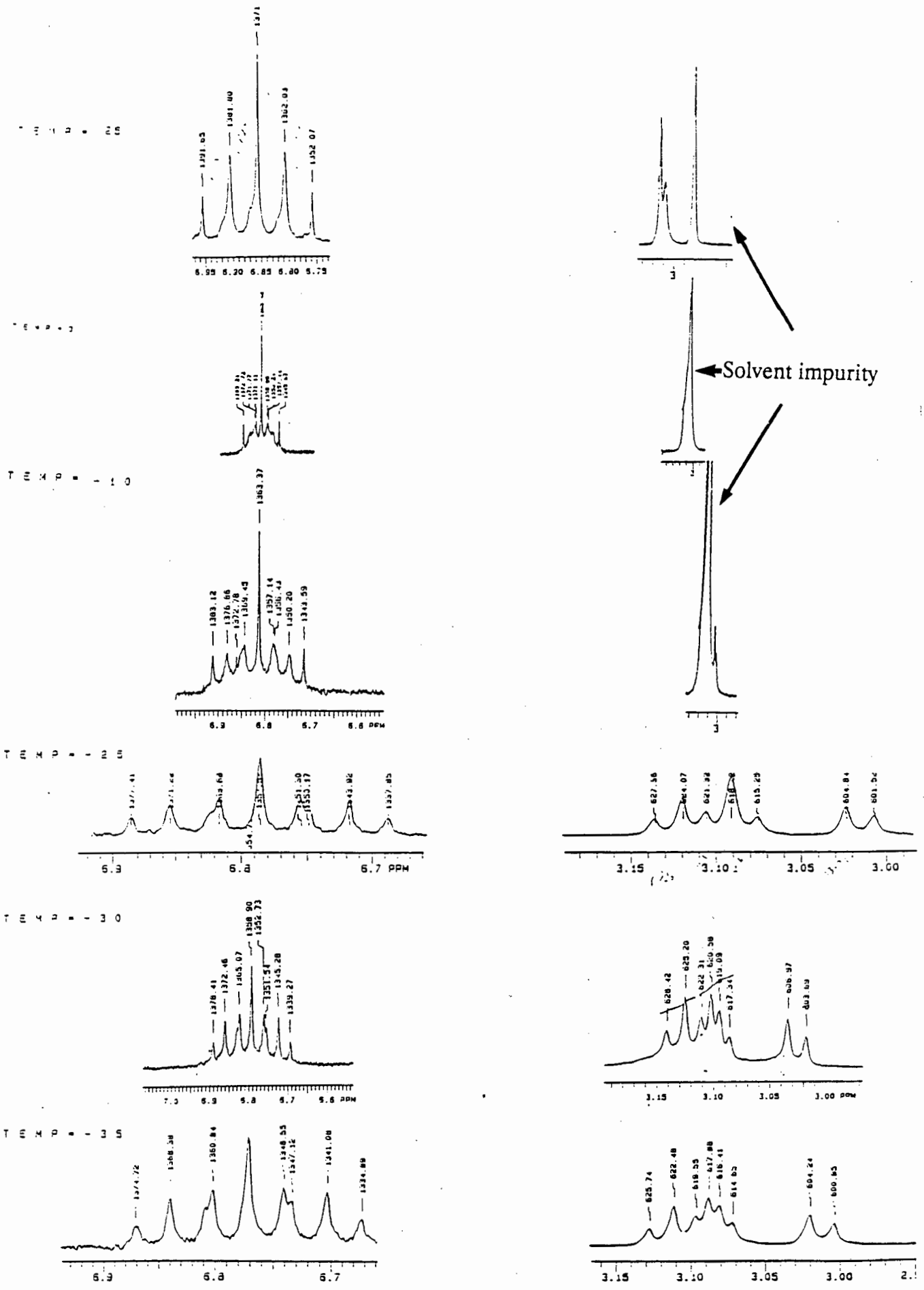

Fig. 14 Variable temperature ^{1}H-NMR spectra for complex 25

The ^1H NMR spectrum of the complex **25** did not change further on cooling to -70 °C (see Table 10 for the ^1H NMR data at low temperatures).

The NMR data at the low temperature limit can be interpreted on the basis of a "frozen out" stucture which is entirely consistent with that found in the solid state.

The change in the spectra at low temperature can be rationalised on the basis of restricted rotation about the C_1 - C_2 and C_2 - C_3 bonds (see Fig. 13). At this temperature with restricted rotation about these bonds, protons H_A and H_B become non-equivalent and the ^1H NMR spectrum observed is that expected for an $AA'BB'X$ spin system.

On warming the solution of complex **25**, the low field triplet of triplets (assigned to H_X) broadens as the temperature increases and becomes a sharp quintet at δ = 6.86 ppm ($J(H_{A,B}H_X)$ = 10.0 Hz), above 25 °C. The two doublet of doublets (assigned to H_A and H_B) coalesce at a temperature in the range, 0 - 10 °C (due to a solvent impurity the exact coalescence temperature was not determined), and then sharpens to a doublet at δ = 3.11 ppm, ($J(H_{A,B}H_X)$ = 10.0 Hz). Thus, at high temperatures when rotation about C_1 - C_2 and C_2 - C_3 (see Figure 13) is rapid on the NMR scale, the ^1H NMR spectrum of the allyl group exhibits peaks expected for an $AA'A''A'''X$ spin system.

Similar changes in the ^1H NMR spectra of the analogous iron complex[29], $[\{CpFe(CO)_2\}_2\{\mu\text{-}(C_3H_5)\}]^+PF_6^-$, **26** (Fig. 15), as well as the corresponding BF_4^- salt of **26** and some related complexes[30] have been reported, although the authors of the latter publication interpreted their results in terms of unsymmetrical hybrid

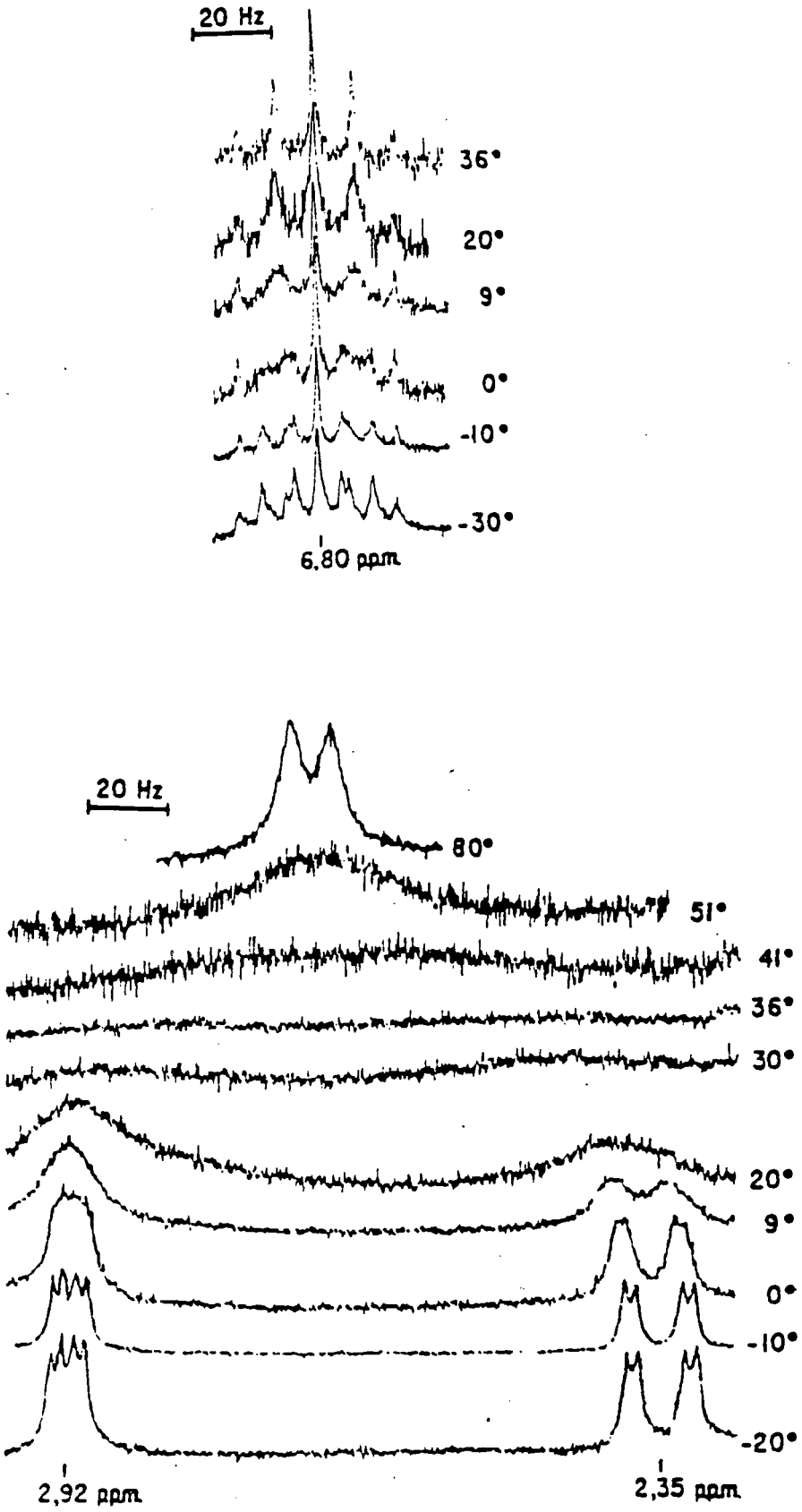

Fig 15 Variable temperature ^{1}H NMR spectra for the complex 26

structures[30]. However, we have shown that in the solid state, the structures of complexes **25** and **26** are essentially symmetrical. Our interpretations of the ^1H NMR spectra for the complex **25** are consistent with those found for the analogous iron complex **26.**

Table 13 **^1H NMR data[a] for the allyl complexes, $[\{CpM(CO)_2\}_2\{\mu\text{-}(C_3H_5)\}]^+PF_6^-$ (M = Fe or Ru) at low temperature (i.e the low temperature limiting spectrum)**

M	H_X	H_A	H_B
Fe	6.80	2.35	2.95
	$^3J(H_AH_X)$ = 14.0 Hz	$^3J(H_AH_X)$ = 14.0 Hz	$^3J(H_BH_X)$ = 6.0 Hz
	$^3J(H_BH_X)$ = 6.0 Hz	$^2J(H_AH_B)$ = 2.8 Hz	$^2J(H_AH_B)$ = 2.8 Hz
Ru	6.75	3.05	3.10
	$^3J(H_AH_X)$ = 13.7 Hz	$^3J(H_AH_X)$ = 13.7 Hz	$^3J(H_BH_X)$ = 6.1 Hz
	$^3J(H_BH_X)$ = 6.1 Hz	$^2J(H_AH_B)$ = 3.2 Hz	$^2J(H_AH_B)$ = 3.2 Hz

[a] measured in d_6-acetone relative to TMS (δ = 0.00 ppm)

Variable temperature ^1H NMR spectra for the analogous mixed metal (Fe and Ru) complex, $[Cp(CO)_2Ru(\mu\text{-}C_3H_5)Fe(CO)_2Cp]^+PF_6^-$, **27**, have been recorded[31] (Fig. 16). This complex shows somewhat different fluxional behaviour to that observed for complexes **25** and **26**. This may be due to the two different groups at each end of the bridging allyl group, C_3H_5, which may lead to two possible isomers, $[Cp(CO)_2RuCH_2CH{=}CH_2Fe(CO)_2Cp]PF_6$ and $[Cp(CO)_2RuCH_2{=}CHCH_2Fe(CO)_2Cp]PF_6$.

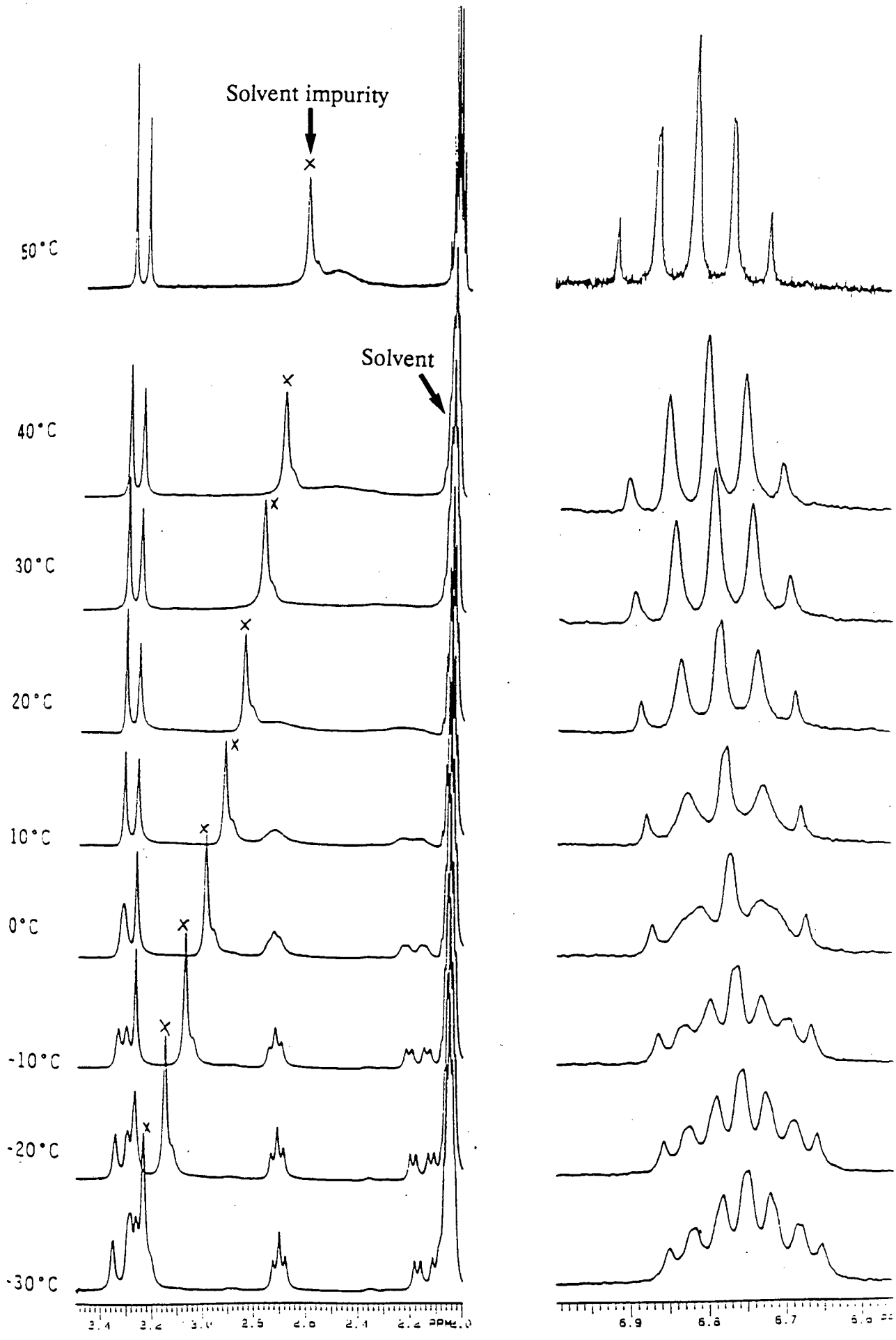

Fig. 16 Variable temperature ^{1}H NMR spectra for the complex 27

2.7.2 *CRYSTAL STRUCTURES OF* $[\{CpM(CO)_2\}_2\{\mu\text{-}(C_3H_5)\}]^+PF_6^-$ (M = Fe or Ru)

Suitable crystals of complexes **25** and **26** for the X-ray crystal structure determination were obtained by slow crystallization from acetone. Both complexes crystallize in space group $P2_1/n$ with Z = 4. Crystal data, experimental details of the data collection and structure refinement of complexes **25** and **26** are reported in Table 14. Selected bond lengths are reported in Tables 15 (for **25**) and 16 (for **26**), and selected bond angles in Tables 17 (for **25**) and 18 (for **26**). Final fractional atomic coordinates are reported in Tables 19 (for **25**) and 20 (for **26**). Perspective views of the iron and ruthenium structures with atomic labelling scheme are shown in Figures 17 and 18 respectively. Figure 19 is a view along the Ru(1) - Ru(2) direction and Figures 20-21 are packing diagrams. As both structures, of complex **25** and **26** are very similar the Figures 19-21 are representative of complex **26** as well.

The X-ray crystal structure of complex **25** is the first to be reported for this compound, whereas preliminary results of the X-ray crystal structure of complex **26** have been briefly reported[32]. The structure of the mixed metal complex $[CpRu(CO)_2\{\mu\text{-}(C_3H_5)\}Fe(CO)_2Cp]PF_6$ was found to be disordered[31]. The Ru-CH_2 lengths in complex **25** exceed 2.180 (9) Å, the value observed in the complex $[CpRu(CO)_2]_2[\mu\text{-}(CH_2)_5]$[2]. Similar variation in M-CH_2 length was observed in complexes **26** and $[CpFe(CO)_2]_2[\mu\text{-}(CH_2)_3]$[32]. The M···CH separation of 2.604 (7) Å is slightly longer in complex **25** than in complex **26** (2.568 (4) Å). This may be because the M···CH attraction is greater in the latter.

Table 14 **Crystal data, experimental details of data collection and structure refinements for $[\{CpM(CO)_2\}_2\{\mu\text{-}(C_3H_5)\}]PF_6$ (M = Fe or Ru)**

	Fe	Ru
Molecular formula	$C_{17}H_{15}O_4Fe_2PF_6$	$C_{17}H_{15}O_4Ru_2PF_6$
M_r/(g mol^{-1})	539.96	630.41
space group	$P2_1/n$	$P2_1/n$
a (Å)	12.614 (4)	12.887 (2)
b (Å)	9.941 (4)	10.101 (2)
c (Å)	16.478 (5)	16.228 (2)
β (°)	108.62 (3)	106.45 (1)
V (Å^3)	1958 (1)	2026.0 (6)
D_c for Z = 4 (g cm^{-1})	1.83	2.07
F(000)	1080	1224
μ(MoKα) (cm^{-1})	16.38	16.15
Crystal dimension (mm)	0.35 × 0.38 × 0.48	0.28 × 0.30 × 0.38
Crystal decay (%)	< 2	< 3
Scan mode	ω - 2θ	ω - 2θ
Scan width (°ω)	(0.85 + 0.35tanθ)	(0.85 + 0.35tanθ)
Aperture width (mm)	(1.12 + 1.05tanθ)	(1.12 + 1.05tanθ)
θ range (°)	1 - 25	1 - 25
% trans. max./min./ave.	85.0/99.9/94.7	88.8/99.9/95.3
Reflection collected	3195	3247
Reflection observed (with $I_{rel} > 2\sigma I_{rel}$)	2872	2827
No. of parameters	288	288
R	0.042	0.041
R_w	0.044	0.043
w	$(\sigma^2F)^{-1}$	$(\sigma^2F)^{-1}$
S	3.70	3.77

Table 15 Selected bond lengths (Å) with e.s.d.s. in parentheses for complex 25

RU(1)	- C(11)	1.878(8)
RU(1)	- C(12)	1.887(8)
RU(1)	- C(111)	2.247(7)
RU(1)	- C(112)	2.248(8)
RU(1)	- C(113)	2.224(8)
RU(1)	- C(114)	2.208(9)
RU(1)	- C(115)	2.229(9)
RU(1)	- C(31)	2.199(6)
RU(2)	- C(21)	1.877(8)
RU(2)	- C(22)	1.892(8)
RU(2)	- C(211)	2.239(8)
RU(2)	- C(212)	2.227(8)
RU(2)	- C(213)	2.199(9)
RU(2)	- C(214)	2.226(9)
RU(2)	- C(215)	2.240(9)
RU(2)	- C(32)	2.604(7)
RU(2)	- C(33)	2.251(8)
P(1)	- F(1)	1.532(9)
P(1)	- F(2)	1.464(11)
P(1)	- F(3)	1.505(11)
P(1)	- F(4)	1.560(7)
P(1)	- F(5)	1.547(6)
P(1)	- F(6)	1.495(11)
C(11)	- O(11)	1.139(10)
C(12)	- O(12)	1.132(10)
C(21)	- O(21)	1.127(10)
C(22)	- O(22)	1.137(9)
C(111)	- C(112)	1.395(14)
C(111)	- C(115)	1.368(12)
C(112)	- C(113)	1.387(11)
C(113)	- C(114)	1.383(17)
C(114)	- C(115)	1.412(17)
C(211)	- C(212)	1.364(10)
C(211)	- C(215)	1.416(15)
C(212)	- C(213)	1.350(15)
C(213)	- C(214)	1.403(17)
C(214)	- C(215)	1.423(13)
C(31)	- C(32)	1.435(12)
C(32)	- C(33)	1.394(13)

Table 16 **Selected bond lengths (Å) with e.s.d.s. in parentheses for complex 26**

FE(1)	- C(11)	1.763(5)
FE(1)	- C(12)	1.771(6)
FE(1)	- C(111)	2.112(4)
FE(1)	- C(112)	2.097(5)
FE(1)	- C(113)	2.093(5)
FE(1)	- C(114)	2.077(5)
FE(1)	- C(115)	2.089(5)
FE(1)	- C(31)	2.112(5)
FE(2)	- C(21)	1.778(5)
FE(2)	- C(22)	1.773(5)
FE(2)	- C(211)	2.101(4)
FE(2)	- C(212)	2.095(5)
FE(2)	- C(213)	2.080(4)
FE(2)	- C(214)	2.090(5)
FE(2)	- C(215)	2.102(5)
FE(2)	- C(32)	2.568(4)
FE(2)	- C(33)	2.135(5)
P(1)	- F(1)	1.563(5)
P(1)	- F(2)	1.525(5)
P(1)	- F(3)	1.571(5)
P(1)	- F(4)	1.565(5)
P(1)	- F(5)	1.552(4)
P(1)	- F(6)	1.532(6)
C(11)	- O(11)	1.143(6)
C(12)	- O(12)	1.131(7)
C(21)	- O(21)	1.130(7)
C(22)	- O(22)	1.139(6)
C(111)	- C(112)	1.402(8)
C(111)	- C(115)	1.392(7)
C(112)	- C(113)	1.398(6)
C(113)	- C(114)	1.386(10)
C(114)	- C(115)	1.421(9)
C(211)	- C(212)	1.400(6)
C(211)	- C(215)	1.405(9)
C(212)	- C(213)	1.379(8)
C(213)	- C(214)	1.413(9)
C(214)	- C(215)	1.408(7)
C(31)	- C(32)	1.418(7)
C(32)	- C(33)	1.398(7)

Table 17 Selected bond angles (°) with e.s.d.s. in parentheses for complex 25

RU(1)	- C(11)	- O(11)	178.8(7)
RU(1)	- C(12)	- O(12)	175.8(6)
RU(2)	- C(21)	- O(21)	174.9(6)
RU(2)	- C(22)	- O(22)	178.4(7)
RU(1)	- C(111)	- C(115)	71.5(5)
RU(1)	- C(111)	- C(112)	72.0(4)
C(112)	- C(111)	- C(115)	109.2(8)
RU(1)	- C(112)	- C(111)	71.9(4)
C(111)	- C(112)	- C(113)	107.3(8)
RU(1)	- C(112)	- C(113)	71.0(5)
RU(1)	- C(113)	- C(112)	72.9(5)
C(112)	- C(113)	- C(114)	108.5(8)
RU(1)	- C(113)	- C(114)	71.2(5)
RU(1)	- C(114)	- C(113)	72.4(6)
C(113)	- C(114)	- C(115)	107.7(9)
RU(1)	- C(114)	- C(115)	72.2(6)
C(111)	- C(115)	- C(114)	107.3(9)
RU(1)	- C(115)	- C(114)	70.7(6)
RU(1)	- C(115)	- C(111)	72.9(5)
RU(2)	- C(211)	- C(215)	71.6(5)
RU(2)	- C(211)	- C(212)	71.8(4)
C(212)	- C(211)	- C(215)	107.4(8)
RU(2)	- C(212)	- C(211)	72.7(5)
C(211)	- C(212)	- C(213)	110.6(8)
RU(2)	- C(212)	- C(213)	71.1(5)
RU(2)	- C(213)	- C(212)	73.4(6)
C(212)	- C(213)	- C(214)	108.6(9)
RU(2)	- C(213)	- C(214)	72.5(6)
RU(2)	- C(214)	- C(213)	70.5(6)
C(213)	- C(214)	- C(215)	106.5(9)
RU(2)	- C(214)	- C(215)	72.0(6)
C(211)	- C(215)	- C(214)	106.8(8)
RU(2)	- C(215)	- C(214)	70.9(5)
RU(2)	- C(215)	- C(211)	71.5(5)
RU(1)	- C(31)	- C(32)	99.9(4)
RU(2)	- C(32)	- C(31)	117.8(4)
C(31)	- C(32)	- C(33)	126.8(7)
RU(2)	- C(32)	- C(33)	59.8(4)
RU(2)	- C(33)	- C(32)	87.9(5)

Table 18 **Selected bond angles (°) with e.s.d.s. in parentheses for complex 26**

FE(1)	- C(11)	- O(11)	178.6(5)
FE(1)	- C(12)	- O(12)	175.0(4)
FE(2)	- C(21)	- O(21)	175.2(4)
FE(2)	- C(22)	- O(22)	178.1(5)
FE(1)	- C(111)	- C(115)	69.8(3)
FE(1)	- C(111)	- C(112)	70.0(3)
C(112)	- C(111)	- C(115)	108.6(5)
FE(1)	- C(112)	- C(111)	71.1(3)
C(111)	- C(112)	- C(113)	108.1(5)
FE(1)	- C(112)	- C(113)	70.3(3)
FE(1)	- C(113)	- C(112)	70.7(3)
C(112)	- C(113)	- C(114)	107.8(5)
FE(1)	- C(113)	- C(114)	70.0(3)
FE(1)	- C(114)	- C(113)	71.2(4)
C(113)	- C(114)	- C(115)	108.7(5)
FE(1)	- C(114)	- C(115)	70.5(4)
C(111)	- C(115)	- C(114)	106.8(5)
FE(1)	- C(115)	- C(114)	69.6(3)
FE(1)	- C(115)	- C(111)	71.6(3)
FE(2)	- C(211)	- C(215)	70.5(3)
FE(2)	- C(211)	- C(212)	70.3(3)
C(212)	- C(211)	- C(215)	107.4(5)
FE(2)	- C(212)	- C(211)	70.8(3)
C(211)	- C(212)	- C(213)	109.1(4)
FE(2)	- C(212)	- C(213)	70.2(3)
FE(2)	- C(213)	- C(212)	71.3(3)
C(212)	- C(213)	- C(214)	108.1(5)
FE(2)	- C(213)	- C(214)	70.5(3)
FE(2)	- C(214)	- C(213)	69.8(3)
C(213)	- C(214)	- C(215)	107.3(5)
FE(2)	- C(214)	- C(215)	70.9(3)
C(211)	- C(215)	- C(214)	108.1(5)
FE(2)	- C(215)	- C(214)	69.9(3)
FE(2)	- C(215)	- C(211)	70.4(3)
FE(1)	- C(31)	- C(32)	99.0(3)
FE(2)	- C(32)	- C(31)	117.9(3)
C(31)	- C(32)	- C(33)	126.3(4)
FE(2)	- C(32)	- C(33)	56.2(3)
FE(2)	- C(33)	- C(32)	90.8(3)

Table 19 **Fractional atomic coordinates ($\times 10^4$) with e.s.d.s. for complex 25**

Atom	x/a	y/b	z/c	Uequiv
RU(1)	3259(0)	4377(1)	1198(0)	35(0)
RU(2)	6791(0)	4326(1)	3926(0)	36(0)
P(1)	5167(2)	9619(2)	2543(1)	66(1)
F(1)	5116(6)	8953(9)	1684(5)	165(4)
F(2)	4991(6)	8398(10)	2971(8)	253(7)
F(3)	5260(7)	10402(13)	3350(6)	232(7)
F(4)	3908(5)	9736(10)	2226(4)	168(4)
F(5)	6408(4)	9431(9)	2859(5)	149(4)
F(6)	5322(14)	10894(8)	2125(8)	310(12)
C(11)	2473(6)	2875(7)	1349(4)	46(3)
O(11)	1980(5)	1975(5)	1432(4)	71(2)
C(12)	4241(6)	3340(7)	806(4)	47(3)
O(12)	4814(5)	2764(6)	526(3)	75(3)
C(21)	5805(6)	3256(7)	4280(4)	46(3)
O(21)	5231(5)	2665(6)	4547(3)	71(3)
C(22)	7580(6)	2824(7)	3753(4)	48(3)
O(22)	8078(4)	1937(5)	3658(4)	68(3)
C(111)	3035(7)	6546(7)	1403(5)	61(3)
C(112)	3565(7)	6419(7)	768(5)	61(3)
C(113)	2872(9)	5754(8)	83(5)	75(4)
C(114)	1929(8)	5465(9)	293(7)	94(4)
C(115)	2037(7)	5967(9)	1125(8)	86(5)
C(211)	6524(7)	6404(7)	4302(5)	62(3)
C(212)	6991(8)	5705(7)	5032(5)	67(4)
C(213)	7974(8)	5252(9)	5025(6)	80(4)
C(214)	8196(7)	5703(9)	4275(8)	93(6)
C(215)	7271(9)	6433(8)	3809(5)	72(4)
C(31)	4147(6)	4075(7)	2557(4)	50(3)
C(32)	5154(7)	4698(7)	2576(4)	51(3)
C(33)	6088(7)	4077(9)	2499(5)	56(3)

Table 20 **Fractional atomic coordinates ($\times 10^4$) with e.s.d.s. for complex 26**

Atom	x/a	y/b	z/c	Uequiv
FE(1)	3328(0)	4531(1)	1254(0)	37(0)
FE(2)	6850(0)	4413(1)	3996(0)	39(0)
P(1)	5250(1)	9762(1)	2613(1)	58(1)
F(1)	5202(3)	8837(4)	1835(3)	125(2)
F(2)	5005(4)	8600(4)	3131(3)	151(3)
F(3)	5319(3)	10760(4)	3367(3)	124(2)
F(4)	3953(4)	9953(6)	2237(3)	168(3)
F(5)	6527(3)	9512(5)	3001(3)	147(3)
F(6)	5495(7)	10944(4)	2104(4)	226(5)
C(11)	2567(4)	3087(5)	1351(3)	48(2)
O(11)	2053(3)	2166(3)	1408(2)	69(2)
C(12)	4333(4)	3634(5)	923(3)	49(2)
O(12)	4946(3)	3109(4)	657(2)	74(2)
C(21)	5819(4)	3499(4)	4293(3)	50(2)
O(21)	5189(3)	2963(4)	4535(2)	71(2)
C(22)	7600(4)	2958(5)	3877(3)	49(2)
O(22)	8103(3)	2046(3)	3796(2)	72(2)
C(111)	3107(4)	6594(4)	1461(3)	57(2)
C(112)	3639(4)	6441(4)	838(3)	55(2)
C(113)	2920(5)	5725(5)	151(3)	63(2)
C(114)	1963(5)	5419(5)	354(4)	75(2)
C(115)	2077(4)	5946(5)	1179(4)	69(3)
C(211)	6610(4)	6384(4)	4364(3)	57(2)
C(212)	7112(5)	5602(5)	5092(3)	61(2)
C(213)	8121(4)	5120(5)	5056(3)	67(2)
C(214)	8282(4)	5616(5)	4300(4)	73(3)
C(215)	7341(5)	6404(5)	3875(3)	64(2)
C(31)	4149(4)	4249(5)	2577(3)	49(2)
C(32)	5186(4)	4869(4)	2643(3)	45(2)
C(33)	6165(4)	4214(5)	2638(3)	51(2)

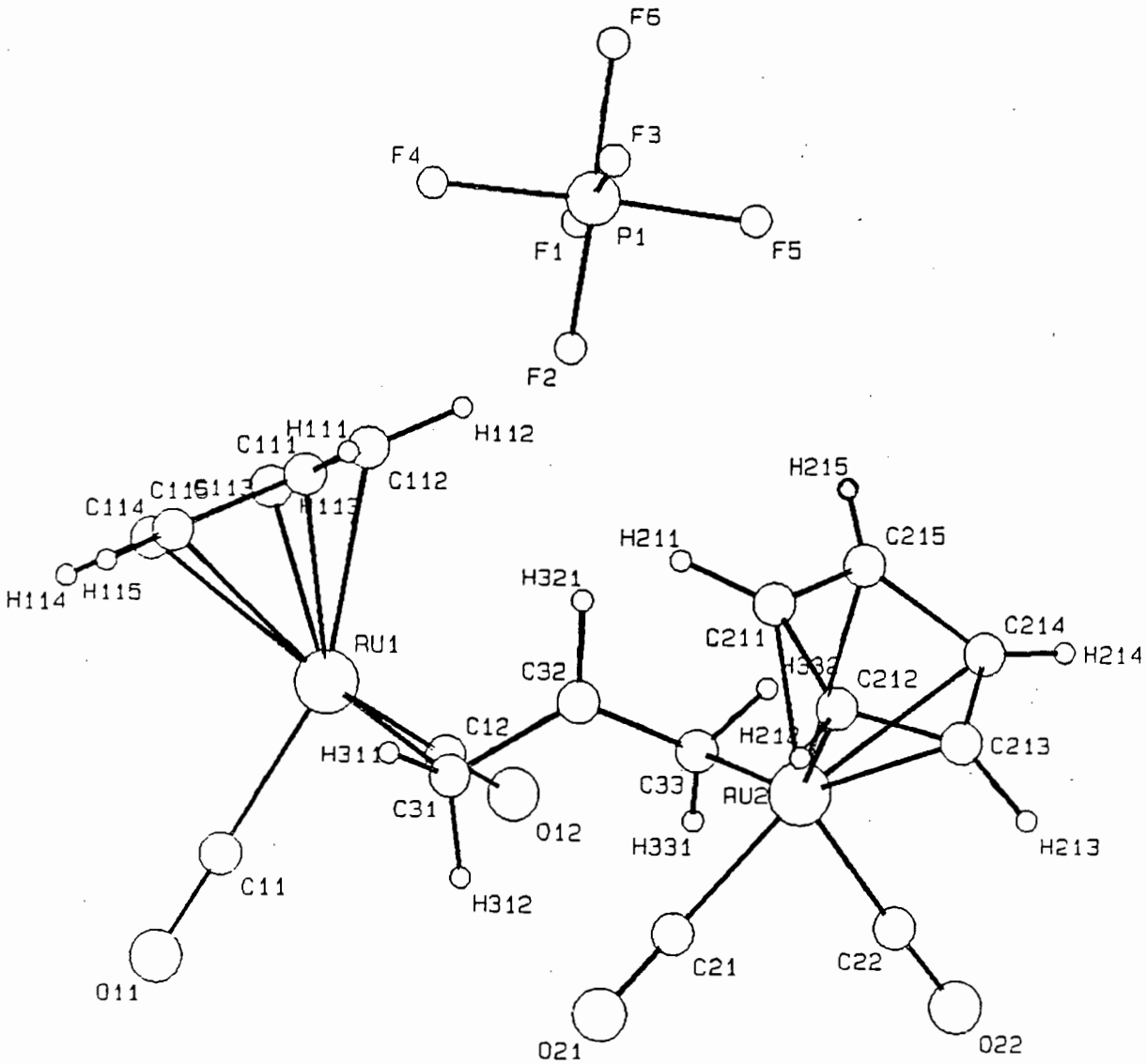

Figure 17 A perspective view of the structure of complex **25** with atomic numbering

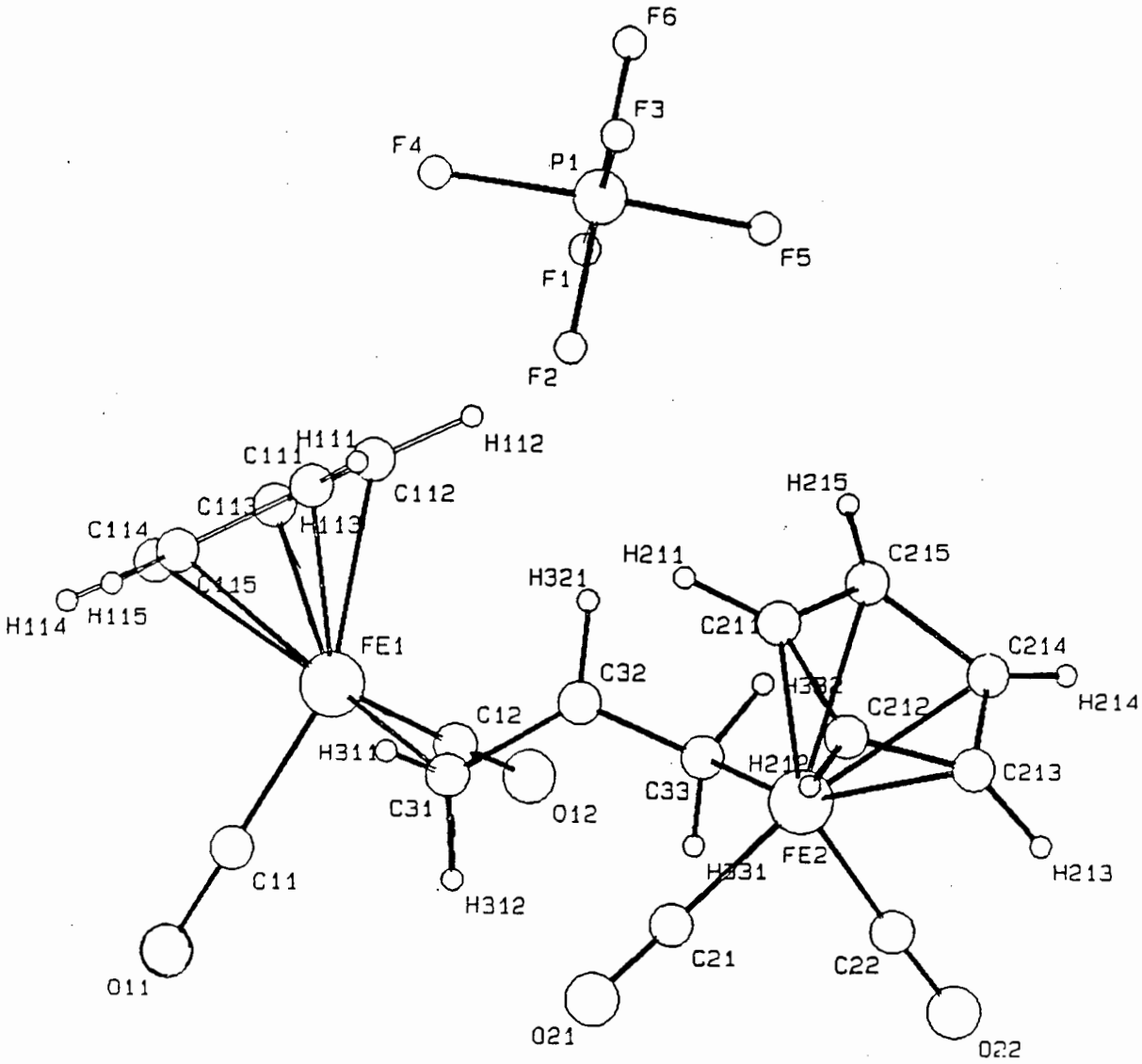

Figure 18 A perspective view of the structure of complex **26** with atomic numbering

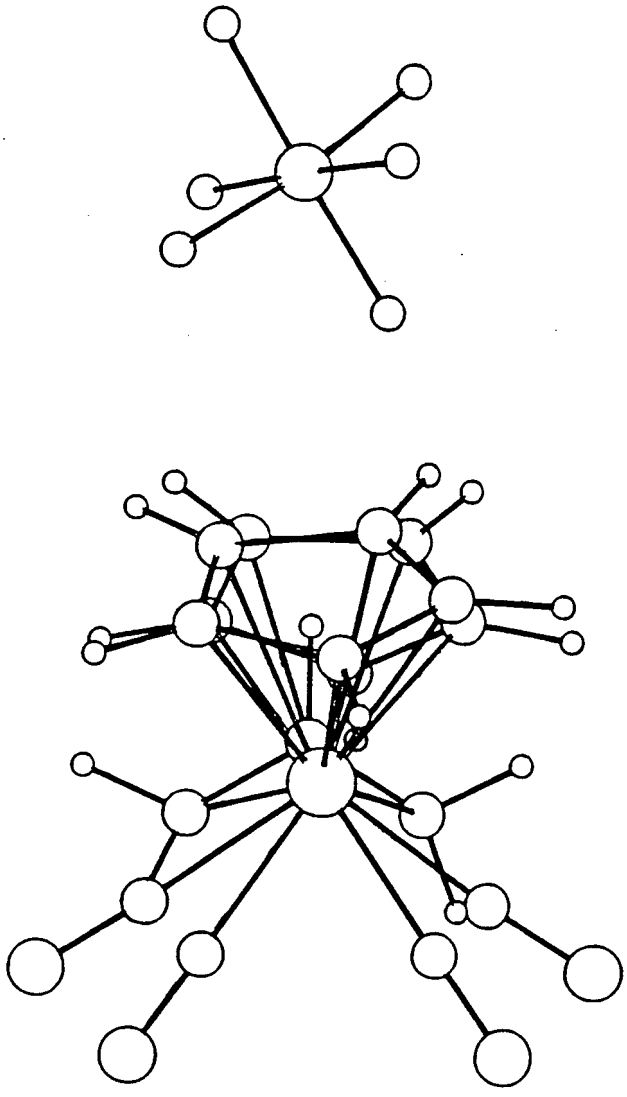

Figure 19 A view along the Ru(1) - Ru(2) direction

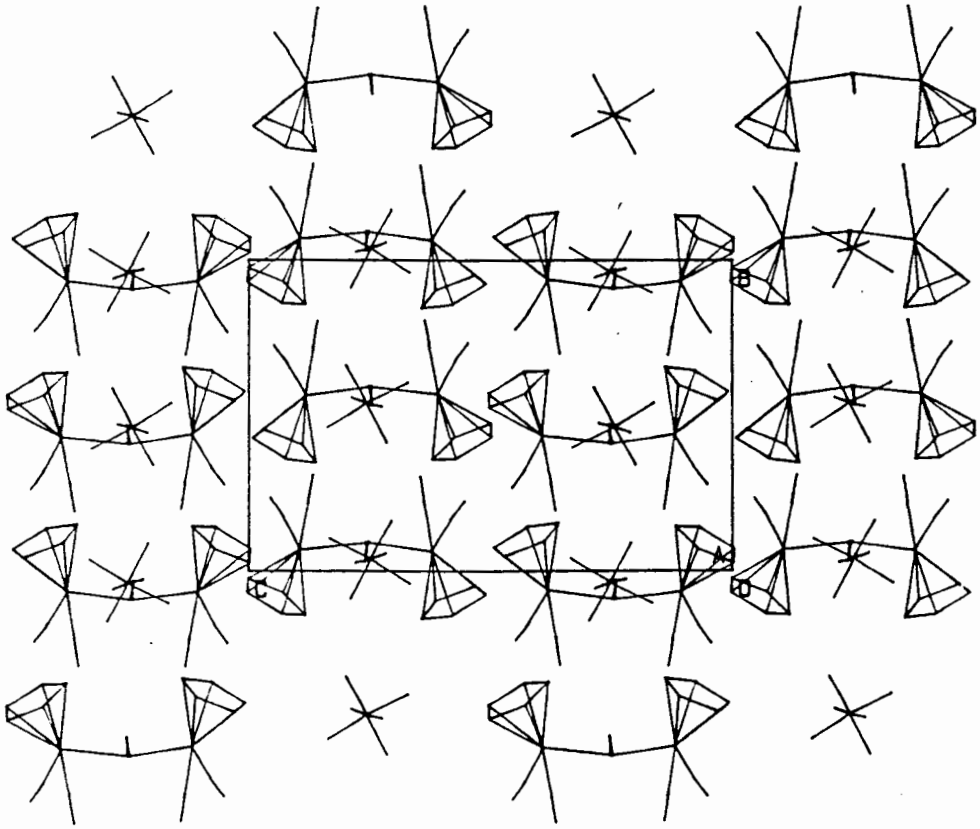

Figure 20 **Packing diagram - a view down a-axis**

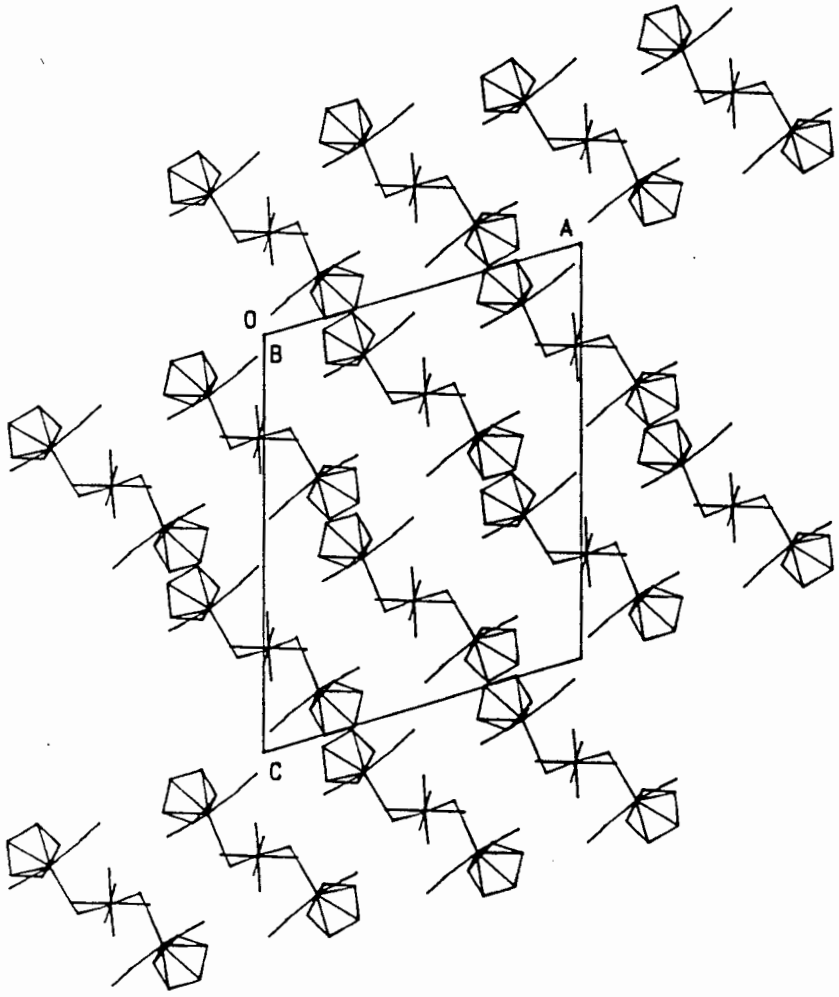

Figure 21 **Packing diagram - a view down b-axis**

2.8 A SEQUENCE OF REACTIONS OF $[CpM(CO)_2]_2[\mu\text{-}(CH_2)_5]$ (M = Fe or Ru) WITH Ph_3CPF_6, CF_3COOH AND NaI

The pentamethylene-bridged complexes $[CpM(CO)_2]_2[\mu\text{-}(CH_2)_5]$ (M = Fe or Ru), were synthesized according to the literature[2,9] methods. A sequence of reactions of these complexes was carried out using trityl salt (Ph_3CPF_6), CF_3COOH and NaI respectively (see Scheme 4), which shows that the alkanediyl chain of the pentamethylene complexes can be converted in high yield to a single organic product which is shown to be 1-pentene. The relevance of this sequence of reaction is described in section 2.9.

WITH Ph_3CPF_6

The reactions of a dichloromethane solution of the pentamethylene-bridged complexes with a slight excess of one equivalent of Ph_3CPF_6 led to a β-hydride abstraction to form the dinuclear alkene alkyl cationic complexes, $[[Cp(CO)_2M\{CH_2{=}CHCH_2CH_2CH_2\}M(CO)_2Cp]^+PF_6^-$ (**28**, M = Fe, a yellow crystalline complex; or **29**, M = Ru, a white crystalline complex) (Eq. 5). These complexes were characterized by standard physical techniques (infrared, ^1H NMR, ^{13}C NMR spectroscopy and elemental analysis, see Table 21). Unlike the allyl complexes, **25** and **26**, the complexes **28** and **29** are soluble in several organic solvents.

TABLE 21 IR, ^{1}H NMR and ^{13}C NMR data for the complexes $[\{CpM(CO)_2\}_2\{\mu\text{-}(C_5H_9)\}]^+PF_6^-$ (M = Fe or Ru)

M	Infrared[a](cm^{-1})	^{1}H NMR[b]	^{13}C NMR[b]	
Fe	2073s	5.87(C_5H_5-Fe^+, 5H, s)	92.12(C_5H_5-Fe^+)	89.10(=CH)
	2036s	5.29(=CH, 1H, m)	86.71(C_5H_5-Fe)	54.73($=CH_2$)
	2003s	4.92(C_5H_5, 5H, s)	42.41($=CH\underline{C}H_2$)	42.15($\underline{C}H_2CH_2Fe$)
	1943s	4.00($=C\underline{H}_2$, 1H, d, J_{cis} = 7.0 Hz)	2.55($\underline{C}H_2Fe$)	
		3.56($=C\underline{H}_2$, 1H, d, J_{trans} = 13.0 Hz)	the CO resonances	
		1.51($C\underline{H}_2C\underline{H}_2Fe$, 4H, m)	were not resolved	
		1.10($C\underline{H}_2Fe$, 2H, m)		
Ru	2082s	6.15(C_5H_5-Ru^+, 5H, s)	92.2(C_5H_5-Ru^+)	89.8(C_5H_5-Ru)
	2039s	5.43($C_5\underline{H}_5$-Ru, 5H, s)	86.5($=\underline{C}H$)	51.6($=\underline{C}H_2$)
	2012s	4.00($=C\underline{H}_2$, 1H, d, J_{cis} = 8.0 Hz)	43.7($=CH\underline{C}H_2$)	43.0($\underline{C}H_2CH_2Ru$)
	1947s	3.93($=C\underline{H}_2$, 1H, d, J_{trans} = 14.0 Hz)	-4.7($\underline{C}H_2Ru$)	
		2.8-1.7($C\underline{H}_2$, 6H, m)	the CO resonances	
		the =CH resonance was not resolved	were not resolved	

[a] in dichloromethane

[b] measured in d_6-acetone relative to TMS (δ = 0.00 ppm)

$$[CpM(CO)_2]_2[\mu\text{-}(CH_2)_5] \xrightarrow{Ph_3CPF_6} [Cp(CO)_2M\{CH_2{=}CHCH_2CH_2CH_2\}M(CO)_2Cp]^+PF_6^-$$

28 M = Fe

29 M = Ru

Eq. 5

The infrared spectrum shows two low frequency and two high frequency ν(CO) bands (Table 21) indicating the presence of an alkene alkyl species, $[Cp(CO)_2M\{CH_2{=}CHCH_2CH_2CH_2\}M(CO)_2Cp]^+PF_6^-$ (M = Fe or Ru). In the ^1H NMR spectra of both these complexes (**28** and **29**) we observe two singlets each (at high and low field) for the Cp ligands, and two doublets each (at δ = 4.0 ppm and at δ = 3.56 ppm, J_{cis} = 7.0 Hz and J_{trans} = 13.0 Hz, Fe; at δ = 4.0 and at δ = 3.93 ppm, J_{cis} = 8 Hz, J_{trans} = 14 Hz, Ru) for the $=CH_2$ protons (Table 21). Both these ^1H NMR data are consistent with the proposed structure of the alkene alkyl complexes (Fig. 22)

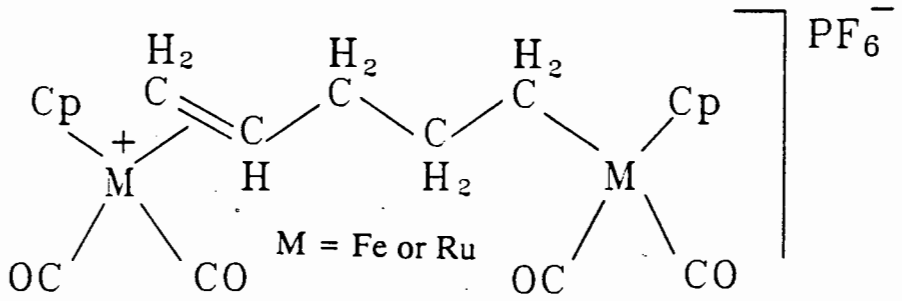

Fig. 22 diagramatic representation of the structure of the alkene alkyl complexes

REACTIONS OF COMPLEXES **28** and **29** WITH CF_3COOH

The reactions of the complexes **28** and **29** with a protic acid, CF_3COOH (in 1 : 25 molar ratio), at room temperature results in the expected quantitative cleavage of metal - carbon bonds (Fe - C and Ru - C) (Eq. 6). Two mononuclear cationic complexes $[Cp(CO)_2M\{CH_2=CHCH_2CH_2CH_3\}]^+BPh_4^-$ (**30**, M = Fe and **31**, M = Ru), as well as the trifluoroacetato complexes, $[CpM(CO)_2\{OC(O)CF_3\}]$, (**32**, M = Fe and **33**, M = Ru) were isolated. $NaBPh_4$ was used to precipitate the cations, see equation 6. These reactions were monitored by infrared spectroscopy. The formation of the complexes, **30** and **31** were confirmed by infrared, ^1H NMR and ^{13}C NMR (Table 22).

$$[Cp(CO)_2M\{CH_2=CHCH_2CH_2CH_2\}M(CO)_2Cp]^+PF_6^-$$

$$\downarrow CF_3COOH$$

$$[Cp(CO)_2M\{CH_2=CHCH_2CH_2CH_3\}]^+PF_6^-$$

$$\downarrow NaBPh_4$$

$$[Cp(CO)_2M\{CH_2=CHCH_2CH_2CH_3\}]^+BPh_4^- \qquad \textbf{30} \quad M = Fe$$

$$\textbf{31} \quad M = Ru$$

$$+$$

$$[CpM(CO)_2\{OC(O)CF_3\}]$$

32 M = Fe

33 M = Ru

Eq. 6

TABLE 22 **IR and ^{1}H NMR data for the complexes $[\{CpM(CO)_2\{CH_2=CHCH_2CH_2CH_3\}]^+BPh_4^-$ (M = Fe or Ru) and ^{13}C NMR data for the complex where M = Ru**

M	Infrared[a](cm^{-1})	^{1}H NMR[b]	^{13}C NMR[b]	
Fe	2072s	5.66(C_5H_5-Fe^+, 5H, s)		
	2036s	5.17(=CH, 1H, m)		
		3.92(=C<u>H</u>$_2$, 1H, d, J_{cis} = 7.0 Hz)		
		3.55(=C<u>H</u>$_2$, 1H, d, J_{trans} = 13.0 Hz)		
		2.45-1.5(C<u>H</u>$_2$C<u>H</u>$_2$, 4H, m)		
		0.95(CH_3, 3H, t)		
Ru	2082s	5.95(C_5H_5-Ru^+, 5H, s)	136.98(*m*-Ph)	126.04(*o*-Ph)
	2039s	5.25(=CH, 1H, m)	122.28(*p*-Ph)	92.13(<u>C</u>$_5H_5$-Ru^+)
		3.90(=C<u>H</u>$_2$, 1H, d, J_{cis} = 8.0 Hz)	86.52(=CH)	51.94(=<u>C</u>H$_2$)
		3.88(=C<u>H</u>$_2$, 1H, d, J_{trans} = 14.0 Hz)	39.70(=CH<u>C</u>H$_2$)	26.69(<u>C</u>H$_2$CH$_3$)
		2.38-1.6(C<u>H</u>$_2$, 4H, m)	13.61(<u>C</u>H$_3$)	
		0.96(CH_3, 3H, t)		

[a] in dichloromethane

[b] measured in d_6-acetone relative to TMS (δ = 0.00 ppm)

We have obtained the qualitative plots of $\ln(I_t/I_o)$ {I_t = intensity of a ν(CO) band (at 1943 and 1947 cm^{-1} for Fe and Ru respectively) at time t; I_o = intensity of the ν(CO) band at t = 0) versus time for the reaction described in equation 6. The plots give two straight lines for the cleavages of the Fe-C and the Ru-C bonds (Fig. 23). Since the concentration of acid is in an excess (25 times), the reaction is not a first order reaction, but rather a pseudo-first order reaction. The plots suggest that the cleavage of the Fe-C bond is approximately five times faster than the Ru-C bond. The rapid cleavage of the Fe-C bond compared to Ru-C bond (under the same reaction conditions and the same acid and complex concentrations) suggests that the former bond is weaker.

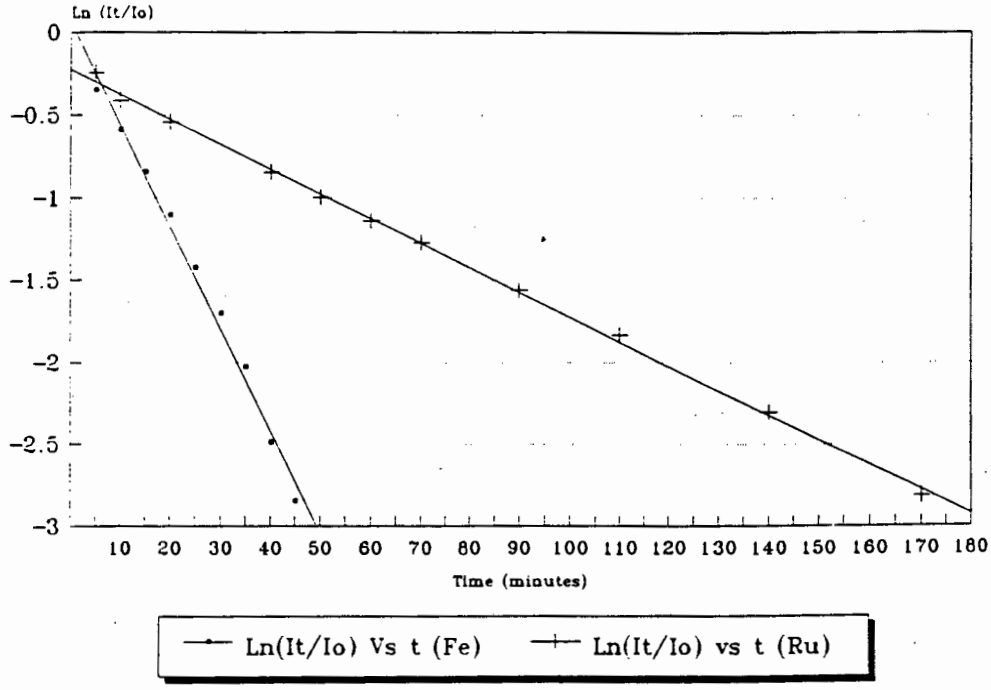

Fig. 23 The plots of $\ln(I_t/I_o)$ vs. time

REACTIONS OF COMPLEXES 30 AND 31 WITH NaI

The mononuclear cationic complexes, **30** and **31**, were subsequently treated with NaI. The reaction was carried out in an NMR tube. The ^1H NMR data showed that the displacement of 1-pentene and the formation of an iodo complex, $[CpM(CO)_2I]$ (M = Fe or Ru), are quantitative (Figure 24 shows a progressive decrease in the intensitiy of the methyl resonances of **30** and **31** and appearance of the methyl resonance of 1-pentene); no other reaction products could be detected by NMR. The ^1H NMR spectrum recorded for an authentic sample of 1-pentene further confirms the displacement of 1-pentene in the above reaction. The above sequence of reactions are summarized in Scheme 4.

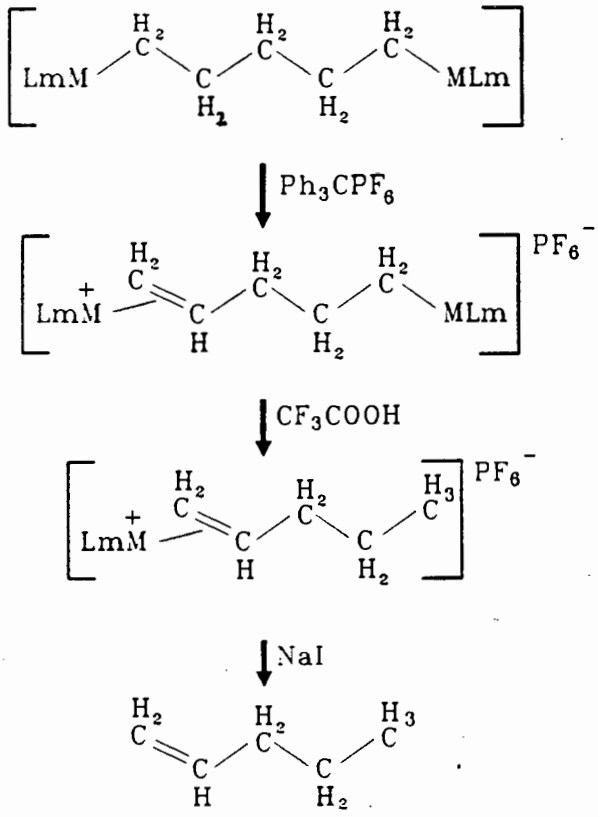

Scheme 4

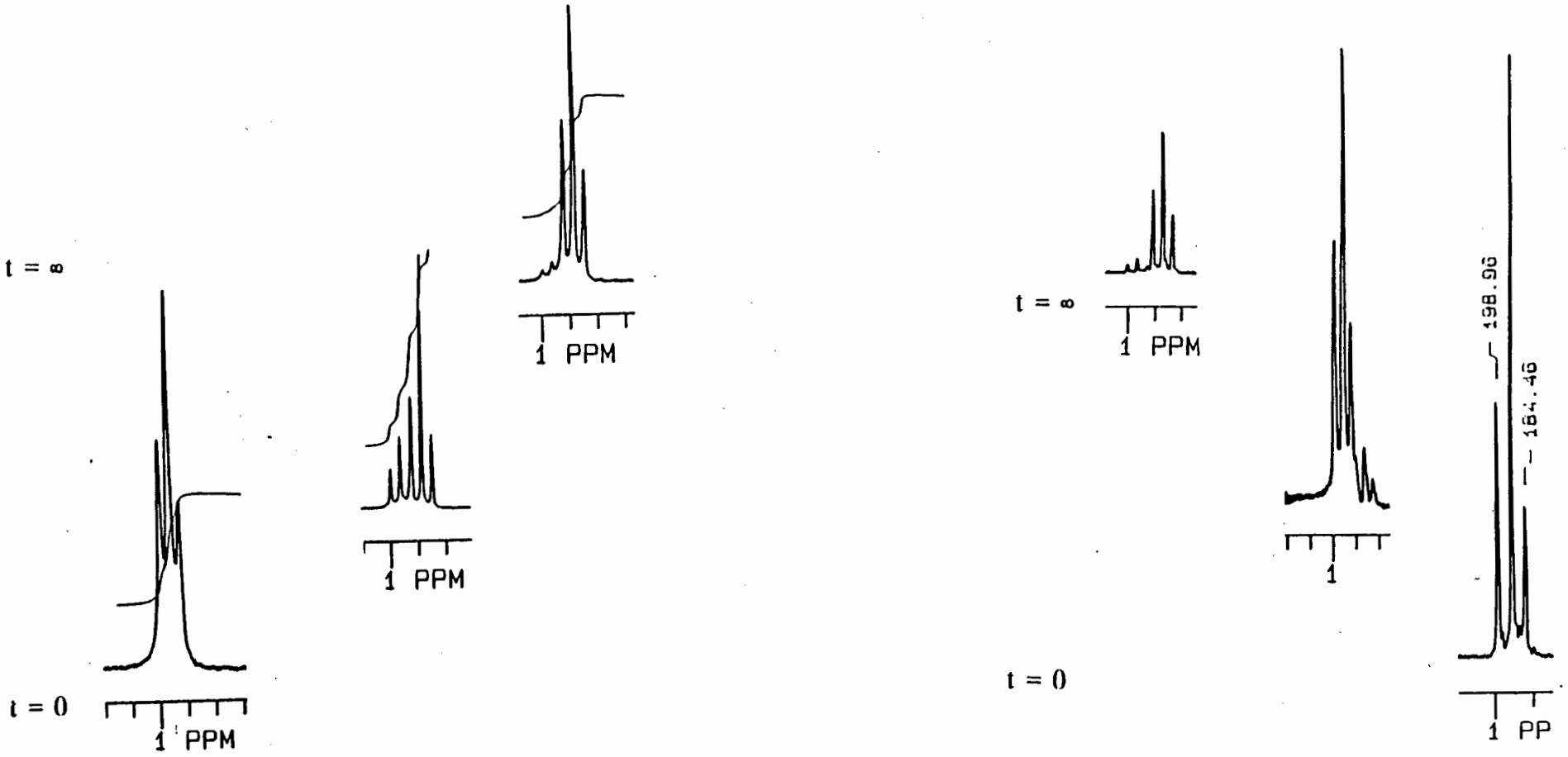

Fig 24 ^{1}H NMR spectra monitoring the reaction of complexes 30 and 31 with NaI.

2.9 THE RELEVANCE OF THE REACTIONS IN SECTION 2.8

Of the many mechanisms proposed[33-35] for the Fischer-Tropsch reaction, the carbide mechanism is favoured by many[36]. This mechanism fails to explain the product distribution observed in the above reaction, particularly that of the 1-alkenes which reach a peak at about C_4, whereas n-alkanes reach a peak at a much higher carbon number (C_8)[37]. Clearly two different intermediates should be responsible for the formation of alkanes and alkenes.

In the proposed carbide mechanism for the Fischer-Tropsch reaction, coupling of two surface methylene species forms the key intermediate[36] **a** (Scheme 5). The intermediate **a** has been proposed to grow along the catalyst surface by interacting with surface methylene to form a polymethylene bridged intermediate[38,39] **b**. The complexes, $[CpM(CO)_2]_2[\mu\text{-}(CH_2)_5]$ (M = Fe or Ru) can be models for the intermediates of type **b**. From our sequence of reactions (Scheme 4) we suggest a possible mechanism for the formation of 1-alkene in the Fischer-Tropsch reaction. The intermediates of type **b**, we believe, are held rigidly on the catalytic surface, and a hydride could be abstracted from the β-carbon (which is accessible to the surface) by a surface species such as $M^{\delta-}\text{-}CH_3{}^{\delta+}$, to form intermediates of type **c**. Since intermediates of types **b** and **c** are sterically demanding, they may be short lived on the surface and could react with M-H to form intermediates of types **d** and **e** respectively. The intermediates of type **d** (which may now be long lived due to less steric demands and can undergo chain growth) could react with M-H surface species to form n-alkanes. The intermediates of type **e** (in which further chain growth can no longer occur) could react with a suitable surface ligand to form the 1-alkenes

(Scheme 5). The intermediates of type **d** can also be formed from the intermediate **a** via the surface ethyl species as shown in the Scheme 5.

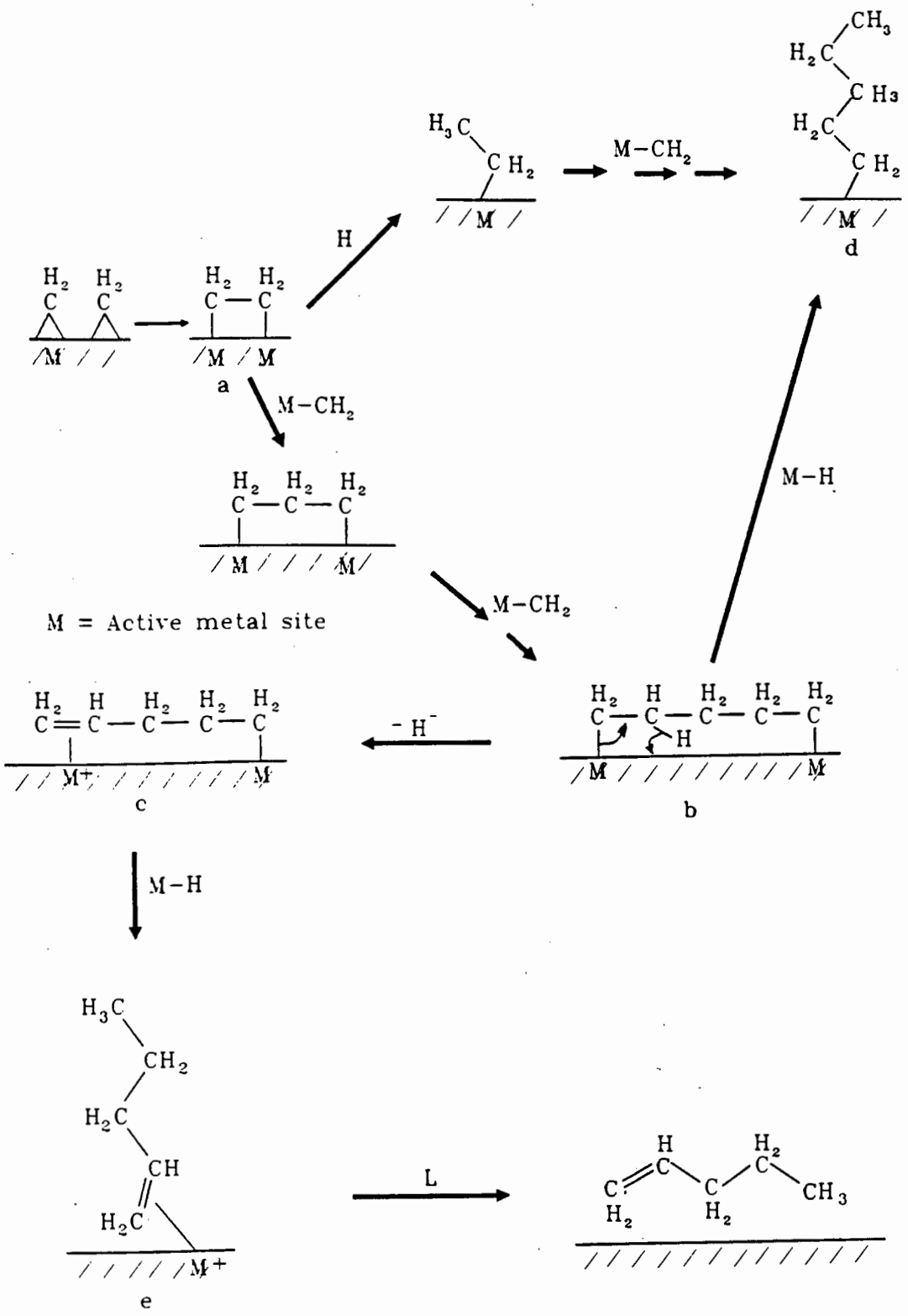

Scheme 5

Ruthenium catalysts are known to give n-alkanes rather than 1-alkenes as products in CO hydrogenation reactions[40]. This may be due to ruthenium being a better hydrogenation catalyst than Fe[41] and the alkenes (as shown in scheme 5) may be hydrogenated to alkanes in secondary reaction[42].

2.10 CONCLUSION

The ethylene-bridged complex $[CpRu(CO)_2]_2[\mu\text{-}(CH_2CH_2)]$ was succesfully synthesized and characterized. The solid state structure of $[CpRu(CO)_2]_2[\mu\text{-}(CH_2CH_2)]$ was also determined.

The reactions of $[CpRu(CO)_2]_2[\mu\text{-}(CH_2CH_2)]$ with donor ligands (PPh_3 and PMe_2Ph) do not appear to give any CO insertion products. The complex $[CpRu(CO)_2]_2[\mu\text{-}(CH_2CH_2)]$ undergoes oxidative demetallation reactions with oxidants such as Ph_3CPF_6 and $AgBF_4$. The reactions of $[CpRu(CO)_2]_2[\mu\text{-}(CH_2CH_2)]$ with acids (CF_3COOH and HCl) give the cationic species $[CpRu(CO)_2(C_2H_4)]^+$. From these latter reactions it appears that the α-carbon in $[CpRu(CO)_2]_2[\mu\text{-}(CH_2CH_2)]$ is slightly electrophilic, i.e. $Ru^{\delta-}\text{-}C^{\delta+}$. The complex $[CpRu(CO)_2]_2[\mu\text{-}(CH_2CH_2)]$ reacts with MeOH to give a methoxyethyl complex $[CpRu(CO)_2(CH_2CH_2OMe)]$. The decomposition of $[CpRu(CO)_2]_2[\mu\text{-}(CH_2CH_2)]$, both in the solid and in solution, leads to the formation of ethylene and the dimer, $[CpRu(CO)_2]_2$.

The cationic complexes $[\{CpM(CO)_2\}_2\{\mu\text{-}(C_3H_5)\}]^+PF_6^-$ (M = Fe or Ru) were also successfully synthesized and characterized. The solid state crystal structures of these complexes $[\{CpM(CO)_2\}_2\{\mu\text{-}(C_3H_5)\}]^+PF_6^-$ (M = Fe or Ru) were also

determined. The fluxional behaviour of the bridging allylic group in $[\{CpRu(CO)_2\}_2\{\mu\text{-}(C_3H_5)\}]^+PF_6^-$ was also studied. As in the complex $[\{CpFe(CO)_2\}_2\{\mu\text{-}(C_3H_5)\}]^+PF_6^-$, the ^1H NMR of the allylic group in complex $[\{CpRu(CO)_2\}_2\{\mu\text{-}(C_3H_5)\}]^+PF_6^-$ exhibits a $AA'BB'X$ spin system at lower temperatures, while an $AA'A''A'''X$ spin system is observed at higher temperatures.

A sequence of reactions of $[CpM(CO)_2]_2[\mu\text{-}(C_5H_{10})]$ (M = Fe or Ru) with Ph_3CPF_6, CF_3COOH and NaI was shown to give 1-pentene as the sole organic product.

2.11 REFERENCES

1. M. C. Cook, N. J. Forrow and S. A. R. Knox, *J. Chem. Soc. Dalton. Trans.*, **1983**, 2435.
2. (a) K. P. Finch, J. R. Moss and M. L. Niven, *Inorg. Chim. Acta*, **1989**, 166, 181; (2) S. J. Archer, K. P. Finch, H. B. Friedrich, J. R. Moss and A. M. Crouch, *Inorg. Chim. Acta*, **1991**, 182, 145.
3. Y. C. Lin, J. C. Calabrese and S. S. Wreford, *J. Am. Chem. Soc.*, **1983**, 105, 167.
4. W. Beck *Polyhedron*, **1988**, 7, 2255.
5. W. Beck and B. Olgemöller, *Chem. Ber.*, **1981**, 114, 867.
6. M. R. Burke, J. Takats, F. W. Grevels and G. J. A. Reuvers, *J. Am. Chem. Soc.*, **1983**, 105, 4092.
7. W. Kaminsky and H. Sinn, *Justus Liebigs Ann. Chem.*, **1975**, 424.
8. J. Breimair, B. Niemer, K. Raab andd W. Beck, *Chem. Ber.*, **1991**, 124, 1059.
9. (a) R. B. King, *Inorg. Chem.*, 85, **1963**, 531; (b) M. E. Brown, K. J. Hindson, J. R. Moss, L. G. Scott, *J. Organomet. Chem.*, **1985**, 282, 255.
10. D. W. Mathieson, Nuclear Magnetic Resonance for the Organic Chemist, Academic Press Inc. **1967**, pp. 110 - 117.
11. K. P. Finch, M. Sc. Thesis, University of Cape Town, **1988**.
12. A. Emeran, M. A. Gafoor, J. K. I. Goslett, Y-H Liao, L. Pimble and J. R. Moss, *J. Organomet. Chem.*, **1991**, 405, 237.
13. T. H. Coffield, J. Kozikowski and R. D. Closson, *J. Organomet. Chem.*, **1957**, 222, 598.

14. C. Masters, Homogeneous Transition Metal Catalysis - A Gentle Art, Chapman Hall (London) **1981.**

15. S. C. Kao, C. H. Thiel and R. Petit, *Organometallics,* **1983**, 2, 914.

16. K. P. Finch, M. A. Gafoor, S. F. Mapolie and J. R. Moss, *Polyhedron,* **1991**, 10, 963.

17. W. Jetz, and W. A. G. Graham, *J. Am. Chem. Soc*, **1967**, 89, 2773.

18. K. Stanley and M. C. Baird, *J. Am. Chem. Soc*, **1975**, 97, 4292.

19. S. Pelling, M. Sc Thesis, University of Cape Town, **1981.**

20. B. K. Blackburn, S. G. Davies and M. Whittaker, *J. Chem. Soc. Chem.* Commun., **1987**, 1344.

21. A. J. Deeming and B. L. Shaw, *J. Chem. Soc. (A),* **1971**, 376.

22. L. F. Johnson and W. C. Jankowski, "Carbon - 13 NMR spectra, A Collection of Assigned, Coded and Indexed Spectra", Wiley, New York, **1972.**

23. J. R. Moss and L. G. Scott, *J. Organomet. Chem.*, **1989**, 363, 351.

24. R. B. King and M. B. Bisnette, *J. Organomet. Chem.*, **1967**, 7, 311.

25. J. W. Faller and B. V. Johnson, *J. Organomet. Chem.*, **1975**, 88. 101.

26. J. W. Johnson and J. R. Moss, *Polyhedron*, **1985**, 4, 563.

27. A. Sanders, T. Bauch, C. V. Magatti, C. Lorenc and W.P. Giering, *J. Organomet. Chem.*, **1976**, 107, 359.

28. N. de Luca and A. Wojcicki, *J. Organomet. Chem.*, **1980**, 193, 359.

29. G. E. Jackson, J. R. Moss and L. G. Scott, *S. Afr. J. Chem.*, **1983**, 36, 69.

30. R.C. Kerber, W. P. Giering, T. Bauch, P. Waterman and E.-H. Chou, *J. Organomet. Chem.*, **1976**, 120, C31.

31. H. B. Friedrich, Ph. D Thesis, University of Cape Town, **1989.**

32. M. Laing, J. R. Moss and J. W. Johnson, *J. Chem. Soc. Chem. Comm.* **1977**, 656.

33. C. K. Rofer-de Poorter, *Chem. Rev.*, **1981**, 81, 447; W. A. Herrmann, *Angew,*

Chem. Int. Ed. Engl., **1982**, 21, 117; C. Masters, *Adv. Organometal. Chem.* **1979**, 17, 61.

34. (a) M. E. Dry, *J. Organomet. Chem.* **1989**, 372, 117; *(b) Catalysis Today*, **1990**, 6, 183.
35. G. Henrici-Olivè and S. Olivè, "The Chemistry of the Catalyzed Hydrogenation of Carbon Monoxide", Springer Verlag, Berlin, **1984**.
36. F. A. Cotton and G. Wilkinson, Advanced Inorganic Chemistry, 5th Ed. Wiley, New York, **1988**, p 1229.
37. Ref. 34 (a), p 147.
38. S. R. Craxford and E. K. Rideal, *J. Chem. Soc.* **1939**, 1604.
39. A. J. Hupert, in "Catalysis in C_1 Chemistry", Ed. W. Kiem, D. Reidel, **1983**, p 287.
40. Ref. 34 (b), p 184.
41. F. R. Hartley, Supported Metal Complex, D. Reidel, Dordrecht **1985**, p 157.
42. M. A. Gafoor and J. R. Moss, manuscript in preparation.

CHAPTER 3

THE SYNTHESIS AND CHARACTERIZATION OF SOME ALKYL AND HALOALKYL COMPLEXES OF RUTHENIUM

3.1 INTRODUCTION

Metal alkyl complexes of the type L_mMR (L_mM = metal with its associated ligands, R = an alkyl group) are the cornerstone of organometallic chemistry and their properties have been studied extensively because of their fundamental importance[1]. These complexes are involved in homogeneous catalysis as key intermediates and can also be models for metal alkyl species in heterogeneous catalysis[2]. These catalytic reactions include the isomerization, polymerization and hydroformylation of alkenes, as well as the Fischer-Tropsch reaction. Metal alkyl complexes of the type $[CpM(CO)_2R]$ are well known[2-7], however, few reactivity studies have been reported. Thus we have now investigated the reactivity of a ruthenium ethyl complex, viz., $[CpRu(CO)_2(CH_2CH_3)]$ (which is a mononuclear C_2 alkyl complex). The reactivity of this complex is compared with the ethylene-bridged complex, $[CpRu(CO)_2]_2[\mu\text{-}(CH_2CH_2)]$ (which is a dinuclear C_2 alkyl complex).

In this chapter we also describe some new functionalized alkyl ruthenium complexes, specifically haloalkyl complexes. The synthesis and properties of transition metal haloalkyl complexes are currently been being explored[8,9]. These complexes have been shown to be precursors to homo- and heterodinuclear $\mu(\alpha,\omega)$ alkanediyl complexes[10], as well as cyclic carbene complexes[11]. Halomethyl complexes of the main group metals have been extensively studied and shown to have many synthetic applications[12-14]. Analogous transition metal complexes of the type $[L_mMCH_2X]$ are well known. However, haloalkyl complexes of the type $[L_mM(CH_2)_nX]$, $n \geq 2$, are less well known, although some complexes of Pt[15,16], Mo, W[17,18], and Fe[9] have been studied. Thus, in our present studies, we have investigated the synthesis and characterization of the mononuclear haloalkyl

ruthenium complexes $[CpRu(CO)_2\{(CH_2)_nX\}]$ (n = 3, X = Cl, Br or I; n = 3 or 4, X = Br or I).

3.2 THE SYNTHESIS, CHARACTERIZATION AND REACTIVITY OF $[CpRu(CO)_2(CH_2CH_3)]$

3.2.1 THE SYNTHESIS AND CHARACTERIZATION OF $[CpRu(CO)_2(CH_2CH_3)]$

SYNTHESIS

Previously, the ethyl complex $[CpRu(CO)_2(CH_2CH_3)]$, **1**, has been reported[3-7] along with some characterization data. In our study the method of Wilkinson[3] was used for the synthesis of this complex, i.e. by the reaction of $Na[CpRu(CO)_2]$ with iodoethane. Complex **1** is an oil at room temperature and is volatile under high vacuum (ca. 0.1 mmHg).

CHARACTERIZATION

IR SPECTROSCOPY

In the infrared spectrum of complex **1** we observe two ν(CO) bands at 2019 and 1959 cm^{-1} (in hexane). No differences were observed in the ν(CO) band positions when compared with the related long chain alkyl complexes[2]. However, these bands are of higher frequency when compared with the dinuclear C_2 alkyl complex $[CpRu(CO)_2]_2[\mu\text{-}(CH_2CH_2)]$, **2** (2007, 1952 cm^{-1} in hexane). This may suggest that

there is less electron density on the Ru metal in complex **1** than in complex **2** and this suggests that the Ru - C(carbonyl) bond is slightly stronger in the latter.

^{1}H NMR SPECTROSCOPY

In the ^{1}H NMR spectrum of complex **1** we observe, as expected, three resonances at δ = 5.23 (s), 1.77 (q, $J_{H,H}$ = 7.6 Hz) and 1.37 ppm (t, $J_{H,H}$ = 7.6 Hz) for the Cp, methylene (α) and methyl protons respectively. Thus the ^{1}H NMR spectrum of the ethyl group of **1** exhibits peaks expected for a A_2X_3 spin system. However, a further splitting of each of the peaks was observed (Fig. 1). This could be attributed to the fact that a departure from the A_2X_3 spin system causes a distinctive "second - order" hyperfine splitting of each component[19]. This hyperfine splitting is observed in the organic compounds of the type CH_3CH_2X (where $X \neq H$)[19].

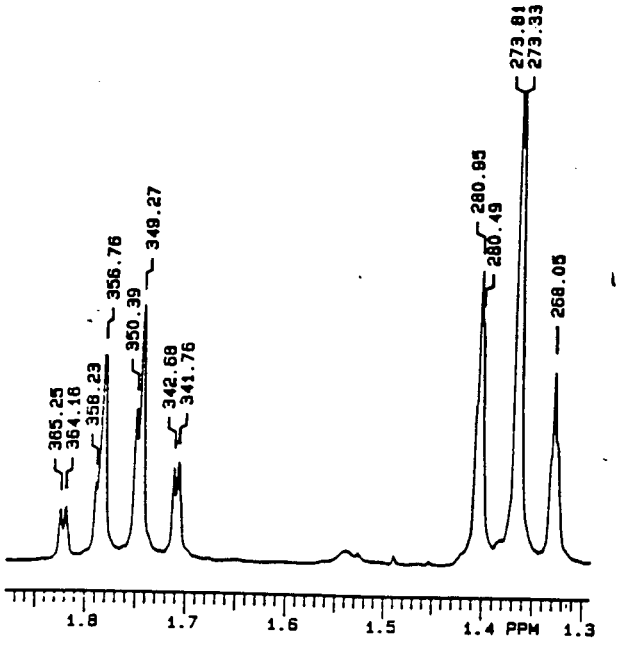

Fig. 1 Resonances due to α and β-protons.

No significant variations were observed for the Cp and α - proton resonances of complex **1** when compared to the analogous long chain alkyl complexes[2]. However, a significant variation was found for the methyl protons (Table 1). This suggests that the effect of the metal is felt by the methyl protons in complex **1** but this effect decreases as the chain length increases, as may be expected and hence the "tail end" of the alkyl chain of these long chain complexes may appear as normal organic hydrocarbons.

Table 1 ^{1}H NMR data[a] for [CpRu(CO)$_2$R]

R	Cp	Ru-CH_2	$(CH_2)_n$	CH_3
C_2H_5	5.23 s	1.77[b] q	-	1.37[b] t
C_6H_{13}[c]	5.19 s	1.60 m	1.24 bs (8H)	0.84 t
C_7H_{15}	5.18 s	1.58 m	1.20 bs (10H)	0.82 t
C_8H_{17}	5.20 s	1.65 m	1.28 bs (12H)	0.88 t
C_9H_{19}	5.22 s	1.65 m	1.27 bs (14H)	0.90 t
$C_{10}H_{21}$	5.14 s	1.60 m	1.23bs (16H)	0.87 t
$C_{11}H_{23}$	5.22 s	1.61 m	1.26 bs (18H)	0.88 t
$C_{12}H_{25}$	5.15 s	1.60 m	1.23 bs (20H)	0.88 t

[a] Measured in $CDCl_3$ relative to TMS (δ = 0.00 ppm)

[b] J = 7.6 Hz; [c] J = 6.5 Hz; t = triplet, m = multiplet, bs = broad singlet

[c] reference 2 for the complexes where R = C_6H_{13} - $C_{12}H_{25}$

^{13}C NMR SPECTROSCOPY

We have obtained the ^{13}C NMR (proton-decoupled as well as proton-coupled) data for complex **1**. In the proton-decoupled ^{13}C NMR spectrum we observe single resonances at δ = 202.4 , 88.6, 24.2 and -10.0 ppm for the carbonyl, Cp, methyl and methylene (α) carbons respectively. The α-carbon resonance, which appears at high field, is characteristic of the carbon bonded to ruthenium. Furthermore, the α-carbon resonance of complex **1** is at significantly higher field position when compared to the related long chain alkyl complexes[2]. This suggests that the electronic environment of the α-carbon is different in complex **1**.

In the proton-coupled ^{13}C NMR spectrum we observe resonances at δ = -10.0 (triplet, $J(^{13}CH)$ = 132.2 Hz), δ = 24.2 (quartet, $J(^{13}CH)$ = 123.1 Hz) and δ = 88.6 ppm (a doublet of quintets, $J(^{13}CH)$ = 177.90 Hz, $J(^{13}CCH)$ = 6.9 Hz) for the α, methyl and the Cp carbons respectively. A further coupling, possibly a long range carbon-hydrogen coupling between nuclei separated by two bonds, was observed for the ethyl group but it was not not well resolved. However, the doublet of quintets was resolved for the Cp carbons of complex **1**. This doublet of quintets is due to the coupling of each Cp carbon to its bonded proton as well as to the remaining four protons of the Cp ligand (see also section 2.3). This long range carbon-hydrogen coupling was observed for the ethylene carbons in the ethylene-bridged complex, **2**.

MASS SPECTROMETRY

We have obtained a low resolution mass spectrum of complex **1**. The spectrum shows ion peaks at m/e 251 and 444 corresponding to $[CpRu(CO)_2(CH_2CH_3)]^+$

and $[CpRu(CO)_2]_2$ respectively. We believe that the $[CpRu(CO)_2]_2$ is formed under the electron impact mass spectral conditions since it was not initially present in the sample. The formation of the dimer, $[CpRu(CO)_2]_2$, could be attributed to the coupling of two "$CpRu(CO)_2$" fragments. Similarly, in the mass spectra of complex **2** and $[CpRu(CO)_2(CH_2CH_2OMe)]$ ion peaks due to the $[CpRu(CO)_2]_2$ were also observed (see sections 2.3 and 2.4.2). However, high resolution mass spectral data would enable definite assignments of the ions to be formed.

The intensities and probable assignments of the peaks due to the fragmentation of complex **1** are presented in Table 2. We suggest that the fragmentation of the complex **1** takes place by successive loss of two CO groups and subsequent loss of a C_2H_5 group. The fragmentation leads to the formation of $[CpRu(CO)(C_2H_5)]^+$ (m/e 223), $[CpRu(C_2H_5)]^+$ (m/e 195) and $[CpRu]^+$ (m/e 167) respectively.

Table 2 MASS SPECTRAL DATA[a] FOR $[CpRu(CO)_2(CH_2CH_3)]$

ION[b]	(m/e)	RELATIVE PEAK INTENSITIES[c]
$[M]^+$	251	10
$[M-\{CO\}]^+$	223	24
$[M-\{2CO\}]^+$	195	21
$[CpRu]^+$	167	100

[a] The ions peaks due to the fragmentation of $[CpRu(CO)_2]_2$ are not included in the above table.

[b] M = $[CpRu(CO)_2(CH_2CH_3)]$, ion refers to probable assignment

[c] peak intensities are relative to base peaks at m/e 167.

3.2.2 THE REACTIVITY OF [CpRu(CO)$_2$(CH$_2$CH$_3$)]

We were interested to compare the reactivity of [CpRu(CO)$_2$(CH$_2$CH$_3$)] with [CpRu(CO)$_2$]$_2$[μ-(CH$_2$CH$_2$)], since both these complexes contain a C_2 alkyl group.

WITH A PROTIC ACID

The reaction of complex **1** with trifluoroacetic acid in $CDCl_3$ was carried out in an NMR tube (Eq. 1).

$$[CpRu(CO)_2(CH_2CH_3)] + CF_3COOH \longrightarrow [CpRu(CO)_2\{OC(O)CF_3\}] + C_2H_6$$

Eq. 1

The ^{1}H NMR data suggests that the reaction leads to the formation of [CpRu(CO)$_2${OC(O)CF$_3$}] and ethane (δ = 5.48 ppm, [(C$_5$H$_5$)Ru(CO)$_2${OC(O)CF$_3$}]; δ = 0.84 ppm, C$_2$H$_6$). From ^{1}H NMR spectroscopy the formation of [CpRu(CO)$_2${OC(O)CF$_3$}] and ethane are quantitative. In contrast, a similar reaction of complex **2** with CF_3COOH leads to the formation of two complexes, viz. [CpRu(CO)$_2$(C$_2$H$_4$)]$^+$ and [CpRu(CO)$_2$OC(O)CF$_3$]; no ethane was detected. This suggests that the α-carbon undergoes an electrophilic attack by CF_3COOH in complex **1**. These results may imply that the α-carbon in complex **1** is slightly nucleophilic (Ru$^{\delta+}$–C$^{\delta-}$) in contrast to complex **2** where there may be a contribution from Ru$^{\delta-}$–C$^{\delta+}$ (see also Chapter 2.4.5).

WITH MeOH

No reaction was observed when complex **1** in MeOH was heated under reflux for 14 days. However, the reaction of complex **2** in refluxing methanol for 5 hours leads to the formation of the methoxyethyl complex $[CpRu(CO)_2(CH_2CH_2OMe)]$ and the dimer, $[CpRu(CO)_2]_2$. This result may also suggest that the α-carbon in complex **2** is slightly electrophilic ($Ru^{\delta-}-C^{\delta+}$). Steric crowding in complex **2** could also be an important factor in the cleavage of Ru–C bond.

WITH TRITYL SALT

The reaction of complex **1** with Ph_3CPF_6 leads to the formation of the expected cationic compound, $[CpRu(CO)_2(C_2H_4)]^+PF_6^-$, **3**, in high yield (Eq. 2).

$$[CpRu(CO)_2(CH_2CH_3)] \xrightarrow{Ph_3CPF_6} [CpRu(CO)_2(C_2H_4)]^+PF_6^- + Ph_3CH$$

Eq. 2

The characterization data obtained for the complex **3** are in good agreement with the literature data[20]. In the above reaction we believe that a β-hydride was abstracted. The reaction of complex **2** with Ph_3CPF_6 takes a different course and leads to the formation of complex **3**. Since a hydride could now not have occurred, we believe that an oxidative demetallation of complex **2** occurs in the latter reaction.

From the comparative study of the data and reactions of these C_2 alkyl complexes (complexes **1** and **2**) several general conclusions can be drawn:

1) the $CpRu(CO)_2$ group has a significant effect on the C_2 alkyl fragments bonded to it, which is reflected in the NMR resonances;
2) the α-carbon atom appears to be slightly nucleophilic in complex **1** ($Ru^{\delta+}-C^{\delta-}$);
3) the α-carbon atom appears to be slightly electrophilic in complex **2** ($Ru^{\delta-}-C^{\delta+}$);
4) the reactivity of complexes **1** and **2** towards Ph_3CPF_6 is selective.

We believe that the comparative study of these C_2 alkyl complexes is relevant to our studies modelling the key intermediates such as **a** and **b** (Scheme 1) that have been proposed in the carbide mechanism of the Fischer-Tropsch reaction[21]. The difference in the reactivity patterns shown by the complexes **1** and **2** may suggest that the intermediates **a** and **b** behave differently on the catalytic surface. Furthermore, we believe that intermediate **a** may be responsible for the initiation of two different types of alkyl intermediates such as **c** and **d**. Such intermediates may eventually lead to the formation of n-alkanes and 1-alkenes respectively via two different routes as shown in scheme 1 and further dicussed in section 2.8.

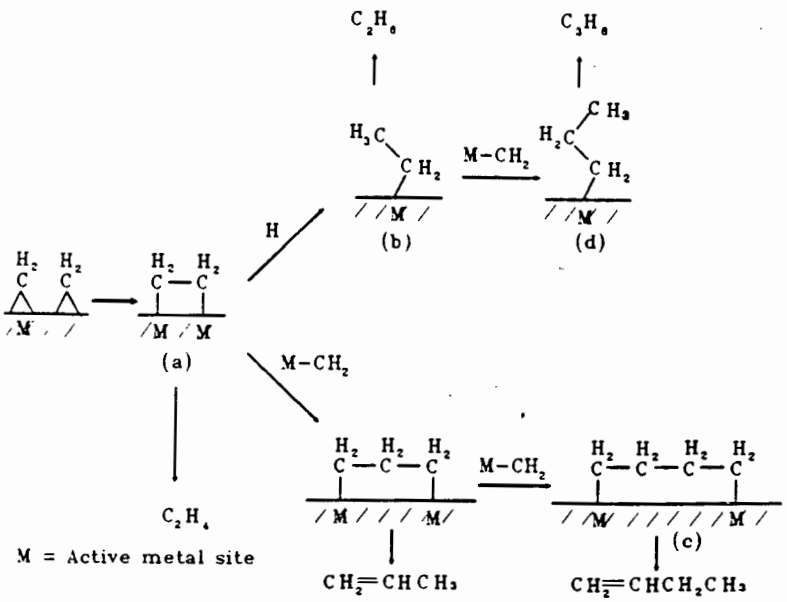

Scheme 1

3.3 THE SYNTHESIS AND CHARACTERIZATION OF SOME HALOALKYL COMPLEXES OF RUTHENIUM

3.3.1 THE SYNTHESIS OF HALOALKYL COMPLEXES

3.3.1.1 THE SYNTHESIS OF $[CpRu(CO)_2\{(CH_2)_nX\}]$ (n = 3, X = Cl or Br; n = 4 or 5, X = Br)

The haloalkyl complexes, $[CpRu(CO)_2\{(CH_2)_nX\}]$ (n = 3, X = Cl or Br ; n = 4 or 5, X = Br) were prepared from the reaction of $Na[CpRu(CO)_2]$ with $X(CH_2)_2X$ (Eq. 3).

$$Na[CpRu(CO)_2] \xrightarrow{X(CH_2)_nX} [CpRu(CO)_2\{(CH_2)_nX\}] + NaX$$

Eq. 3

This route has also been used to prepare other transition metal haloalkyl compounds[22,23]. The bromoalkyl and chloropropyl complexes were obtained in relatively good yield, but difficulty was experienced in isolation of these haloalkyl complexes from the unreacted dihaloalkanes, $X(CH_2)_nX$. This difficulty increases as n increases, because as the length of the alkyl chain increases the boiling point increases. These complexes are colourless oils at room temperature. The above reactions were carried out at low temperatures (-78 °C) to prevent the formation of dinuclear alkanediyl complexes, $[CpRu(CO)_2]_2[\mu\text{-}(CH_2)_n]$ (n = 3, 4 or 5). These alkanediyl complexes are formed at high temperatures presumably by the reaction of initially formed $[CpRu(CO)_2\{(CH_2)_nX\}]$ with $Na[CpRu(CO)_2]$.

3.3.1.2 THE CONVERSION OF $[CpRu(CO)_2\{(CH_2)_nBr\}]$ TO $[CpRu(CO)_2\{(CH_2)_nI\}]$ (n = 3, 4 or 5)

The reaction of bromoalkyl iron and molybdenum complexes with NaI has been shown to give iodoalkyl complexes[22]. We show that in a similar way the complexes $[CpRu(CO)_2(CH_2)_nBr]$ (n = 3, 4 or 5) can be converted to the iodoalkyl analogues (Eq. 4).

$$[CpRu(CO)_2(CH_2)_nBr] \xrightarrow{NaI} [CpRu(CO)_2\{(CH_2)_nI\}] + NaBr$$

(Eq. 4)

The above reaction is best monitored by ^1H NMR spectroscopy. The ^1H NMR spectra reveal the up-field shift of the CH_2X resonance as X changes from Br to I. The conversion of bromoalkyl to iodoalkyl complexes is quantitative. However, it is rather difficult to convert the chloropropyl complex, viz. $[CpRu(CO)_2\{(CH_2)_3Cl\}]$, to its iodo analogue[24]. All the above iodoalkyl complexes are colourless oils at room temperature, except for the complex where n = 3, the iodopropyl is a low melting crystalline solid.

3.3.2 THE CHARACTERIZATION OF HALOALKYL COMPLEXES

The haloalkyl complexes were characterized by infrared, NMR spectroscopy (^1H, ^{13}C as well as COSY and HETCOR {n = 3 or 5}), and mass spectroscopy.

INFRARED SPECTROSCOPY

In the IR spectra we observe no significant shift in the ν(CO) bands for the bromo- and iodoalkyl complexes, $[CpRu(CO)_2\{(CH_2)_nX\}]$. However, There is a slight trend towards low frequency, as the alkyl chain length increases (See Table 3). This suggests that the electron withrawing effect of halogens decreases as the chain length increases.

Table 3 Data (IR, M.P. Yield) for $[CpRu(CO)_2\{(CH_2)_nX\}]$

n	X	YIELD (%)	M.P. (°C)	IR ν(CO)[a](cm^{-1}) (in hexane)	
3	Cl	76	Oil	2021	1964
	Br	64	Oil	2022	1965
	I[b]	71	37-39	2022	1965
4	Br	69	Oil	2020	1961
	I	75	Oil	2020	1961
5	Br	74	Oil	2019	1960
	I	79	Oil	2019	1960

[a] all peaks are sharp and very strong

[b] data from reference 22

NMR SPECTROSCOPY

In the ^1H NMR spectra for these haloalkyl complexes we observe that the Cp proton resonances are not affected by either n or X. However, X affects the shift of the CH_2X resonances. These resonances are shifted by 0.2 ppm up-field as X changes from Br to I. We also observe that the α-proton resonances appear at high field for the complexes where n = 3 and 4, while the γ-proton resonances appear at high field for the complex where n = 5 (see Figures 3 and 4). A possible explanation may be that there is an interaction of the metal atom with the γ-protons, causing shielding of the γ-protons (Fig. 2); with this interaction being pronounced in complexes where n = 5.

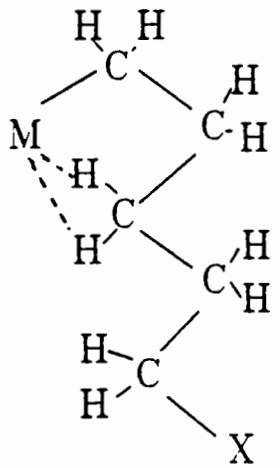

Fig. 2

Table 4 ^{1}H NMR[a] Data for the complexes [CpRu(CO)$_2${(CH$_2$)$_n$X}]

n	X	Cp	$C\underline{H_2}X$	α-$C\underline{H_2}$	β-$C\underline{H_2}$	γ-$C\underline{H_2}$	δ-$C\underline{H_2}$
3	Cl	5.23	3.42t(J = 7.2 Hz)	1.60m	1.97q(J = 7.0 Hz)		
	Br	5.24	3.31t(J = 7.0 Hz)	1.59m	2.05		
	I	5.21	3.08t(J = 7.2 Hz)	1.56m	2.04		
4	Br	5.24	3.43t(J = 6.7 Hz)	1.64m	1.64	1.85m	
	I	5.21	3.18t(J = 6.6 Hz)	1.64m	1.64	1.84m	
5	Br	5.21	3.38t(J = 6.9 Hz)	1.60m	1.60	1.42m	1.85m(J = 7.1 Hz)
	I	5.22	3.17t(J = 6.9 Hz)	1.56m	1.56	1.37m	1.83m(J = 7.2 Hz)

[a] measured in $CDCl_3$ relative to TMS (δ = 0.00 ppm), α-$C\underline{H_2}$ refers to those protons on the carbon α to ruthenium etc.,

t = triplet, q = quintet, m = multiplets

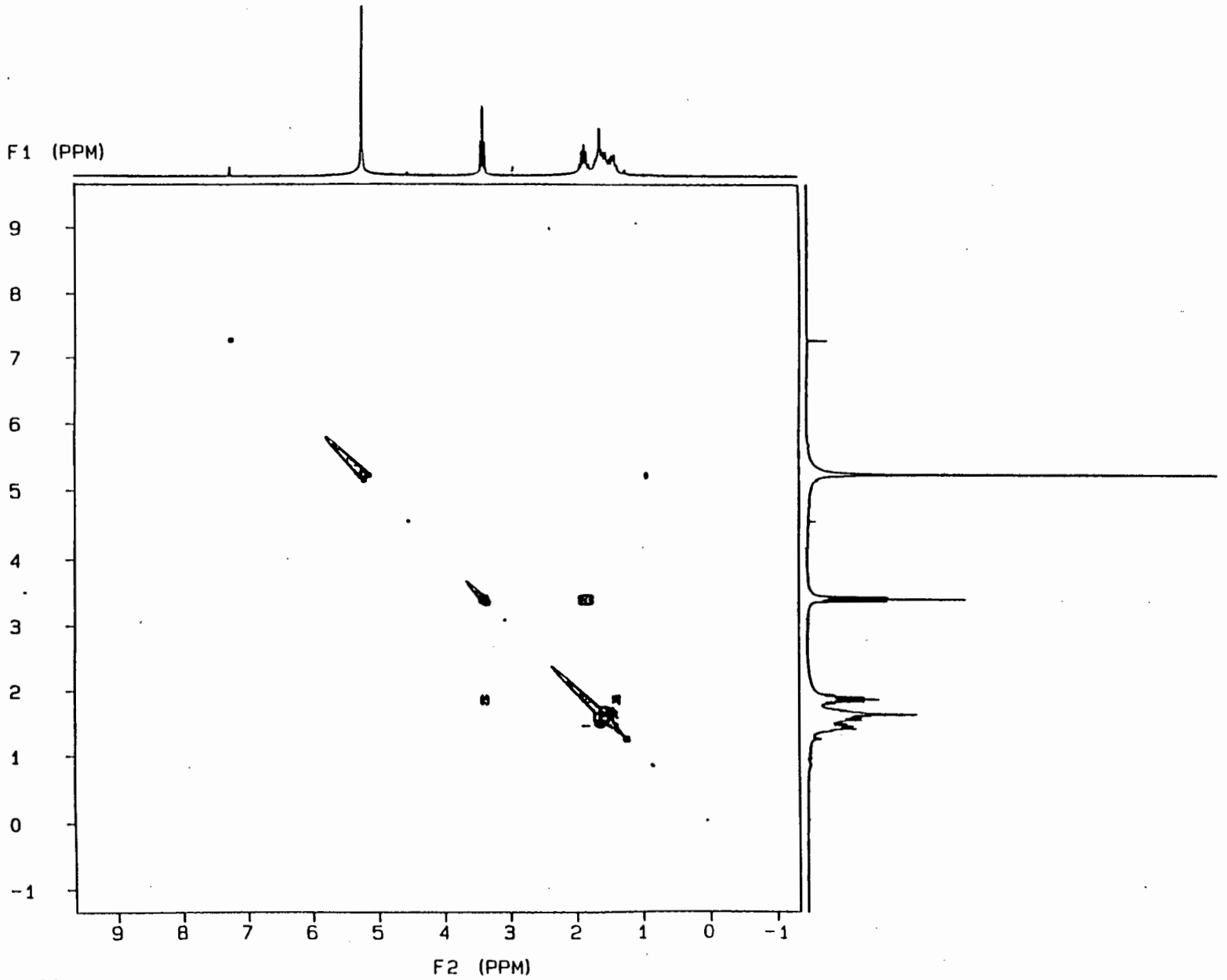

Fig. 3 COSY of [CpRu(CO)$_2${(CH$_2$)$_5$Br}]

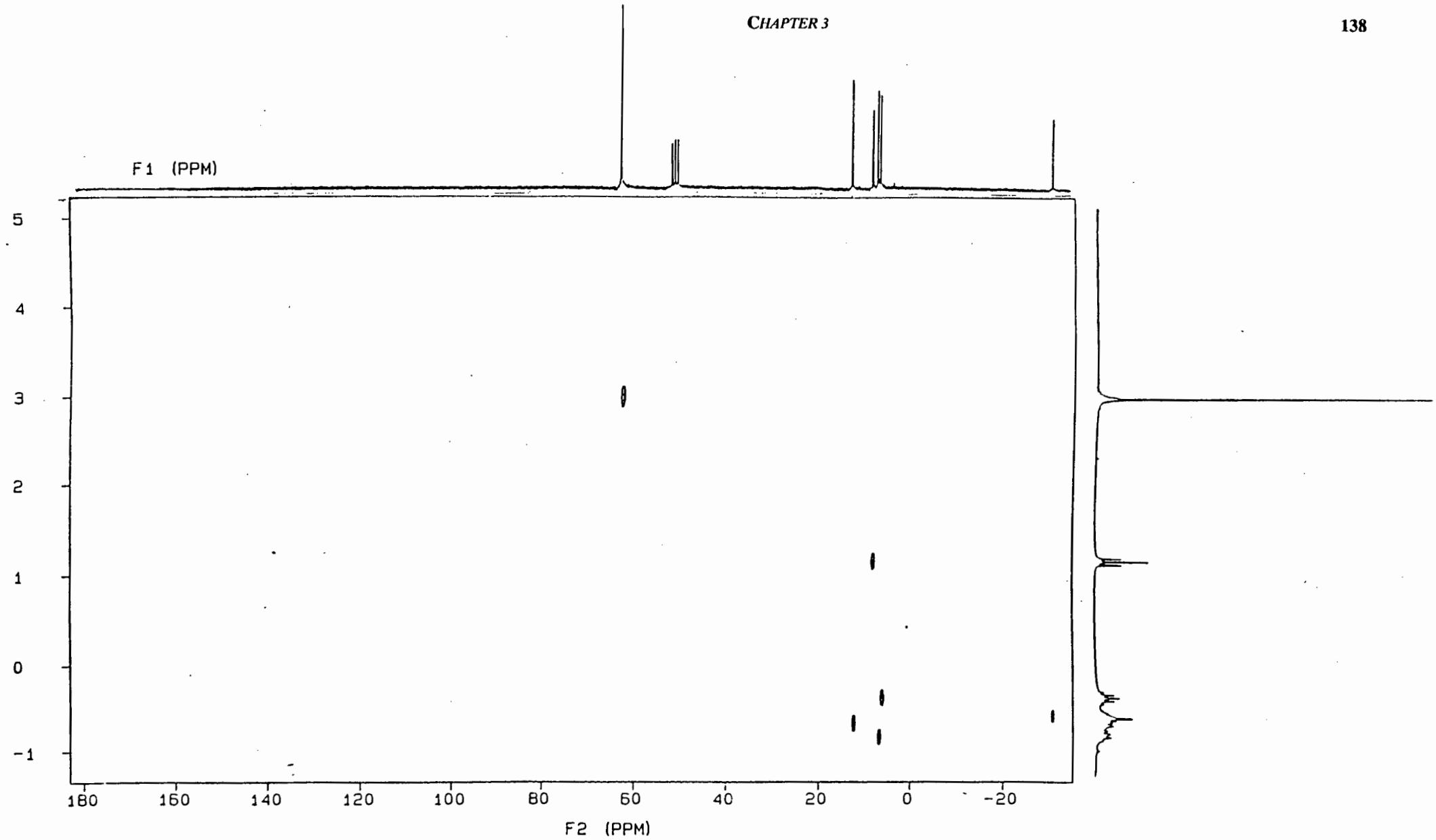

Fig. 4 HETCOR of $[CpRu(CO)_2\{(CH_2)_5Br\}]$

In the ^{13}C NMR spectra for the haloalkyl complexes we observe no variations in the resonances due to CO and Cp carbons. However, the α-carbon resonances in the complex where n = 3 are at higher field than those complexes where n = 4 or 5 (Table 5). This implies that the effect of halogens on the α-carbon resonances diminishes as the alkyl chain length increases. Furthermore, the α-carbon resonance for the complex where n = 3 is at higher field for X = Br than for X = I, which may indicate an interaction between the metal atom with the γ - CH_2 - X bond; with this interaction being stronger for the iodoalkyl complex (X = I). This type of interaction was also proposed by Monaghan and Puddephatt[15] for the complex [Pt(Phen)(Me_2)I{(CH_2)$_3$}].

Furthermore, in the ^{13}C NMR spectra we observe an up-field shift of ca. 26 ppm for the CH_2X resonances as X changes from Br to I (see Figures 5 and 6).

Table 5 ^{13}C **NMR data[a] for the complexes** $[CpRu(CO)_2\{(CH_2)_nX\}]$

n	X	CO	Cp	$\underline{C}H_2X$	α-$\underline{C}H_2$	β-$\underline{C}H_2$	γ-$\underline{C}H_2$	δ-$\underline{C}H_2$
3	Br	201.78	88.41	36.19	-7.29	42.48		
	I[b]	201.80	88.40	10.10	-4.50	43.50		
4	Br[b]	202.10	88.50	33.80	-5.30	37.40	37.40	
	I[b]	201.10	88.50	7.40	-5.60	40.10	38.00	
5	Br	202.32	88.49	34.22	-4.12	38.69	33.14	32.51
	I	202.31	88.49	7.58	-4.10	38.50	35.51	33.29

[a] measured in $CDCl_3$ relative to TMS (δ = 0.00 ppm)

[b] reference 22

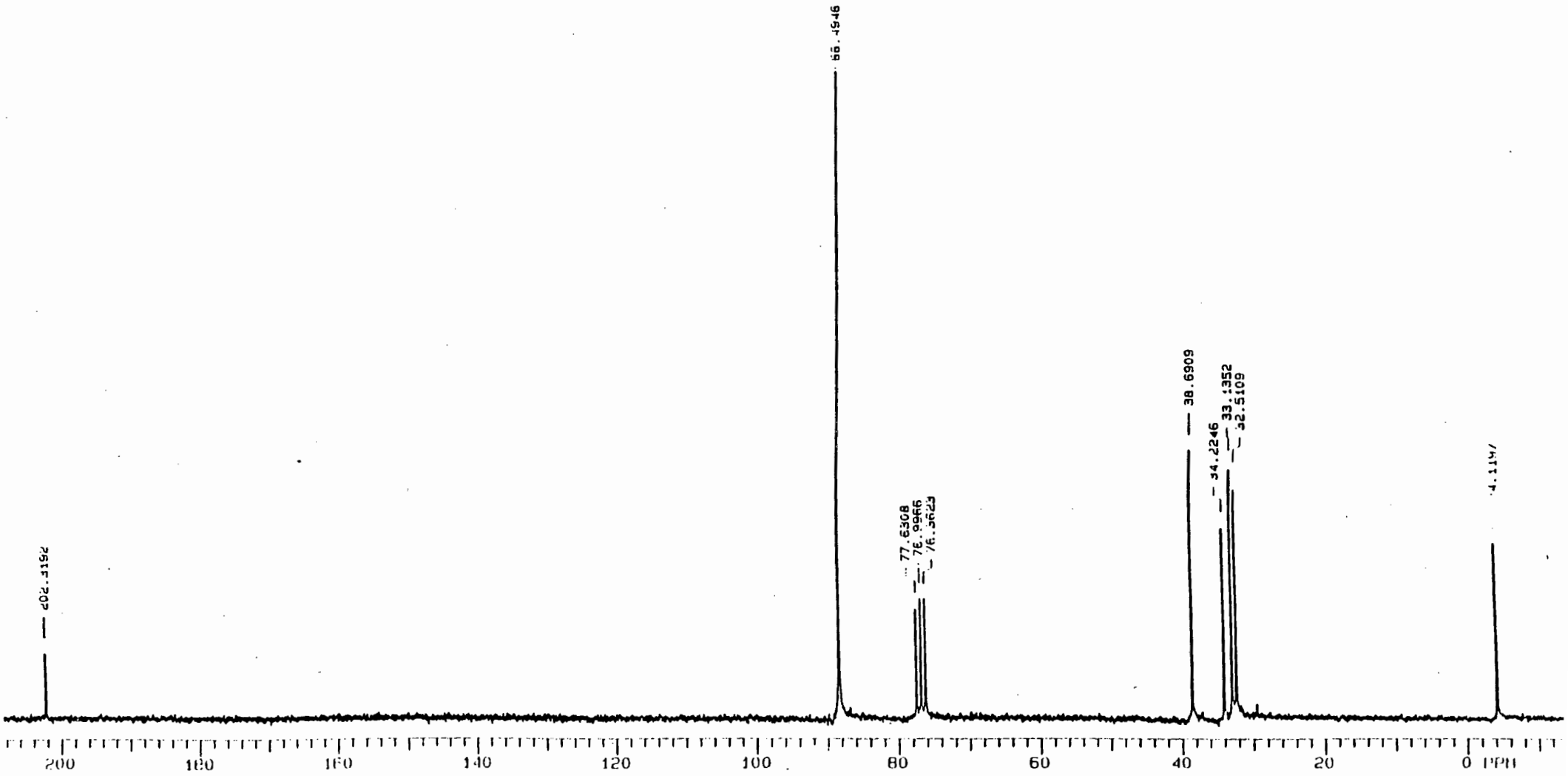

Fig. 5 ^{13}C NMR spectrum for $[CpRu(CO)_2\{(CH_2)_5Br\}]$

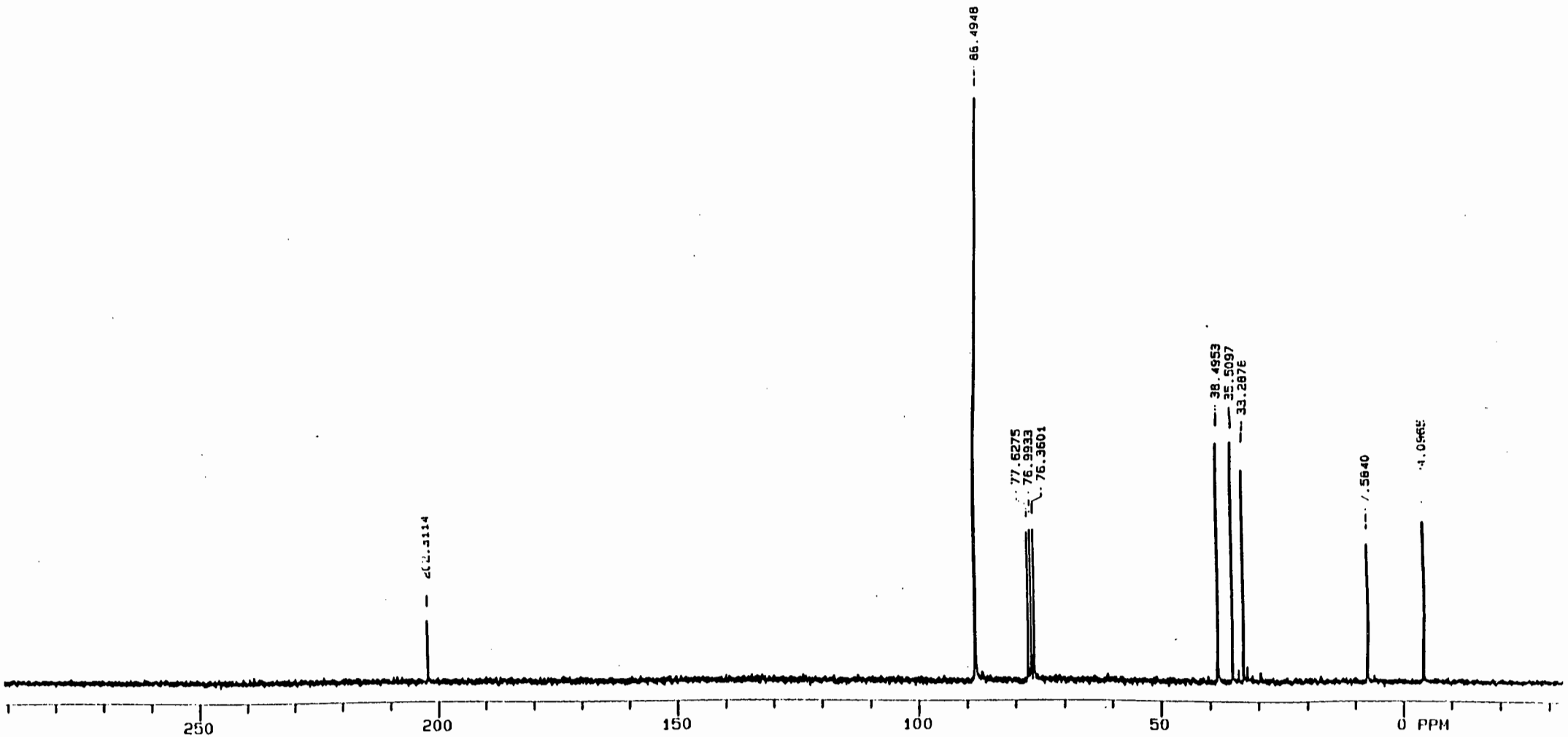

Fig. 6 ^{13}C NMR spectrum for $[CpRu(CO)_2\{(CH_2)_5I\}]$

MASS SPECTROMETRY

We have obtained low resolution mass spectra of the haloalkyl complexes, $[CpRu(CO)_2\{(CH_2)_nX\}]$ (n = 3, 4 or 5, X = Br; n = 3 or 4 X = I). The molecular ion peaks were observed for all the above haloalkyl complexes, except for the complexes where n = 3. The isotopic patterns in the spectra are not well resolved. However, the spectra indicate that the ruthenium haloalkyl complexes behave identically to their iron analogues under the electron impact mass spectral conditions. The intensities and probable assignments of peaks are presented in tables 6-8.

Table 6 MASS SPECTRA DATA FOR $[CpRu(CO)_2\{(CH_2)_3X\}]$ (X = Br or I)

ION[a]	RELATIVE PEAK INTENSITIES[b]	
	X = Br	X = I
$[M]^+$	-	-
$[M-\{(CH_2)_3\}]^+$	36	69
$[M-\{(CO)(CH_2)_3\}]^+$	39	34
$[M-\{2(CO)(CH_2)_3\}]^+$	37	31
$[M-\{(CH_2)_3X\}]^+$	19	13
$[M-\{(CO)(CH_2)_3X\}]^+$	38	31
$[M-\{2(CO)(CH_2)_3X\}]^+$	100	100

[a] M = $[CpRu(CO)_2(CH_2)_3X]$ (X = Br or I), ion refers to probable assignment

[b] peak intensities are relative to base peaks at m/e 167

Table 7 MASS SPECTRA DATA FOR $[CpRu(CO)_2\{(CH_2)_4X\}]$ (X = Br or I)

ION[a]	RELATIVE PEAK INTENSITIES[b]	
	X = Br	X = I
$[M]^+$	6	3
$[M-\{CO\}]^+$	3	-
$[M-\{2(CO)\}]^+$	13	33
$[M-\{(CO)(CH_2)_4X\}]^+$	33	32
$[M-\{2(CO)(CH_2)_4X\}]^+$	100	100
$[M-\{(CH_2)_4\}]^{+c}$	-	-
$[M-\{(CO)(CH_2)_4\}]^+$	19	16
$[M-\{2(CO)(CH_2)_4\}]^+$	23	18

[a] M = $[CpRu(CO)_2(CH_2)_4X]$ (X = Br or I), ion refers to probable assignment

[b] peak intensities are relative to base peaks at m/e 167

[c] same in low resolution as [M-{2CO}]

Table 8 MASS SPECTRA DATA FOR $[CpRu(CO)_2\{(CH_2)_5Br\}]$

ION[a]	RELATIVE PEAK INTENSITIES[b]
$[M]^+$	7
$[M-\{CO\}]^{+c}$	
$[M-\{2(CO)\}]^{c+}$	
$[M-\{2(CO)(CH_2)_5Br\}]^+$	100
$[M-\{(CO)(CH_2)_5Br\}]^+$	50
$[M-\{(CH_2)_5\}]^+$	16
$[M-\{2(CO)(CH_2)_5\}]^+$	22
$[M-\{(CO)(CH_2)_5\}]^+$	32

[a] M = $[CpRu(CO)_2(CH_2)_5Br]$, ion refers to probable assignment

[b] peak intensities are relative to base peaks at m/e 167

[c] peaks due to this ion were observed in the complexes where n = 3 or 4

The molecular ion (for complexes where n = 4, X = Br or I; n = 5, X = Br) as well as the fragmentation patterns in the mass spectra of the haloalkyl complexes further confirm the structure of these complexes.

3.3.3 REACTIONS OF $[CpRu(CO)_2\{(CH_2)_nI\}]$ (n = 3,4) with $Na[CpMo(CO)_3]$

We have carried out the reactions of $[CpRu(CO)_2\{(CH_2)_nI\}]$ (n = 3, 4) with $Na[CpMo(CO)_3]$. The infrared evidence suggests that the reactions lead to the formation of the heterobimetallic complexes, $[Cp(CO)_2Ru(CH_2)_nMo(CO)_3Cp]$ (IR ν(CO): 2019, 2012, 1975, 1960 and 1936 cm^{-1} {in hexane} for n = 3; 2010, 1944 and 1921 cm^{-1} {in THF} for n = 5). The infrared data compares well with the data

obtained for the analogous iron/molybdenum complexes $[Cp(CO)_2Fe(CH_2)_nMo(CO)_3Cp]$[10]. However, we did not isolate the heterobimetallic ruthenium-molybdenum complexes, since the complexes were unstable and decompose rapidly on attempting to purify them on a chromatography column.

3.4 CONCLUSION

We have successfully carried out the synthesis and characterization of the mononuclear ethyl complex $[CpRu(CO)_2(CH_2CH_3)]$ and studied some reactions. We have also found that the reactivities of the C_2 alkyl complexes, viz. $[CpRu(CO)_2(CH_2CH_3)]$ and $[CpRu(CO)_2]_2[\mu\text{-}(CH_2CH_2)]$, are significantly different.

The haloalkyl complexes were also successfully synthesized and characterized. The bromoalkyl complexes are easily synthesized at low temperatures, while their iodo analogues are best obtained from the reaction of $[CpRu(CO)_2\{(CH_2)_nBr\}]$ with NaI. These haloalkyl complexes could be good precursors to homo- and heteronuclear complexes.

3.5 REFERENCES

1. F. A. Cotton and G. Wilkinson, *Advanced Inorganic Chemistry, 5th ed. Wiley, New York* **1988** p. 1122.
2. A. Emeran, M. A. Gafoor, J. K. I. Goslett, Y-H Liao, L. Pimble and J. R. Moss, *J. Organomet. Chem.,* **1991**, 405, 237.
3. A. Davison, J. A. McCleverty and G. Wilkinson, *J. Chem. Soc.*, **1963**, 1133.
4. R. J. Kasluaskas and M. S. Wrighton, *Organometallics*, **1982**, 1, 602.
5. K. A. Mahmoud, A. J. Rest and H. G. Alt, *J. Chem. Soc. Dalton Trans.*, **1985**, 1365.
6. J. A. S. Howell, and A. J. Rowan, *J. Chem. Soc. Dalton Trans.*, **1980**, 1845.
7. M. F. Joseph, J. A. Page and M. C. Baird, *Organometallics*, **1984**, 3, 1749.
8. H. B. Friedrich and J. R. Moss, *Adv. Organomet. Chem.,* **1991**, 33 325.
9. H. B. Friedrich, P. A. Makhesha, J. R. Moss and B. K. Williamson, *J. Organomet. Chem.,* **1990**, 384, 325.
10. H. B. Friedrich, J. R. Moss and B. K. Williamson, *J. Organomet. Chem.,* **1990**, 394, 313.
11. (a) C. P. Casey and L.J. Smith, *Organometallics*, **1979**, 21, 1897; (b) J. M. Garner, A. Irving and J. R. Moss, *Organometallics*, **1990**, 9, 2836.
12. D. Seyferth and H. Shih, *J. Org. Chem.*, **1974**, 39, 2329.
13. J. Barluenga, P. J. Campers, J.C. Garcia-Martin, M. A. Roy and G. Asensio, *Synthesis*, **1979**, 893 (and references therein).
14. D. Seyferth and S. B. Andrews, *J. Org. Chem.*, **1971**, 30, 151 (and references therein)
15. P. K. Monaghan and R. J. Puddephatt, *Inorg. Chim. Acta.,* **1983**, 76, L237.
16. J. D. Scott and R. J. Puddephatt, *Organometallics*, **1986**, 5, 1538.

17. F. A. Cotton and C. M.Lukehart *J. Am. Chem. Soc.*, **1971**, 93, 2672.

18. V. A. Osborn and M. J. Winter, *Polyhedron*, **1986**, 5, 435 (and references therein).

19. D. W. Mathieson, "Nuclear Magnetic Resonance for the Organic Chemist", Academic Press Inc., **1967**, p. 166.

20. J. W. Faller and B. V. Johnson, *J. Organomet. Chem.*, **1975**, 88, 101.

21. F. A. Cotton and G. Wilkinson, "Advanced Inorganic Chemistry, 5th ed. Wiley, New York" **1988** p. 1229.

22. H. B. Friedrich, Ph. D. Thesis, University of Cape Town, **1990**.

23. K. P. Finch, M. Sc. Thesis, University of Cape Town, **1988**.

24. H. B. Friedrich and J. R. Moss, unpublished results.

CHAPTER 4

EXPERIMENTAL

4.1 GENERAL

All reactions were carried out under nitrogen (unless otherwise stated) using standard Schlenk tube techniques.

Tetrahydrofuran (THF), hexane, heptane and toluene were distilled from sodium. Acetone and dichloromethane were distilled from anhydrous $CaCl_2$.

The chemical reagents were obtained from the suppliers shown in parentheses: PPh_3 (Merck), PMe_2Ph (Strem), mono- and dialkyl halides (Aldrich), Ph_3CPF_6 (Alpha Products), CF_3COOH (Aldrich), $AgBF_4$ (Merck) and $Ru_3(CO)_{12}$ (Strem). These reagents were used without further purification. NaI was dried before use, by heating at 150 °C at 0.1 mm Hg for five hours. HCl was prepared from the reaction of NaCl with H_2SO_4 and was not dried.

The alkanediyl complexes, $[CpM(CO)_2]_2[\mu\text{-}(CH_2)_n]$ (M = Fe or Ru, n = 3 or 5), were prepared by the literature methods[1,2]. $[CpRu(CO)_2]_2$ was prepared by the method of Knox and Doherty[3]. Alumina (BDH, active neutral, Brockman grade 1) was deactivated before use.

Melting points were recorded on a Kofler hot-stage microscope (Reichert Thermovar) and are uncorrected. Microanalyses were performed by the University of Cape Town Microanalytical Laboratory. Infrared spectra were recorded on a Perkin - Elmer 983 spectrometer in solution cells using NaCl windows or as HCBD mulls between NaCl plates. ^1H NMR and ^{13}C NMR spectra as well as COSY, HETCOR and variable temperature NMR experiments were obtained using a Varian XR 200 spectrometer.

Low resolution mass spectra were recorded with a VG Micromass 16F spectrometer, operating at 70 eV ionising voltage. The source temperature was raised from room temperature until the spectrum was observed. Differential Scanning Calorimetry (DSC) traces were recorded on a Perkin-Elmer PC Series under a nitrogen atmosphere with heating rate of 20 °C / min. X-ray crystal analyses were carried out on an Enraf Nonius CAD4 diffractometer, using MoKα (λ = 0.7107 Å) radiation. The data were corrected for Lorentz-polarization effects and an empirical absorption correction was applied[4]. The structures were solved using SHELX76[5]. Complex neutral atom scattering factors were taken from Cromer and Mann[6] for non-hydrogen atoms and from Stewart, Davidson and Simpson[7] for H, with dispersion corrections from Cromer and Liberman[8]. Molecular parameters were calculated using PARST[9] and drawings obtained using PLUTO[10].

4.2 EXPERIMENTAL DETAILS PERTAINING TO CHAPTER 2

PREPARATION OF $[CpRu(CO)_2]_2[\mu\text{-}(CH_2CH_2)]$, 1

Method (i) : A solution of $Na[CpRu(CO)_2]$ (0.55 g, 2.25 mmol) in THF (20 ml) was added dropwise over 5 min to dichloroethane (0.11 g, 1.13 mmol) at -78 °C with stirring in the dark. The solution was allowed to reach room temperature. After ca. 2 hours the solvent was removed under reduced pressure and the orange-brown residue was extracted with hexane/CH_2Cl_2 (1:1) (3 × 50 ml). The extract was filtered and solvents were removed under reduced pressure. The resulting solid was crystallized from CH_2Cl_2 at -78 °C yielding a pale yellow crystalline solid, complex **1**

(yield, 43 %). Found: C, 40.3; H, 3.0 %. $C_{16}H_{14}O_4Ru_2$ requires C, 40.68; H, 2.99 %. For the characterization data of complex **1**, see Tables 1 - 6 (chapter 2).

Method (ii): A solution of $Na[CpRu(CO)_2]$ (0.10 g, 0.39 mmol) in THF (5 ml) was added dropwise over 5 min to a solution of $[CpRu(CO)_2(C_2H_4)]^+PF_6^-$ {see later} (0.16 g, 0.39 mmol) in THF (10 ml) at 0 °C with stirring. This solution was stirred further at room temperature for ca. three hours. The solvent was removed under reduced pressure leaving an orange-brown residue. This was extracted with hexane : CH_2Cl_2 (19 : 1) (3 × 40 ml). The extract was filtered and solvents were removed under reduced pressure. The resulting solid, complex **1**, was crystallized from hexane at -78 °C (yield 30 %).

REACTION OF COMPLEX **1** *WITH CO IN THF*

A solution of complex **1** (0.05 g, 0.11 mmol) in THF (6 ml) was placed in an autoclave which was then charged with CO (50 atm). The reaction mixture was stirred at room temperature for ca. 10 hours, after which time the gases were vented and the reaction mixture evaporated to dryness. The resulting solid (0.045 g) was identified as complex **1**, indicating that no reaction of complex **1** with CO had occurred.

REACTION OF COMPLEX **1** *WITH CO IN MeOH*

In a similar way, a solution of complex **1** (0.05 g, 0.11 mmol) in distilled MeOH (6 ml) was charged with CO (50 atm) in an autoclave. The reaction mixture was stirred at room temperature for ca. 8 hours, after which time the gases were vented and the reaction mixture evaporated. The resulting semi-crystalline solid was

extracted with hexane and filtered; the filtrate was then concentrated and the product cooled to -78 °C which afforded a yellow precipitate. This precipitate was identified as the dimer, $[CpRu(CO)_2]_2$ (61 %), whereas the oil obtained from the mother liquor was identified as the methoxyethyl complex, $[CpRu(CO)_2(CH_2CH_2OCH_3)]$, (26 %).

REACTION OF COMPLEX **1** *WITH MeOH*

Complex **1** (0.10 g, 0.21 mmol) in distilled MeOH (10 ml) was heated under reflux for 5 hours. The solvent was removed under reduced pressure leaving a yellow-orange residue which was extracted with hexane. The extract was filtered, concentrated and cooled to -78 °C which afforded a yellow precipitate. The precipitate was identified as the dimer, $[CpRu(CO)_2]_2$ (57 %), whereas the oil obtained from the mother liquor was identified as the methoxyethyl complex, $[CpRu(CO)_2(CH_2CH_2OCH_3)]$, (29 %). For the characterization data for the product, see Table 7 (Chapter 2).

REACTION OF $Na[CpRu(CO)_2]$ *WITH* $Cl(CH_2CH_2)OCH_3$

A solution of $Na[CpRu(CO)_2]$ (0.28 g, 1.13 mmol) in THF (12 ml) was added dropwise over 5 min to chloroethyl methyl ether, $Cl(CH_2CH_2)OCH_3$, (0.11 g, 1.13 mmol) at -78 °C with stirring. The solution was allowed to reach room temperature. After 3 hours the solvent was removed under reduced pressure and the orange-yellow residue was extracted with hexane. As above the precipitate was identified as the dimer, $[CpRu(CO)_2]_2$ (60 %), whereas the oil obtained as above. This oil was identified as the methoxyethyl complex, $[CpRu(CO)_2(CH_2CH_2OCH_3)]$,

(30 %). Found: C, 42.3; H, 4.1 %. $C_{10}H_{12}O_3Ru$ requires C, 42.74; H, 4.30 %. For more characterization data for the product, see Table 7 (chapter 2).

REACTION OF COMPLEX **1** *WITH* PMe_2Ph

Complex **1** (0.10 g, 0.21 mmol) and PMe_2Ph (0.90 g, 0.7 mmol) in THF were heated under reflux for ca. 55 hours. The solvent was removed under reduced pressure and the residue taken up in CH_2Cl_2 which was then chromatographed on an alumina column. Elution with CH_2Cl_2/hexane (1 : 1) gave a pale yellow band from which a yellow oil containing the disubstituted complex $[CpRu(CO)(PMe_2Ph)]_2[\mu\text{-}(CH_2CH_2)]$ (38 %) was obtained.

REACTION OF COMPLEX **1** *WITH* Ph_3CPF_6

Ph_3CPF_6 (0.12 g, 0.32 mmol) was added to a solution of complex **1** (0.10 g, 0.21 mmol) in CH_2Cl_2 (8 ml) and the solution stirred for 30 min at room temperature. The solvent was removed and the residue dissolved in a minimum of acetone. Addition of diethyl ether to the solution gave fine, white microcrystals which were washed with ether and dried to give $[CpRu(CO)_2(C_2H_4)]^+PF_6^-$ (60 %). IR (CH_2Cl_2) ν(CO): 2079 and 2038 cm^{-1}; ^1H NMR data: δ = 6.18 ppm (C_5H_5, 5H, s) and δ = 4.05 ppm (CH_2CH_2, 4H, s). The other complex formed in the reaction was identified (IR) as the dimer, $[CpRu(CO)_2]_2$.

REACTION OF COMPLEX **1** *WITH* $AgBF_4$

Similarly, $AgBF_4$ (0.06 g, 0.32 mmol) was added to a solution of complex **1** (0.11 g, 0.21 mmol) in CH_2Cl_2 (8 ml) and the solution stirred for 30 min at room

temperature. The solvent was removed and the residue dissolved in a minimum of acetone. Addition of excess of diethyl ether to the solution gave a light brown precipitate which was identified by IR as the cationic ethylene complex, $[CpRu(CO)_2(C_2H_4)]^+PF_6^-$.

REACTION OF COMPLEX **1** *WITH* CF_3COOH

Trifluoroacetic acid, CF_3COOH, (0.09 g, 0.78 mmol) was added to a solution of complex **1** (0.03 g, 0.08 mmol) in CH_2Cl_2 (8 ml) at room temperature. An immediate reaction occurs with a distinct colour change from pale yellow to a violet-red. The solvent was removed under reduced pressure resulting in a violet-red oil. A methanol solution of $NaBPh_4$ was added to a concentrated methanol solution of the violet-red oil resulting in an immediate precipitation of a white solid which was filtered and dried to give white microcrystals of $[CpRu(CO)_2(C_2H_4)]^+BPh_4^-$ (51 %) (identified by IR and ^1H NMR spectroscopy). The fluoroacetato complex, $[CpRu(CO)_2\{OC(O)CF_3\}]$ {IR (CH_2Cl_2): 2061, 2015 and 1688 cm^{-1}} and traces of the dimer, $[CpRu(CO)_2]_2$ were obtained from the filtrate.

REACTION OF COMPLEX **1** *WITH HCl*

A slight excess of an equimolar amount of HCl (dissolved in $CDCl_3$) was added to a solution of complex **1** (0.02 g, 0.04 mmol) in $CDCl_3$ (0.6 ml) in an NMR tube. ^1H NMR spectra were recorded before and after the addition of HCl. ^1H NMR : δ = 5.43 ppm (C_5H_5, 5H, s,) corresponds to $[CpRu(CO)_2Cl]$; δ = 5.27 ppm (C_5H_5, 5H, s) corresponds to $[CpRu(CO)_2]_2$ and δ = 6.1 ppm (C_5H_5, 5H, s,), δ = 4.1 ppm (CH_2CH_2, 4H, s) correspond to $[CpRu(CO)_2(C_2H_4)]^+$.

REACTION OF COMPLEX 1 *WITH BROMINE*

A similar NMR spectroscopic technique was employed in this reaction. A slight excess of an equimolar amount of Br_2 was added to a solution of complex **1** (0.02 g, 0.04 mmol) in $CDCl_3$ (0.6 ml) placed in an NMR tube. ^1H NMR data: a resonance at δ = 5.43 ppm (C_5H_5, 5H, s,) corresponds to [$CpRu(CO)_2Br$] and resonances at δ = 6.1 ppm (C_5H_5, 5H, s,) and δ = 4.1 ppm (CH_2CH_2, 4H, s) correspond to $[CpRu(CO)_2(C_2H_4)]^+$, whereas a resonance at δ = 3.64 ppm corresponds to $Br(CH_2CH_2)Br$ (see section 2.4.6 for more details).

THERMAL DECOMPOSITION OF COMPLEX 1

A solution of complex **1** (0.02 g, 0.04 mmol) in C_6D_6 (0.6 ml) was placed in a high pressure thick-walled NMR tube[11]. The NMR tube was then connected to a vacuum line and evacuated while cooling at -196 °C and sealed off after several freeze thaw cycles. The sealed NMR tube was allowed to reach room temperature in a fume hood, since condensed O_2 or excess pressure can lead to an explosion.

The NMR tube was then heated in a silicone oil bath at temperatures in the range 80 - 90 °C and the ^1H NMR spectra were recorded at t = 0, 0.75, 3, 122 and 312 hrs (see section 2.5).

CRYSTALLIZATION OF COMPLEX 1

Single crystals suitable for X-ray analysis were prepared by a slow recrystallization of complex **1** from a concentrated, filtered solution of dichloromethane at room temperature in the dark. After ca. 10 days a few crystals had formed and a suitable one was selected for X - ray structural determination.

REACTION OF $[CpFe(CO)_2]_2[\mu\text{-}(CH_2)_3]$ *WITH* Ph_3CPF_6

Ph_3CPF_6 (0.59 g, 1.52 mmol) was added to a solution of $[CpFe(CO)_2]_2[\mu\text{-}(CH_2)_3]$ (0.40 g, 1.01 mmol) in CH_2Cl_2 (20 ml) and the solution was stirred for 30 min at room temperature[12,13]. The solvent was removed and the residue was dissolved in a minimum of acetone. Addition of ether to the solution gave fine, red microcrystals which were filtered, washed with ether and dried to give $[\{CpFe(CO)_2\}_2\{\mu\text{-}(C_3H_5)\}]^+PF_6^-$ (yield 69 %). For more characterization data for the product, see Table 12 (Chapter 2).

REACTION OF $[CpRu(CO)_2]_2[\mu\text{-}(CH_2)_3]$ *WITH* Ph_3CPF_6

Ph_3CPF_6 (0.42 g, 1.08 mmol) was added to a solution of $[CpRu(CO)_2]_2[\mu\text{-}(CH_2)_3]$ (0.35 g, 0.72 mmol) in CH_2Cl_2 (10 ml) and the solution was stirred for 30 min at room temperature. The solvent was removed and the residue was dissolved in a minimum of CH_2Cl_2. Addition of hexane to the solution gave bright yellow fine needle-like crystals which were filtered, washed with hexane and dried to give $[\{CpRu(CO)_2\}_2\{\mu\text{-}(C_3H_5)\}]^+PF_6^-$ (yield 62 %; m.p. 202 - 204 °C). Found: C, 32.6;

H, 2.5 %. $C_{17}H_{15}F_6O_4PRu_2$ requires C, 32.39; H, 2.40 %. Infrared, ^1H NMR and ^{13}C NMR data for the product are given in Table 12 (Chapter 2).

RECRYSTALLIZATION OF $[\{CpM(CO)_2\}_2\{\mu\text{-}(C_3H_5)\}]^+PF_6^-$ (M = Fe or Ru)

Single crystals suitable for X-ray analysis were prepared by a slow recrystallization of the cationic complexes, $[\{CpM(CO)_2\}_2\{\mu\text{-}(C_3H_5)\}]^+PF_6^-$ (M = Fe or Ru) from a concentrated, filtered acetone solution at room temperature. After ca. 5 days a few crystals had formed and suitable ones were selected for X - ray structural determination.

REACTION OF $[CpFe(CO)_2]_2[\mu\text{-}(CH_2)_5]$ WITH Ph_3CPF_6

Ph_3CPF_6 (0.55 g, 1.42 mmol) was added to a solution of $[CpFe(CO)_2]_2[\mu\text{-}(CH_2)_5]$ (0.40 g, 0.94 mmol) in CH_2Cl_2 (10 ml) and the solution was stirred for 10 min at room temperature[14]. The solvent was removed and the residue was redissolved in a minimum of acetone. Addition of ether to the solution gave yellow microcrystals which were filtered, washed with ether and dried to give $[\{CpFe(CO)_2\}_2\{\mu\text{-}(C_5H_9)\}]^+PF_6^-$ (yield 68 %). This is an improved procedure to that reported previously for this complex[13]. For more characterization data for the product, see Table 21 (Chapter 2).

REACTION OF $[CpRu(CO)_2]_2[\mu\text{-}(CH_2)_5]$ WITH Ph_3CPF_6

Similarly, Ph_3CPF_6 (0.06 g, 0.147 mmol) was added to a solution of $[CpRu(CO)_2]_2[\mu\text{-}(CH_2)_5]$ (0.05 g, 0.097 mmol) in CH_2Cl_2 (8 ml) and the solution

was stirred for 10 min at room temperature[14]. The solvent was concentrated. Addition of hexane to the solution gave yellow-orange fine microcrystals which were purified as before to give $[\{CpRu(CO)_2\}_2\{\mu\text{-}(C_5H_9)\}]^+PF_6^-$ (yield 70 %; m.p. 141 - 145 °C). Found: C, 34.3; H, 2.9 %. $C_{19}H_{19}F_6O_4PRu_2$ requires C, 34.66; H, 2.91 %. Infrared, ^1H NMR and ^{13}C NMR data for the product are given in Table 21 (Chapter 2).

REACTION OF $[\{CpFe(CO)_2\}_2\{\mu\text{-}(C_5H_9)\}]^+PF_6^-$ WITH CF_3COOH

Trifluoroacetic acid, CF_3COOH, (0.88 g, 0.77 mmol) was added to a solution of $[\{CpFe(CO)_2\}_2\{\mu\text{-}(C_5H_9)\}]^+PF_6^-$ (0.18 g, 0.31 mmol) in CH_2Cl_2 (10 ml) at room temperature. The reaction was monitored by infrared spectroscopy. A series of IR spectra were recorded at 5 min intervals. After one hour the solvent from the reaction mixture was removed under reduced pressure resulting in a maroon-red oil. A methanol solution of $NaBPh_4$ was added to a concentrated methanol solution of the maroon-red oil resulting in an immediate yellow precipitation which was filtered and dried to give $[CpFe(CO)_2(CH_2{=}CHCH_2CH_2CH_3)]^+BPh_4^-$ (yield 90 %). For the infrared, ^1H NMR and ^{13}C NMR characterization data, see Table 22 (Chapter 2). The other product, the fluoroacetato complex $[CpFe(CO)_2\{OC(O)CF_3\}]$ was obtained from the filtrate; IR (CH_2Cl_2): 2061, 2015 and 1683 cm^{-1}.

REACTION OF $[\{CpRu(CO)_2\}_2\{\mu\text{-}(C_5H_9)\}]^+PF_6^-$ WITH CF_3COOH

Similarly, trifluoroacetic acid, CF_3COOH, (0.46 g, 0.40 mmol) was added to a solution of $[\{CpRu(CO)_2\}_2\{\mu\text{-}(C_5H_9)\}]^+PF_6^-$ (0.10 g, 0.16 mmol) in CH_2Cl_2 (5 ml) at room temperature. The reaction was monitored by infrared spectroscopy. A series of IR spectra were recorded from t = 0 to t = 300 min. After five hours the

a violet-red oil. A methanol solution of $NaBPh_4$ was added to a concentrated methanol solution of the violet-red oil resulting in an immediate yellow precipitate which was filtered and dried to give $[CpRu(CO)_2(CH_2=CHCH_2CH_2CH_3)]^+BPh_4^-$ (yield 66 %; m.p. 112 - 114 °C). The fluoroacetato complex, $[CpRu(CO)_2\{OC(O)CF_3\}]$ was also isolated from the filtrate. For the infrared, ^1H NMR and ^{13}C NMR characterization data, see Table 22 (Chapter 2).

REACTION OF $[CpFe(CO)_2(CH_2=CHCH_2CH_2CH_3)]^+BPh_4^-$ WITH NaI

A d_6-acetone solution (0.6 ml) of the cationic complex, $[CpFe(CO)_2(CH_2=CHCH_2CH_2CH_3)]^+BPh_4^-$ (0.03 g, 0.06 mmol), was treated with 2 equiv. of NaI at room temperature in an NMR tube. The reaction was monitored by means of ^1H NMR spectroscopy. The ^1H NMR spectra indicated a quantitative displacement of 1-pentene and the formation of $[CpFe(CO)_2I]$.

REACTION OF $[CpRu(CO)_2(CH_2=CHCH_2CH_2CH_3)]^+BPh_4^-$ WITH NaI

Similarly, a d_6-acetone solution (0.6 ml) of the cationic complex, $[CpRu(CO)_2(CH_2=CHCH_2CH_2CH_3)]^+BPh_4^-$ (0.03 g, 0.05 mmol), was treated with 2 equiv. of NaI at room temperature in an NMR tube. The ^1H NMR spectra indicated a quantitative displacement of 1-pentene and the formation of $[CpRu(CO)_2I]$.

4.3 EXPERIMENTAL DETAILS PERTAINING TO CHAPTER 3

REACTION OF [CpRu(CO)$_2$(CH$_2$CH$_3$)] WITH CF$_3$COOH

A solution of [CpRu(CO)$_2$(CH$_2$CH$_3$)] (0.02 g, 0.08 mmol) in CDCl$_3$ (0.6 mmol) was treated with an excess of one equivalent of CF$_3$COOH at room temperature in an NMR tube. ^{1}H NMR spectrum indicated the quantitative formation of ethane from the ethyl complex, [CpRu(CO)$_2$(CH$_2$CH$_3$)].

ATTEMPTED REACTION OF [CpRu(CO)$_2$(CH$_2$CH$_3$)] WITH MeOH

The complex [CpRu(CO)$_2$(CH$_2$CH$_3$)] (0.05 g, 0.20 mmol) in MeOH (10 ml) was heated under reflux for 14 days. The IR spectra indicated that no reaction had occurred.

REACTION OF [CpRu(CO)$_2$(CH$_2$CH$_3$)] WITH Ph$_3$CPF$_6$

Ph$_3$CPF$_6$ (0.15 g, 0.60 mmol) was added to a solution of [CpRu(CO)$_2$(CH$_2$CH$_3$)] (0.16 g, 0.40 mmol) in CH$_2$Cl$_2$ (8 ml) and the solution was stirred for 1 hour at room temperature[15]. The solvent was removed and the residue was dissolved in a minimum of CH$_2$Cl$_2$. Addition of hexane to the solution gave white microcrystals which were filtered, washed with hexane and dried to give [CpRu(CO)$_2$(C$_2$H$_4$)]$^+$PF$_6^-$ (yield 61 %).

PREPARATION OF [CpRu(CO)$_2${(CH$_2$)$_3$Br}]

A solution of Na[CpRu(CO)$_2$] (0.33 g, 1.34 mmol) in THF (10 ml) was added dropwise over 15 min to 1,3-dibromopropane (0.28 g, 1.40 mmol) at -78 °C with stirring. The solution was allowed to attain room temperature. After 1 hour the solvent was removed under reduced pressure and the orange-brown oily residue was extracted with hexane (4 × 50 ml). The extract was filtered, concentrated and chromatographed on an alumina column. Elution with hexane gave a colourless fraction from which a colourless oil of the haloalkyl complex [CpRu(CO)$_2${(CH$_2$)$_3$Br}] was obtained (yield 64 %).

PREPARATION OF [CpRu(CO)$_2${(CH$_2$)$_3$Cl}]

Similarly, a solution of Na[CpRu(CO)$_2$] (0.14 g, 0.57 mmol) in THF (10 ml) was added dropwise over 5 min to 1,3-dichloropropane (0. 60 g, 0.57 mmol) at -10 °C with stirring. The solution was allowed to attain room temperature. After 1 hour the solvent was removed under reduced pressure and the orange-brown oily residue was extracted with hexane (3 × 40 ml). The extract was filtered, concentrated and recrystallized from hexane at -78 °C to give a chloropropyl complex, [CpRu(CO)$_2${(CH$_2$)$_3$Cl}], (which is a colourless oil at room temperature; yield 76 %).

PREPARATION OF [CpRu(CO)$_2${(CH$_2$)$_4$Br}]

Similarly, a solution of Na[CpRu(CO)$_2$] (0.28 g, 1.15 mmol) in THF (10 ml) was added dropwise over 5 min to 1,4-dibromobutane (0.25 g, 1.15 mmol) at -78 °C with

stirring. The solution was allowed to attain room temperature. After 45 min the solvent was removed under reduced pressure and the orange-brown oily residue was extracted with hexane (4 × 40 ml). The extract was filtered, concentrated and chromatographed on an alumina column. The first colourless fraction eluted with hexane gave a colourless oil of $[CpRu(CO)_2\{(CH_2)_4Br\}]$ (yield 69 %).

PREPARATION OF $[CpRu(CO)_2\{(CH_2)_5Br\}]$

Similarly, a solution of $Na[CpRu(CO)_2]$ (0.55 g, 2.25 mmol) in THF (10 ml) was added dropwise over 5 min to 1,5-dibromopentane (0.52 g, 2.25 mmol) at -78 °C with stirring. The product was isolated and purified as above (yield 74 %).

PREPARATION OF $[CpRu(CO)_2\{(CH_2)_3I\}]$

A solution of $[CpRu(CO)_2\{(CH_2)_3Br\}]$ (0.18 g, 0.52 mmol) in acetone (10 ml) was treated with two equivalents of NaI (0.16 g, 1.04 mmol) at room temperature. The solution was stir for ca. 30 hours. The solvent was removed under reduced pressure and the residue was extracted with hexane. The extract was filtered, concentrated and chromatographed on an alumina column. The first colourless fraction eluted with hexane gave a crystalline solid of $[CpRu(CO)_2\{(CH_2)_3I\}]$ (yield 71% m.p. 37 - 39 °C).

PREPARATION OF [CpRu(CO)$_2${(CH$_2$)$_4$I}]

Similarly, a solution of [CpRu(CO)$_2${(CH$_2$)$_4$Br}] (0.18 g, 0.50 mmol) in acetone (8 ml) was treated with two equivalents of NaI (0.15 g, 1.0 mmol) at room temperature. The solution was allowed to stir for ca. 24 hours. The iodobutyl complex (a colourless oil at room temperature) was isolated and purified as above (yield 75 %).

PREPARATION OF [CpRu(CO)$_2${(CH$_2$)$_5$I}]

In a similar way, a solution of [CpRu(CO)$_2${(CH$_2$)$_5$Br}] (0.23 g, 0.61 mmol) in acetone (8 ml) was treated with two equivalents of NaI (0.19 g, 1.24 mmol) at room temperature. The solution was allowed to stir at this temperature for ca. 28 hours to yield the iodopentyl complex, [CpRu(CO)$_2${(CH$_2$)$_5$I}] (a colourless oil at room temperature, yield 79 %).

For the characterization data for all these haloalkyl complexes, see Tables 2 - 4 (chapter 3).

REACTION OF [CpRu(CO)$_2${(CH$_2$)$_3$I}] WITH Na[CpMo(CO)$_3$]

A solution of Na[CpMo(CO)$_3$] (0.09 g, 0.39 mmol) in THF (10 ml) was added dropwise over 5 min to the [CpRu(CO)$_2${(CH$_2$)$_3$I}] (0.15 g, 0.37 mmol) at -78 °C with stirring. The solution was allowed to attain room temperature. An infrared spectrum recorded after 60 hours showed ν(CO) bands at 2019, 2012, 1975, 1960 and 1936 cm^{-1} in hexane. The solvent was removed under reduced pressure and the orange-brown residue was extracted with CH_2Cl_2. The extract was filtered, concentrated and transferred to an alumina column. A rapid decomposition of this

crude product takes place on the column. However, the product was not further investigated.

REACTION OF $[CpRu(CO)_2\{(CH_2)_5I\}]$ WITH $Na[CpMo(CO)_3]$

A solution of $Na[CpMo(CO)_3]$ (0.12 g, 0.50 mmol) was added dropwise to the $[CpRu(CO)_2\{(CH_2)_5I\}]$ (0.20 g, 0.48 mmol) at -78 °C. The solution was allowed to attain room temperature. An infrared spectrum recorded after 60 hours showed ν(CO) bands at 2010, 1944 and 1921 cm^{-1} in THF. The crude product decomposes rapidly on the column and the product was not further investigated. However, other purification methods such as recrystallization could be employed.

4.4 REFERENCES

1. M.E.Brown, K.J.Hindson, J.R.Moss and L.G.Scott, *J. Organomet. Chem.*, **1985**, 282, 255.
2. K. P. Finch, J.R.Moss and M. L. Niven , *Inorg. Chim. Acta*, **1989**, 166, 867.
3. N.M.Doherty and S.A.R.Knox, *Inorg. Synth.*, **1989**, 25, 179.
4. A. C. T. North, D. C. Phillips and F. S. Mathews: *Acta Crystallogr.*, **1968**, A24, 351
5. G. M. Sheldrick: The SHELX-76 program system, in Computing in Crystallography, H. Schenk, R. Olthof-Hazekamp, H. von Koningsveld and G. C. Bassi, eds. (Delft University press) **1978**, p. 34
6. D. T. Cromer and J. B. Mann: *Acta Crystallogr.*, **1968**, A24, 321
7. R. F. Stewart, E. R. Davidson and W. T. Simpson: *J. Chem. Phys.*, **1965**, 42, 3175.
8. D. T. Cromer and D. Liberman: J. Chem. Phys. **1970**, 53, 1891.
9. M. Nardelli: Comput. Chem., **1983**, 7, 95.
10. W. D. S. Motherwell: The PLUTO program for molecular drawings (Cambridge University, unpublished).
11. B.J.Burger and J.E.Bercaw, *submitted for publication*.
12. R.B.King and M.B.Bisnette, *J. Organomet. Chem.*, **1967**, 7, 311.
13. J.W.Johnson and J.R.Moss, *Polyhedron*, **1985**, 4, 563.
14. K.P.Finch, M.A.Gafoor, S.F.Mapolie and J.R.Moss, *Polyhedron*, **1991**, 10, 1991.
15 J.W.Faller and B.V.Johnson, *J. Organomet. Chem.*, **1975**, 88, 101.